AD_____

Award Number: W81XWH-04-1-0909

TITLE: Role of the ARF Tumor Suppressor in Prostate Cancer

PRINCIPAL INVESTIGATOR: Leonard B. Maggi, Jr., Ph.D.
Jason D. Weber, Ph.D.
Arul M. Chinnaiyan, M.D., Ph.D.
Paul J. Goodfellow, Ph.D.
Adam S. Kibel, M.D.
Jeffrey D. Milbrandt
Peter A. Humphrey, M.D., Ph.D.

CONTRACTING ORGANIZATION: Washington University
Saint Louis, MO 63110

REPORT DATE: October 2006

TYPE OF REPORT: Annual Summary

PREPARED FOR: U.S. Army Medical Research and Materiel Command
Fort Detrick, Maryland 21702-5012

REPORT DOCUMENTATION PAGE

Form Approved
OMB No. 0704-0188

1. REPORT DATE	2. REPORT TYPE	3. DATES COVERED
01-10-2006	Annual Summary	1 Oct 2004 – 30 Sep 2006

4. TITLE AND SUBTITLE

Role of the ARF Tumor Suppressor in Prostate Cancer

5a. CONTRACT NUMBER

5b. GRANT NUMBER
W81XWH-04-1-0909

5c. PROGRAM ELEMENT NUMBER

6. AUTHOR(S)
Leonard B. Maggi, Jr., Ph.D.
Jeffrey D. Milbrandt Ph.D
Jason D. Weber, Ph.D.
Peter A. Humphrey, M.D.
Arul M. Chinnaiyan, M.D., Ph.D.
Paul J. Goodfellow, Ph.D.
Adam S. Kibel, M.D.

5d. PROJECT NUMBER

5e. TASK NUMBER

5f. WORK UNIT NUMBER

7. PERFORMING ORGANIZATION NAME(S) AND ADDRESS(ES)

Washington University
Saint Louis, MO 63110

8. PERFORMING ORGANIZATION REPORT NUMBER

9. SPONSORING / MONITORING AGENCY NAME(S) AND ADDRESS(ES)
U.S. Army Medical Research and Materiel Command
Fort Detrick, Maryland 21702-5012

10. SPONSOR/MONITOR'S ACRONYM(S)

11. SPONSOR/MONITOR'S REPORT NUMBER(S)

12. DISTRIBUTION / AVAILABILITY STATEMENT
Approved for Public Release; Distribution Unlimited

13. SUPPLEMENTARY NOTES
Original contains colored plates: ALL DTIC reproductions will be in black and white.

14. ABSTRACT

The nucleolar tumor suppressor ARF plays an important role in the tumor surveillance of human cancer. We have found that ARF expression is absent from highly proliferative prostate adenocarcinomas and this correlates with the increased expression of the p53-independent target of NPM. We have created and characterized an immortalized ARF-null prostate epithelial cell line. In addition we have shown that alterations in NPM levels can have dramatic affects on the androgen-dependent cancer cell line, LNCaP, but not PC3 cells which are androgen-independent. We have previously shown that ARF inhibits NPM's nuclear export and cell cycle progression in a p53-indpendent manner. Under this proposal we have defined the mechanism by which this happens. Specifically, ARF binds to NPM preventing its ability to carry both small and large ribosomal subunits out of the nucleus. This results in a decrease in protein synthesis and growth rates contributing to ARF's tumor suppressor function. We are beginning to further define the role of ARF in prostate cell growth. These studies are opening the door to new therapeutic targets in prostate cancer; namely protein synthesis.

15. SUBJECT TERMS
ARF, Prostate Cancer, Tumor Suppression, Nucleophosmin, Protein Synthesis

16. SECURITY CLASSIFICATION OF:				18. NUMBER OF PAGES	19a. NAME OF RESPONSIBLE PERSON
					USAMRMC
a. REPORT	b. ABSTRACT	c. THIS PAGE			19b. TELEPHONE NUMBER *(include area code)*
U	U	U	UU	120	

Standard Form 298 (Rev. 8-98)
Prescribed by ANSI Std. Z39.18

Table of Contents

INTRODUCTION

Prostate cancer is the second leading cause of cancer related deaths in the US male population (*1*). With the development of prostate specific antigen (PSA) screening the number of prostate cancer cases identified has risen, and the number of deaths has begun to decrease. However, the molecular mechanisms underlying the development and progression of prostate cancer are still largely unknown. The most mutated gene associated with human cancer in general, the p53 tumor suppressor, has been reported to play a role in the development and progression of prostate cancer (*2*, *3*). p53 is regulated by the ARF tumor suppressor which imparts its control over cell proliferation though both p53-dependent and –independent mechanisms, with the former involving the nucleolar sequestration of the p53 negative regulator, Mdm2 and the latter only recently discovered by our laboratory (*4*, *5*). While tumors of epithelial cell origin are rare in *Arf*- or *p53*-null mice, animals lacking both *Arf* and *p53* display numerous tumors of this type demonstrating a role for ARF in preventing epithelial cell tumorigenesis (*6*-*9*). In addition, introduction of ARF into $p53^{-/-}$ MEFs results in cell cycle arrest (*9*). In numerous human cancers, the frequency of loss of the *Arf* tumor suppressor is second only to mutation of p53, providing critical evidence of *Arf*'s role in preventing tumorigenesis throughout the body, irregardless of cell type. However, the result of loss of ARF function in the prostate is unknown. The preliminary data for my original proposal indicated that prostate adenocarcinomas typically maintain wild type p53 (97%), but lose ARF (96%) expression. These data suggest ARF loss may play a role in the development and/or progression of prostate cancer. The goal of this study is to understand the role of the *Arf* tumor suppressor in prostate cell growth. We hypothesize that ARF utilizes p53-dependent and –independent mechanisms to regulate prostate cell proliferation.

	p53	p21	Mdm2	ARF	NPM
-	60 (97%)	65 (100%)	32 (53%)	51 (96%)	35 (56%)
+	2 (3%)	0 (0%)	28 (47%)	2 (4%)	28 (44%)

Table 1. Protein Expression in Prostate Adenocarcinomas Human prostate tissue samples were analyzed by immunohistochemistry for the indicated proteins. Proteins were scored for their expression above (+) or at/below (-) wild type levels. The number of samples scored positive or negative is indicated with the percentage of the positive or negative in parentheses.

BODY

Creation of an $Arf^{-/-}$ Prostate Epithelial Cell Line

To begin to address the role of ARF in PEpC growth, prostates were isolated from 8 week old $Arf^{+/+}$ and $Arf^{-/-}$ mice. The organs were diced into pieces approximately $1mm^3$ in size and plated in defined media to select for prostate epithelial cell growth. As shown in Figure 1, cells cultures were grown from isolated prostates. Cells from the $Arf^{-/-}$ prostates grew well, but the wild-type cells were unable to proliferate beyond the 2nd passage. The $Arf^{-/-}$ prostate cells were then subjected to a 3T3 protocol in which $3x10^5$ cells were passaged every 3 days to demonstrate their proliferative capacity. As shown in Figure 2A, the $Arf^{-/-}$ prostate cells were

able to be passaged 15 times without inhibition in growth indicating they are immortal. In fact the Arf-/- prostate cells have been passaged over 40 times without a decrease in growth (data not shown). In addition, an *Arf*$^{-/-}$ prostate cell growth curve shows that the cells can grow to confluency in a 10 cm dish (Figure 2B). Finally, *Arf*$^{-/-}$ prostate cells are not transformed as they cannot form colonies in soft agar (Figure 2C). Taken together these data indicate that the cell line created from *Arf*$^{-/-}$ prostates are immortal but not transformed.

To verify that the cultured cells were in fact epithelial in origin, *Arf*$^{-/-}$ prostate cells were seeded onto glass cover slips in defined media and incubated overnight. The cells were fixed and stained with antibodies against prostate epithelial (anti-CD38) and stromal (anti-CD54) markers (*10*). As shown in Figure 3, the *Arf*$^{-/-}$ prostate cells stained strongly for CD-38, the prostate epithelial marker, but showed almost no CD-54 signal indicating the cells were epithelial in origin not stromal.

After passaging the *Arf*$^{-/-}$ PEpC several times, we next determined if they maintained genomic integrity. *Arf*$^{-/-}$ PEpC (passage 20) were fixed and DNA was stained with propidium iodide (PI) and DNA content was analyzed by flow cytometry. As shown in Figure 4A, the *Arf*$^{-/-}$ PEpC contain 2N and 4N DNA with little to no >4N cells indicating these cells can maintain a proper DNA content. In addition, late passage *Arf*$^{-/-}$ PEpC were subjected to a colcemid block and metaphase spread analysis to determine chromosome number. As shown in Figure 4B, *Arf*$^{-/-}$ PEpC maintain normal chromosome number over several passages. Taken together these data demonstrate that *Arf*$^{-/-}$ PEpC remain diploid.

Since *Arf*$^{-/-}$ PEpC remain diploid as shown in Figure 4, this indicates that while the cells have lost *Arf*, p53 function remains intact. To verify this, *Arf*$^{-/-}$ PEpC were treated with etoposide to induce DNA strand breaks which will activate a p53 response. As shown in Figure 5A, treatment with 50 mM etoposide for 18 h results in cell cycle arrest. To show this is a p53-dependent cell cycle arrest the levels of p21, a downstream target of p53, were determined by western blot. As shown in Figure 5B, p21 was induced in response to etoposide treatment indicating that Arf-/- PEpC have an intact p53 response. In addition to having an intact p53 response to DNA damage, ARF expression in *Arf*$^{-/-}$ PEpC should also result in cell cycle arrest. As shown in Figure 6, overexpression of p19ARF in *Arf*$^{-/-}$ PEpC results in the inhibition of cell cycle progression indicating that this cell line has an intact ARF response.

In addition to expression of prostate epithelial markers, PEpC require androgen signaling for survival (*11*). As shown in Figure 7E, the Arf-/- PEpC express the androgen receptor by western blot analysis. Using an androgen receptor antagonist, bicalutamide from AstraZeneca, I was able to demonstrate that *Arf*$^{-/-}$ PEpC do not proliferate well (Figure 7A and B) as shown by a growth curve. In addition, treatment of *Arf*$^{-/-}$ PEpC with bicalutamide for 48 h blocks BrdU incorporation into replicating DNA (Figure 7C). Taken together these data indicate that *Arf*$^{-/-}$ PEpC express the androgen receptor and require androgen signaling for growth.

Previous studies have shown that Androgen Receptor signaling is required for phosphorylation of NPM, a p53-independent target of the ARF nucleolar tumor suppressor (*12, 13*). As shown in Figure 7D, inhibition of androgen receptor signaling in *Arf*$^{-/-}$ PEpC with bicalutamide results for 96 h results in a loss in phosphorylation of NPM at Thr198 (top panel).

This correlates with a decrease in total NPM levels in these cells (Figure 7B bottom panel). Interestingly, the androgen independent prostate tumor cell line PC3 has a detectable level of NPM (data not shown) indicating that androgen independence may result from the ability to stabilize NPM in the absence of androgen receptor activity.

mTOR Pathway activation regulates NPM expression at the translational level.

Given the growth promoting properties of androgen receptor signaling and its affects on NPM in our *Arf*$^{-/-}$ PEpC, we wanted to examine the regulation of *Npm* expression. NPM is a classic mitogen-induced protein, with changes in its expression correlating with growth factor stimulation. In an effort to understand the regulation of NPM expression, we examined the underlying mechanism of NPM induction and demonstrate that hyperproliferative signals emanating from oncogenic H-Ras^{V12} cause tremendous increases in NPM protein expression. NPM protein accumulation was dependent on mTOR activation, as rapamycin completely prevented NPM induction. Consistent with this finding, genetic ablation of *Tsc1*, a major upstream inhibitor of mTOR, resulted in NPM protein induction through increased translation of existing NPM mRNAs. Increases in NPM protein accumulation were suppressed by re-introduction of TSC1. Induction of NPM through *Tsc1* loss resulted in a greater pool of actively translating ribosomes in the cytoplasm, higher overall rates of protein synthesis and increased cell proliferation, all of which were dependent on efficient NPM nuclear export. NPM protein accumulation in the absence of *Tsc1* promoted the nuclear export of maturing ribosome subunits, providing a mechanistic link between TSC1/mTOR signaling, NPM-mediated nuclear export of ribosome subunits, protein synthesis levels, and cell growth. (SEE ATTACHED Manuscript #1 IN APPENDICIES, "TSC1 Sets the Rate of Ribosome Export and Protein Synthesis Through Nucleophosmin Translation").

Nucleophosmin (NPM/B23) is a p53-independent target of nucleolar ARF tumor suppression.

Our lab and others have previously shown that the nucleolar tumor suppressor, ARF, can bind to NPM (*5*). We have also shown that ARF inhibits NPM nuclear/cytoplasmic trafficking which correlates with an inhibition of cell cycle progression in a p53-indpendent manner (*5*). However, the underlying mechanism of how ARF-induced inhibition of NPM nuclear export regulates cell cycle progression remained undiscovered.

NPM is a key regulator in the regulation of a number of processes including centrosome duplication, maintenance of genomic integrity, and ribosome biogenesis. While the mechanisms underlying NPM function are largely uncharacterized, NPM loss results in severe dysregulation of developmental and growth-related events. We determined that NPM utilizes a conserved CRM1-dependent nuclear export sequence in its amino terminus to enable its shuttling between the nucleolus/nucleus and cytoplasm. In search of NPM trafficking targets, we biochemically purified NPM-bound protein complexes from HeLa cell lysates. Consistent with NPM's proposed role in ribosome biogenesis, we isolated ribosomal protein L5 (rpL5), a known chaperone for the 5S rRNA. Direct interaction of NPM with rpL5 mediated the colocalization of NPM with maturing nuclear 60S ribosomal subunits, as well as newly exported and assembled 80S ribosomes and polysomes. Inhibition of NPM shuttling or loss of *NPM* blocked the nuclear

export of rpL5 and 5S rRNA, resulting in cell cycle arrest and demonstrating that NPM and its nuclear export provide a unique and necessary chaperoning activity to rpL5/5S (SEE ATTACHED PAPER #1 IN APPENDICIES, "Nucleophosmin is Essential for Ribosomal Protein L5 Nuclear Export").

NPM is a critical target of ARF tumor suppression while, in the absence of *ARF*, NPM is capable of transforming cells. In addition to our preliminary findings that ARF is under expressed in 96% of prostate adenocarcinomas, more detailed analysis of NPM levels show that over 82% of proliferating (Ki-67 positive) prostate adenocarcinomas overexpress NPM with 44% grossly overexpressing the gene. We have reported the mechanism for NPM's regulation of cell growth; NPM directs the nuclear export of both 40S and 60S ribosomal subunits. Transduction of NPM shuttling-defective mutants or loss of *Npm*, inhibited nuclear export of both the 40S and 60S ribosomal subunits, reduced the available pool of cytoplasmic polysomes, and diminished overall protein synthesis without affecting ribosomal RNA processing. Modest increases in NPM expression amplified the export of newly synthesized ribosomal RNAs, resulting in increased rates of protein synthesis and indicating that NPM is rate-limiting in this pathway. These results support the idea that NPM-regulated ribosome export is a fundamental process in growth and cellular transformation (SEE ATTACHED MANUSCRIPT #2 IN APPENDICIES, "Nucleophosmin Directs Ribosome Nuclear Export and Cell Growth").

We next examined the effects of inhibition of NPM shuttling on S phase entry of two human prostate cancer cell lines, androgen-dependent LNCaP and androgen independent PC3. As shown in Figure 8, overexpression of NPM or the NPM shuttling mutant NPMdL did not alter BrdU incorporation into replicating DNA. However, the androgen-dependent cell line, LNCaP, showed a high sensitivity to inhibition of NPM shuttling (>5 fold decrease, Figure 9B). Interestingly, the level of wild type NPM overexpression also affected BrdU incorporation. As shown in Figure 9A (arrows), high levels of NPM expression resulted in an inhibition of BrdU incorporation into replicating DNA (>5 fold Figure 9B). However, lower levels of expression showed a slight increase in the number of BrdU positive cells (Figure 9B). Taken together with the data from the $Arf^{-/-}$ PEpC which show sensitivity of NPM levels to androgen signaling (figure 7D), and the data showing high NPM levels in prostate adenocarcinomas (SEE ATTACHED MANUSCRIPT #2 IN APPENDICIES, "Nucleophosmin Directs Ribosome Nuclear Export and Cell Growth") this data indicates that targeting protein synthesis could be a useful therapeutic target for the treatment of prostate cancer.

To examine the effects of *Arf* loss on PEpC protein synthesis rate, wild-type and $Arf^{-/-}$ PEpC were labeled with ^{35}S-Methionine for the indicated times and total trichloroacetic acid-precipitable proteins were counted for label incorporation. As shown in figure 10, $Arf^{-/-}$ PEpC produce 4-fold more protein over a 24 time course than an equal number of wild type PEpC. These data indicate that *Arf* is required to regulate protein synthesis in PEpC.

Our previous studies have shown that NPM can transform immortalized $Arf^{-/-}$ MEFs. While loss of *Arf* results in an increase in protein synthesis rates of PEpC, overexpression of NPM cannot increase growth rates as determined by foci assay (Figure 11A), nor transform them as determined by colony formation in soft agar (Figure 11B). In addition, classical transforming genes such as a constitutively active *RasV12* and *Myc* alone and in combination cannot increase

growth rates of (Figure 11A) or transform (Figure 11B) *Arf*$^{-/-}$ PEpC. This is not unprecedented as bone marrow derived cells isolated from *Arf*$^{-/-}$ mice could not be transformed with RasV12 or Myc alone (*14*). However, in combination RasV12 and Myc overexpression were able to transform *Arf*$^{-/-}$ bone marrow derived cells. Previous work by Trotta and colleagues (*15*) has shown loss of Pten, the negative regulator of PI3K, to promote prostate tumorigenesis. Therefore we obtained two activated PI3K constructs (PI3K^{E545K}, PI3K^{H1047R}, (*16*) and overexpressed them in the *Arf*$^{-/-}$ PEpC in combination with Ras^{V12}. As shown in Figure 13, overexpression of Ras^{V12} alone or in combination with any of the PI3K constructs did not result in increase proliferation (Foci Assay, bottom panel). However, in combination with Ras^{V12}, the activate PI3K mutants (PI3K^{E545K}, PI3K^{H1047R}) were able to induce the growth of colonies in soft agar (top panels). These data show that loss of *Arf* in conjunction with Ras^{V12} and PI3K signals can induce the transformation of PEpC.

To further support these findings we have performed Electron Microscopy on Mouse Embryo Fibroblasts (MEF) isolated from *Npm*$^{+/+}$ and *Npm* hypomorphic (*Npm*$^{h/h}$) mice. As shown in Figure 13, loss of *Npm* results in a thickening of the nuclear membrane (arrows) indicating a buildup of ribosomal subunits that cannot exist the nucleus (upper panels). In the cytoplasm of *Npm*$^{h/h}$ MEF there is also a paucity of rough endoplasmic reticulum compared to wild-type cells (diamond headed arrows, upper panels) indicating a decrease in protein synthetic capability. To confirm that the electron dense areas at the nuclear membrane are indeed ribosomes building up at nuclear pores, immunogold labeling studies will be performed. There are difficulties getting two antibodies to label under the same conditions and these technical difficulties are being worked out. Finally, the morphology of the nucleolus in markedly altered with a large increase in vacant areas in *Npm*$^{h/h}$ nucleoli versus *Npm*$^{+/+}$ nucleoli (bottom panels).

We next wanted to define the regions of NPM that are required for nuclear export (Crm1 binding), interaction with the ribosome (L5 binding), and ribosome export. To that end, a NPM deletion panel was created. Overlapping 30 amino acid sections of GFP-tagged NPM were deleted using a QuickChange Mutagenesis kit. The expression of the deletion panel is shown in Figure 14A by western blot. Subcellular localization of the mutants was determined by fluorescence microscopy (Figure 14C). Deletion of amino acids 1 to 120 resulted in an increased pan nuclear localization of the GFP signal as compared to the nucleolar localization of wild type GFP-NPM. Deletion of the c-terminal regions of NPM also results in more nuclear staining than wild type, but not to the extent of the n-terminal mutant. A schematic of the NPM protein (Figure 14B) shows that the pan nuclear signal resulting from the n-terminal mutants results from disruptions of the oligomerization domain of NPM. These localization data correlate with NPM-Crm1 biding. As shown in Figure 15B, the same mutants that show increase nucleoplasmic localization also show decreased Crm1 binding. Interestingly, the oligomerization of NPM does not seem to be essentially required for L5 binding as only 3 deletions prevent L5-NPM interactions (Δ1-30, Δ20-50, and Δ180-210, Figure 15A). Examining export of newly synthesized ribosomes by the deletion mutants reveals both N-terminal as well as C-terminal regions to have an effect (figure 16). While not directly mirroring the protein interaction data, these findings show regions of NPM to be necessary for ribosome export. The reason for the disparity in results could be that the deletion mutants are not dominant negative in their actions and therefore cannot overcome wild type NPM in the cells. Taken together these data indicate that NPM oligomerization, which has been reported to be essential for NPM function (*17*), is

required for nuclear export and Crm1 binding, but no for ribosome (L5) interaction. However, more data is necessary to draw definitive conclusions.

Taken together these data provide evidence that ARF can regulate PEpC growth and proliferation through its interaction with NPM. The effects on the other ARF-interacting proteins will be explored, but as discussed below, due to the initial difficulties determining the signals required for transformation of the *Arf*$^{-/-}$ PEpC, these studies could not be completed.

Difficulties and actions taken

Due to the difficulty in transforming *Arf*$^{-/-}$ PEpC, I have not yet been able to assess the response of the ARF-interacting genes, *Mdm2*, *Bop1*, and *Npm* to true transforming signals in the prostate. Since my annual report, I finally have been able to transform the *Arf*$^{-/-}$ PEpC with a combination of Ras^{V12} and activated PI3K (PI3K^{E545K}, PI3K^{H1047R}). However, I have just obtained this data and could not perform the experiments to assess the effects on ARF-interacting genes before the writing of this final report. I have also not been able to complete the third task of the statement of work as I did not see the value of determining the effects of the ARF-interacting genes on PEpC cell growth and transformation when I could not determine the transforming signals initially. Now that I have the transforming upstream signals in hand I can begin to determine their effects on the expression of the ARF-interacting genes and form a more directed assessment of their affects on *Arf*$^{-/-}$ PEpC cell growth and proliferation. I have been able to prepare and validate NPM and BOP1 Real Time Primers and standard plasmids for quantifying mRNA levels (data not shown).

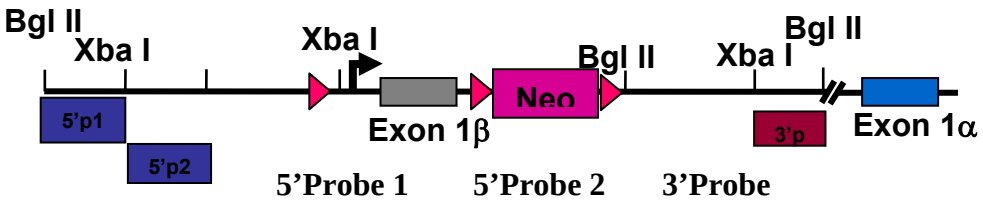

	5'Probe 1 Bgl II Digest	5'Probe 2 Xba I Digest	3'Probe Bgl ll Digest
Wild Type	**9100**	**4900**	**9100**
Neo/1β	**5400**	**2000**	**5400**
Δ Neo/1β	**3800**	**2000**	**5400**
Δ Neo/Δ 1β	**3000**	**4200**	**5400**
Neo/Δ 1β	**4600**	**5800**	**5400**

While I have tried to begin examining NPM and BOP1 protein levels in prostate tumor samples by immunohistochemistry, technical difficulties have prevent me from obtaining conclusive data. I have purchased new prostate tumor samples from Zymed in order to test new antibody dilutions.

I have continued to run into difficulty cloning the targeting vector for creation of the conditional *Arf* knockout mouse (see figure 17). I have been able to clone both homology arms individually into the targeting vector. However, all attempts to get the 2nd homology arm,

weather it be the 5' or 3' homology arm into the targeting vector have failed. The CpG island just 5' to Arf exon 1β is causing problems and results in the deletion of a portion of the 5'HA around exon 1β. Three other members of the lab have attempted the cloning reaction from beginning to end. I have attempted using several different bacterial cell lines (DH5a, JM109, XL10 Gold, ABLE C, and SCS110) some of which are defective in recombination genes or are purported to tolerate "toxic" plasmids. I have attempted to clone into two new targeting vectors since my previous report to no avail. I have begun to construct a new targeting vector and am in the process of cloning of the homology arms. I am using essentially the same strategy as described in my proposal, but will be inserting the Lox-Neo-Lox into the LoxP site 5' of Exon1β to hopefully disrupt the effects of the CpG island on the initial cloning. The extra LoxP site will be inserted at down stream of Exon1β where the Lox-Neo-Lox is currently depicted.

While doing this, I have begun a study to look at the effects of ARF loss on a conditional knockout model of prostate cancer. Work performed by Dr Henry Sucov's lab (*18*, *19*) shows that selective deletion of the RXRα results in PIN lesions but does not result in metastatic prostate cancer. I have received these RXRα floxed mice from Dr Sucov as well as the Pb-Cre mice from the NCI. I am breeding the Pb-Cre as well as the RXRα floxed mice onto the $Arf^{-/-}$ background and will then cross the Pb-Cre/$Arf^{-/-}$ mice to the $RXR\alpha^{fl/fl}/Arf^{-/-}$ mice to determine the effects of *Arf* loss on the progression and extent of disease in the mice. We have obtained the Pb-Cre/$Arf^{-/-}$ mice and are beginning to obtain litters of the $RXR\alpha^{fl/fl}/Arf^{-/-}$ mice.

KEY RESEARCH ACCOMPLISHMENTS

- Isolated and established wild-type and *Arf*$^{-/-}$ prostate epithelial cell lines.
- Wild-type prostate epithelial cells have limited proliferation in culture.
- *Arf*$^{-/-}$ prostate epithelial cells are immortal in culture, but not transformed.
- *Arf*$^{-/-}$ prostate epithelial cells maintain ploidy as well as an intact p53 response in culture.
- *Arf*$^{-/-}$ prostate epithelial cells make 4-fold more protein over a 24 h time course than wild-type cells.
- NPM is a potent transforming oncogene in the absence of *Arf* in Mouse Embryo Fibroblasts but not in Prostate Epithelial Cells.
- Ras^{V12} and PI3K activated mutants can combine to induce *Arf*$^{-/-}$ prostate epithelial cell transformation.
- The N-terminal oligomerization domain of NPM is necessary for proper NPM localization and influences NPM-mediated ribosome export.
- NPM is overexpressed in 82% and highly overexpressed in 44% of proliferating prostate adenocarcinomas.

- "Nucleophosmin is Essential for Ribosomal Protein L5 Nuclear Export", Yue *et al*. *Molecular and Cellular Biology* (2006) **26**:3798-3809.

- "TSC1 Sets the Rate of Ribosome Export and Protein Synthesis Through Increased Nucleophosmin Translation Pelletier *et al.* *Cancer Research* (2006) *Accepted for publication.*

- "Nucleophosmin Directs Ribosome Nuclear Export and Cell Growth", Maggi *et al*. Manuscript in preparation for submission to *EMBO Journal*.

- "ARF-null Prostate Epithelial Cell Transformation Requires PI3K Pathway Activation," *Maggi et al.* Manuscript in preparation for submission to *Cancer Research*.

REPORTABLE OUTCOMES

- "Nucleophosmin is Essential for Ribosomal Protein L5 Nuclear Export", Yue *et al*. *Molecular and Cellular Biology* (2006) **26**:3798-2809.
- "TSC1 Sets the Rate of Ribosome Export and Protein Synthesis Through Increased Nucleophosmin Translation", Pelletier *et al.* *Cancer Research* (2006) Accepted for publication.
- "What is the role of the ARF tumor suppressor in Prostate Tumorigenesis?" Oral Presentation at the Washington University Signaling/Cell Cycle Group (December 2004).
- "Regulation of Growth and Transformation by Nucleophosmin-mediated Ribosome Export" Invited Oral Presentation at the 2nd Annual Washington University Postdoc Symposium (February 2006).

- "Nucleophosmin Directs Ribosome Nuclear Export and Cell Growth" Co-Winner of Best Poster at the 1st Annual Washington University Signaling/Cell Cycle Retreat (April 2006).
- "Nucleophosmin Directs Ribosome Nuclear Export and Cell Growth" Poster presentation at the Mechanisms and Models of Cancer Meeting at Cold Spring Harbor Laboratories (August 2006).
- Creation and characterization of an *Arf*$^{-/-}$ prostate epithelial cell line.
- Creation and characterization of a NPM deletion mutant panel.
- Promotion from Postdoctoral Research Scholar to Research Instructor in Molecular Oncology at Washington University School of Medicine, St. Louis, MO.

CONCLUSIONS

The nucleolar tumor suppressor ARF plays an important role in the tumor surveillance of human cancer. We have found that ARF expression is absent from highly proliferative prostate adenocarcinomas and this correlates with the increased expression of the p53-independent target of NPM. We have created and characterized an immortalized ARF-null prostate epithelial cell line. In addition we have shown that alterations in NPM levels can have dramatic affects on the androgen-dependent cancer cell line, LNCaP, but not PC3 cells which are androgen-independent. We have previously shown that ARF inhibits NPM's nuclear export and cell cycle progression in a p53-indpendent manner. Under this proposal we have defined the mechanism by which this happens. Specifically, ARF binds to NPM preventing its ability to carry both small and large ribosomal subunits out of the nucleus. This results in a decrease in protein synthesis and growth rates contributing to ARF's tumor suppressor function. In addition we have shown that NPM expression level is controlled through an mTOR dependent pathway. One upstream activator of mTOR is PI3K, and we have shown that PI3K activation is required along with Ras pathway activation to transform *Arf*$^{-/-}$ prostate epithelial cells. We are beginning to further define the role of the ARF tumor suppressor pathway in prostate cell growth.

The promising result of PI3K combining with the Ras pathway to transform *Arf*$^{-/-}$ PEpC finally opens the door to examining the downstream targets of these pathways, namely the ARF-interacting proteins. Unfortunately these results come at the end of the grant period and the results cannot be given at this time. The examination of NPM has shed a new light on the possibility of the pathways controlling protein synthesis to be targeted for anticancer therapeutics.

While development of the conditional ARF knockout mouse continues, a parallel strategy has begun looking at the conditional knockout of known prostate cancer genes on the *Arf*-null background to determine *Arf*'s role if any in prostate cancer progression. A time consuming endeavor, the results are not yet known, but will provide more insight into the role of the ARF tumor suppressor pathway in prostate cancer.

This proposal was designed to investigate the role of the nucleolar tumor suppressor ARF in the development of prostate cancer. I have generated a substantial amount of data which is laying the foundation for future studies. I have isolated and characterized an immortal prostate epithelial cell line. In addition, I have defined a novel and very important mechanism for ARF-induced cell cycle arrest that is independent of p53. The role of NPM and protein synthesis in

prostate cancer is an exciting and emerging field of study which has also defined a pathway with promising therapeutic targets for prostate cancer treatment.

REFERENCES

1. A. Jemal *et al.*, *CA Cancer J Clin* **54**, 8 (January 1, 2004, 2004).
2. P. L. Fernandez, L. Hernandez, X. Farre, E. Campo, A. Cardesa, *Pathobiology* **70**, 1 (2002).
3. S. R. Downing, P. J. Russell, P. Jackson, *Can J Urol* **10**, 1924 (Aug, 2003).
4. C. J. Sherr, J. D. Weber, *Curr Opin Genet Dev* **10**, 94 (Feb, 2000).
5. S. N. Brady, Y. Yu, L. B. Maggi, Jr., J. D. Weber, *Mol Cell Biol* **24**, 9327 (Nov, 2004).
6. T. Kamijo, S. Bodner, E. van de Kamp, D. H. Randle, C. J. Sherr, *Cancer Res* **59**, 2217 (May 1, 1999).
7. T. Jacks *et al.*, *Curr Biol* **4**, 1 (Jan 1, 1994).
8. T. Kamijo *et al.*, *Cell* **91**, 649 (Nov 28, 1997).
9. J. D. Weber *et al.*, *Genes Dev* **14**, 2358 (Sep 15, 2000).
10. A. Y. Liu, L. D. True, *Am J Pathol* **160**, 37 (Jan, 2002).
11. B. J. Feldman, D. Feldman, *Nat Rev Cancer* **1**, 34 (Oct, 2001).
12. S. Tawfic, M. O. Olson, K. Ahmed, *J Biol Chem* **270**, 21009 (Sep 8, 1995).
13. S. Tawfic, S. A. Goueli, M. O. Olson, K. Ahmed, *Cell Mol Biol Res* **39**, 43 (1993).
14. D. H. Randle, F. Zindy, C. J. Sherr, M. F. Roussel, *Proc Natl Acad Sci U S A* **98**, 9654 (Aug 14, 2001).
15. L. C. Trotman *et al.*, *PLoS Biol* **1**, E59 (Dec, 2003).
16. S. J. Isakoff *et al.*, *Cancer Res* **65**, 10992 (Dec 1, 2005).
17. B. Y. Yung, P. K. Chan, *Biochim Biophys Acta* **925**, 74 (Jul 16, 1987).
18. J. Huang *et al.*, *Cancer Res* **62**, 4812 (Aug 15, 2002).
19. X. Wu *et al.*, *Mech Dev* **101**, 61 (Mar, 2001).

APPENDICIES

1. "TSC1 Sets the Rate of Ribosome Export and Protein Synthesis Through Increased Nucleophosmin Translation", Pelletier *et al. Cancer Research* (2006) Accepted for publication.

2. "Nucleophosmin is Essential for Ribosomal Protein L5 Nuclear Export", Yue *et al*. *Molecular and Cellular Biology* (2006) **26**:3798-2809.

3. "Nucleophosmin Directs Ribosome Nuclear Export and Cell Growth", Maggi *et al*. Submitted (2006).

4. Curriculum Vitae: Leonard B. Maggi, Jr., Ph.D.

SUPPORTING DATA

Figure 1. *Arf*$^{-/-}$ Prostate Cell Cultures.

Figure 2. *Arf*$^{-/-}$ Prostate Cells are Immortal not Transformed.

Figure 3. *Arf*$^{-/-}$ Prostate Cells are Epithelial Cells**.**

Figure 4. *Arf*$^{-/-}$ PEpC are Diploid.

Figure 5. *Arf*$^{-/-}$ PEpC Have an Intact p53 Response.

Figure 6. p19ARF Overexpression Inhibits *Arf*$^{-/-}$ PEpC Cell Cycle Progression.

Figure 7. Androgen Receptor Signaling is required for *Arf*$^{-/-}$ PEpC Growth.

Figure 8. PC3 Cell S Phase Progression Is Not Affected By NPM Shuttling.

Figure 9. LNCaP Cell S Phase Progression Is Affected By Inhibition of NPM Shuttling or High Expression of NPM.

Figure 10. *Arf* loss Increases Protein Synthesis Rates of PEpC.

Figure 11. *Arf*$^{-/-}$ PEpC Cannot Be Transformed.

Figure 12. *Arf*$^{-/-}$ PEpC Can Be transformed by Ras and PI3K mutants.

Figure 13. Loss of *Npm* Inhibits Ribosome Nuclear Export and Alters Nucleolar Morphology.

Figure 14. Expression and Localization of NPM Deletion Mutants.

Figure 15. Regions of NPM required for L5 and CRM-1 interaction.

Figure 16. Regions of NPM required for rRNA Export.

TSC1 Sets the Rate of Ribosome Export and Protein Synthesis Through Nucleophosmin Translation

Corey L. Pelletier[1], Leonard B. Maggi, Jr.[1], Suzanne N. Brady[1], Danielle K. Scheidenhelm[2], David H. Gutmann[2] and Jason D. Weber[1, 3]*

[1]Department of Internal Medicine, Division of Molecular Oncology, Siteman Cancer Center, Washington University School of Medicine, St. Louis, MO 63110, USA

[2]Department of Neurology, Washington University School of Medicine, St. Louis, MO 63110, USA

[3]Department of Cell Biology, Washington University School of Medicine, St. Louis, MO 63110, USA

Running Title: TSC1 regulates ribosome export through Nucleophosmin

Keywords: TSC1/translation/Nucleophosmin/ribosome/mTOR

* Please address correspondence to:
Jason D. Weber, Ph.D.
Department of Medicine
Division of Molecular Oncology
Washington University School of Medicine
Campus Box 8069
660 S. Euclid Avenue
St. Louis, MO 63110, USA
Tel: (314) 747-3896
Fax: (314) 747-2797
jweber@im.wustl.edu

ABSTRACT

Nucleophosmin (NPM/B23) is a nucleolar phosphoprotein that has been implicated in numerous cellular processes. In particular, NPM interacts with nucleolar components of newly synthesized ribosomes to promote ribosome nuclear export. NPM is a classic mitogen-induced protein, with changes in its expression correlating with growth factor stimulation. In this study, we examined the underlying mechanism of NPM induction and demonstrate that hyperproliferative signals emanating from oncogenic H-Ras^{V12} cause tremendous increases in NPM protein expression. NPM protein accumulation was dependent on mTOR activation, as rapamycin completely prevented NPM induction. Consistent with this finding, genetic ablation of *Tsc1*, a major upstream inhibitor of mTOR, resulted in NPM protein induction through increased translation of existing NPM mRNAs. Increases in NPM protein accumulation were suppressed by re-introduction of TSC1. Induction of NPM through *Tsc1* loss resulted in a greater pool of actively translating ribosomes in the cytoplasm, higher overall rates of protein synthesis and increased cell proliferation, all of which were dependent on efficient NPM nuclear export. NPM protein accumulation in the absence of *Tsc1* promoted the nuclear export of maturing ribosome subunits, providing a mechanistic link between TSC1/mTOR signaling, NPM-mediated nuclear export of ribosome subunits, protein synthesis levels, and cell growth.

INTRODUCTION

NPM/B23 is a 38-kilodalton protein localized to the granular regions of the nucleolus (1). Numerous studies have linked NPM to cell proliferation (2-6). Activation of murine lymphocytes and immortalized fibroblasts by various growth factors is associated with a rapid and prominent increase in NPM protein expression (3). In addition, NPM is present at elevated levels in various lymphoma and malignant cell lines, correlating NPM protein induction with the transduction of mitogenic signals (2). Recent knock-out studies have revealed that NPM is essential for embryonic development, specifically for proper development of the central nervous and hematopoetic systems (7, 8). Moreover, loss of NPM greatly diminishes cell growth and proliferation, underscoring its critical role in these two processes (6, 7).

In addition to its role in mitogenesis and embryonic development, NPM has been recognized as having roles in protein chaperoning (9), regulation of p53 (10), and centrosome duplication (7, 11). Additionally, NPM binds nucleic acids (12-14), cleaves pre-rRNA (15), and associates with maturing pre-ribosomal ribonucleoprotein particles in the nucleolus (16), promoting rRNA processing. Based on these activities and its localization in the nucleolus, NPM has been implicated as a critical regulator of the general process of ribosome biogenesis. In eukaryotic cells, ribosome biogenesis is a highly coordinated multi-step process that begins in the nucleolus (17). During rRNA processing, the rRNA particles associate with numerous ribosomal proteins and the 5S rRNA to assemble the large (L, 60S) and small (S, 40S) ribosomal subunits, which are then transported to the cytoplasm and assembled with nascent mRNAs to direct protein synthesis (18). Recent findings from our lab have demonstrated that NPM interacts

directly with maturing ribosomal subunits and aids in their efficient nuclear export (19), placing NPM in a key position to relay growth cues to protein synthesis.

Appropriate regulation of ribosome biogenesis and translation is necessary to maintain accurate cellular growth and proliferation. A key signaling component known to regulate growth, at least in part, by coordinating protein biosynthesis, is the mammalian target of rapamycin (mTOR). TOR is an evolutionarily conserved protein serine-threonine kinase that controls translation efficiency, cell cycle progression and ribosomal biogenesis through its ability to integrate nutrient and mitogenic signals (20). When complexed with its cellular receptor FK-506-binding protein 12, the immunosuppressive drug rapamycin directly binds to mTOR (21). This inhibits mTOR-dependent downstream signaling, resulting in delayed cell cycle progression in most cell types (22). Recent insight into upstream regulators of mTOR have revealed a tumor suppressor complex composed of two proteins, TSC1 and TSC2, that functions by acting as a GAP for mTOR's activator, Rheb, a Ras-like protein (23-26). In patients with TSC, loss of either *Tsc1* or *Tsc2* gene expression leads to hyperactivation of the mTOR pathway, and results in the widespread formation of benign and malignant tumors.

To understand how growth signals are relayed to the ribosome biogenesis machinery, we hypothesized that NPM might act as a key nucleolar sensor of growth signals. Indeed, NPM protein levels increased in response to proliferative signals and this induction was regulated not at the level of transcription, but rather solely at the translational level. We also found that induction of NPM by growth signals was sensitive to rapamycin, clearly placing NPM translation downstream of mTOR activation. Additionally, we demonstrate that the TSC1 protein is a critical regulator of this pathway,

with loss of *Tsc1* promoting dramatic increases in NPM protein, thereby leading to an increased pool of actively translating ribosomes and a higher overall rate of protein synthesis. These processes were dependent on functional NPM, firmly establishing NPM at the interface between TSC function and ribosome biogenesis.

MATERIALS AND METHODS

Cell Culture and Reagents – Low-passage (3-6) primary MEFs (ArtisOptimus, Carlsbad, CA) were established and maintained as described (27). *Tsc1*$^{-/-}$*/p53*$^{-/-}$ MEFs were isolated as previously described (28). Quiescence was achieved by maintaining cells that were ~30% confluent in media containing 0.1% fetal bovine serum for 48 hours. Cells were stimulated with either human recombinant PDGF-BB (Calbiochem) (10 ng/mL) or 10% fetal bovine serum. LY294002, and rapamycin (Cell Signaling Technology) were used at final concentrations of 15 μM and 100 nM, respectively. Total RNA was isolated using Trizol following the manufacturer's specifications.

Plasmid Constructs – pBabe-H-RasV^{12} was a gift from Martine Roussel (St. Jude Children's Research Hospital). His-NPM and His-NPMdL constructs (19) were subcloned into the retroviral pSRα-MSCV-tkNEO plasmid for production of retrovirus as previously described (6). Full-length human *TSC1* cDNA cloned into the MSCV retroviral vector was used to express TSC1 in *Tsc1*/*p53*$^{-/-}$ MEFs. pRK7-HA-S6K1 and pRK7-3HA-eIF4E were provided by John Blenis (Harvard University).

Viral Production and Infection – Collected retrovirus (6) was used to infect target cells for 1-5 days in the presence of 10 μg/ml polybrene (Sigma). For pBabe.puro retroviral vector infections, MEFs were selected in 2.0 μg/ml puromycin. For pSRα retroviral vector infections, MEFs were selected in 0.8 mg/ml G418. The efficiency of infections was generally 100% as assessed by puromycin or G418 selection and β-galactosidase staining. For the production of lentiviruses encoding shRNAs targeting either luciferase

or NPM, 293Ts were transfected with Fugene 6, using a three-plasmid system: pHCMV.G (envelope), CMVΔR8.2 (packaging) and either pFLRu-YFP-shLuc or pFLRu-YFP-shNPM. The following oligos (hairpin loop in italics, antisense in bold) were annealed and cloned into the pFLRu-YFP vector (Y. Feng and G. Longmore, unpublished, Washington University), to yield shRNAs targeting the 3'UTR of NPM: 5'-GCCAAGAATGTGTTGTCAAA*TTCAAGAGA***TTAGACAACACATTCTTGGC**TTT TT-3' (forward oligo) 3'-CGGTTCTTACACAACAGTTT*AAGTTCTCT***AATC TGTTGTGTAAGAACCG**AAAAA-5' (reverse oligo). MEFs were infected for four hours with lentiviral-containing culture media, supplemented with 8 μg/ml protamine sulfate. MEFs were cultured in the presence of 2 ug/ml puromycin for 48 hours. Following puromycin selection, the cells were trypsinized, counted and re-plated for subsequent western blot, growth curve, foci formation and soft-agar assays.

Western Blots –Harvested cells were resuspended and sonicated in lysis buffer (50 mM Tris-HCl, pH 7.4, 120 mM NaCl, 0.5% NP-40, 1 mM EDTA, pH 7.4, 10 μg/ml aprotinin, phosphatase inhibitors, and 0.5 mM phenylmethylsulfonyl fluoride). Proteins (100 μg) were separated on 10-12.5% SDS-containing polyacrylamide gels. Separated proteins were transferred to polyvinylidene difluoride membranes (Millipore, Boston, MA). Membranes were probed with the following antibodies: γ-tubulin, cyclin D1, NPM, Ras, HA and His (Santa Cruz Biotechnology); AKT, phospho-AKT (Thr^{308}), TSC1, and phospho-S6 (Cell Signaling Technology). Sheep anti-goat (Zymed), goat anti-rabbit and goat anti-mouse (Bio-Rad) IgG (H+L) horseradish peroxidase conjugates were added as

the secondary antibodies and specific protein bands were visualized using ECL (Amersham).

Northern blot analysis- Total RNA (8-10 μg) was denatured and fractionated by gel electrophoresis using a 1% agarose gel containing 2.2 M formaldehyde. RNA was transferred by capillary action in 10X SSPE (1.5M NaCl, 100mM NaH_2PO_4, 10mM EDTA, pH 7.4) to Hybond-NX Membrane (Amersham). The membrane was cross linked with a Hoeffer UV autolinker and stained with methylene blue for visualization of 18S and 28S RNAs. Membranes were blocked with Rapidhyb Buffer (Amersham) containing 100 μg/ml salmon sperm DNA (Sigma) for 1 hour at 65˚C before hybridization to a ^{32}P-labeled probe specific for NPM in Rapidhyb Buffer with 100 μg/ml salmon sperm DNA for 4 hours at 65˚C. Membranes were washed once with 2X SSC (0.3M NaCl, 30mM sodium citrate, pH 7.0)/0.1% SDS at room temperature for 20 minutes, and twice with 1X SSC/0.1%SDS at 65˚C for 15 minutes. Gels were autoradiographed at -80˚C with intensifying screens. Methylene Blue-stained 18S and 28S rRNAs were used as internal loading controls.

The complete mouse NPM cDNA (accession number M33212) was used as a probe and was radiolabeled with [α-^{32}P]dCTP by random priming using the rediprime II kit (Amersham) according to the manufacturer's specifications.

Labeling of Cellular Protein with ^{35}S-Methionine and Immunoprecipitation of NPM - $1x10^5$ cells were seeded in six-well plates in triplicate, cultured in DMEM without methionine (GIBCO) for 30 min and incubated in the presence of 100 μCi [^{35}S]-protein

labeling mix (Amersham) for various time points. Cells were washed twice with phosphate-buffered saline and lysed with 1% Triton X-100 PBS buffer. For the ^{35}S-methionine incorporation assay, total protein was precipitated from lysates with 10% trichloroacetic acid and pelleted. Pellets were subjected to liquid scintillation counting to measure incorporated cpm. For NPM pulse label experiments, NPM proteins were immunoprecipitated from 500 μg total cellular protein lysates with a monoclonal antibody recognizing NPM (Zymed) and Protein A/G Sepharose. Precipitated NPM proteins were separated by SDS-PAGE and detected by autoradiography.

Ribosome fractionation - $3x10^6$ cells were treated with 50 μg/ml cyclohexamide for 10 minutes prior to trypsinization and lysis, and fractionation was carried out over a 10-45% sucrose gradient in a Beckman SW41 rotor at 36,000 rpm. Gradients were fractionated and RNA absorbance at 254 nm was continuously monitored to detect ribosomal subunits.

Subcellular fractionation – Equal numbers of wild-type MEFs were resuspended in HEPES buffer (10 mM HEPES, pH 7.4 with 4 mM $MgCl_2$, 1 mM PMSF, 10 μg/ml leupeptin, 10 μg/ml aprotinin, 1 μg/ml pepstatin, 1 mM NaF, 10 mM $NaVO_4$, β-glycerophosphate) followed by passage (15x) through a 25-guage needle. Lysed cells were pelleted and the supernatant was saved as the cytoplasmic fraction. The pellet was resuspended in fractionation buffer (10 mM Tris pH 7.5, 10 mM NaCl, 1 mM EDTA, 0.5 mM EGTA, 4 mM $MgCl_2$, 1 mM PMSF, 10 μg/ml leupeptin, 10 μg/ml aprotinin, 1 μg/ml pepstatin), dounced (20x) with a B pestle, layered over a 1 ml cushion of sucrose (45%

w/v in fractionation buffer), and centrifuged. The pellet was washed three times by overlaying the pellet with ddH_2O and centrifuging. The pellet was resuspended in TRIZOL (Invitrogen).

Ribosomal RNA Export – MEFs were infected with retroviruses encoding His-NPM or His-NPMdL and incubated at 48 h at 37°C after infection. Cells were incubated in methionine-free media for 15 min and labeled with 50 μCi/ml L-[methyl-^{3}H]-methionine (Amersham Biosciences) for 30 min. The radiolabel was washed away and the cells incubated in a 10-fold excess of cold methionine-containing media for 2 hours. Cells ($2x10^6$) were harvested, counted, and equal numbers of cells were fractionated into cytoplasm and nuclei as described above. Total RNA was isolated from the cytosolic and nuclear fractions with TRIZOL, and fractionated by gel electrophoresis using a 1% agarose gel containing 2.2M formaldehyde. RNA was transferred by capillary action in 20X SSC to Hybond-NX Membrane. The membrane was cross-linked, sprayed with EN^{3}HANCE Spray (Perkin Elmer) and subjected to autoradiography.

Foci Formation and Proliferation Assays - Tsc1$^{-/-}$/p53$^{-/-}$ MEFs were infected with control or His-NPMdL retroviruses, and siLuciferase or siNPM lentiviruses. For foci formation, cells were seeded (1.5×10^3) on 100 mm dishes, grown for 12 days in complete medium, fixed in 100% MeOH and stained for 10 min with Giemsa (Sigma). To assay proliferation, infected cells were seeded (1×10^4) in triplicate wells of a 6-well plate and counted once a day over the course of 6 days.

Densitometry and Image Analysis – Autoradiograms were scanned using a FluoroChem8900 (Alpha Innotech), and densities were determined using NIH ImageJ version 1.33 software.

RESULTS

NPM Protein is Induced by Serum, PDGF and H-Ras^{V12} in an LY294002-Sensitive Manner.

To investigate whether NPM protein expression is associated with proliferation of low passage wild-type mouse embryonic fibroblasts (MEFs), cells were synchronized in G0 by serum deprivation, and then induced to enter the cell cycle simultaneously by addition of serum (FBS) (29). Cyclin D1 expression increased upon serum stimulation, indicating that the wild-type MEFs were successfully synchronized in G0 and simultaneously induced to enter the cell cycle (Fig. 1A, G1/S transition is at 12 hours for MEFs) (30). A three-fold increase in NPM protein was observed by 8 hours after serum stimulation, with levels peaking at a six-fold increase 24 hours post-stimulation. The heterogeneous nature of serum signaling presents a significant barrier in defining the upstream activator or activators of NPM induction. Thus, in an effort to more clearly define a growth factor signaling pathway, platelet-derived growth factor (PDGF) was used to stimulate cells into cell cycle entry. Once again, low passage wild-type MEFs were starved of mitogen to synchronize them and subsequently driven into cycle by the addition of PDGF. PDGF induced cellular proliferation as well as a significant induction of NPM protein expression (Fig. 1A). Because H-Ras is a common activator of a multitude of PDGF- and serum-stimulated signaling pathways, (31, 32), we tested whether expression of a constitutively-active H-Ras (Ras^{V12}) would increase expression of NPM in wild-type MEFs. Upon 48 hours of Ras^{V12} expression, NPM protein was significantly induced (10-fold, Fig. 1B).

In an attempt to define which pathway downstream of growth factor activation was responsible for NPM induction, pharmacological inhibition was used to block PI-3-kinase and ERK signals. Wild-type MEFs were serum-starved and then released into cycle by serum stimulation in the presence and absence of inhibitor. LY294002, an inhibitor of the PI-3-kinase pathway (33, 34), significantly blocked NPM expression after serum stimulation (Fig. 1C) while addition of UO126 did not affect NPM protein expression (data not shown). Unphosphorylated AKT was used as a loading control and phospho-AKT (Thr-308) demonstrated that PI-3-kinase, which phosphorylates AKT at this site (35), was effectively inhibited by LY294002 (Fig. 1C). Given that serum-induced expression of NPM is sensitive to LY294002, we tested whether Ras^{V12}-induced increases in NPM protein expression were sensitive as well. LY294002 was added to both empty vector and Ras^{V12}-infected MEFs, and samples were collected 48 hours post-infection. As expected, LY294002 caused NPM levels to decrease in asynchronously growing, vector-infected cells (Fig. 1D). In addition, the presence of LY294002 significantly inhibited the Ras^{V12}-induced increase in NPM protein expression (Fig. 1D), demonstrating that both mitogenic and oncogenic stimulation of NPM protein expression are sensitive to PI-3K inhibition.

Rapamycin Decreases NPM Levels in Asynchronously Growing and Ras^{V12}-Infected Cells.

In order to assess the role of downstream PI-3K effectors, specifically mTOR, in regulating NPM protein induction, we employed the selective mTOR inhibitor, rapamycin (Rap). Addition of rapamycin to wild-type MEFs grown in serum caused a

dramatic decrease in NPM protein expression (Fig. 2A). Levels of phosphorylated S6, a downstream target of mTOR activity, also declined in the presence of rapamycin, as expected (36) (Fig. 2A). We next tested whether rapamycin was able to block NPM induction in response to oncogenic Ras^{V12}. Similar to results observed in asynchronous cells growing in serum, western blot analysis demonstrated that NPM protein induction by oncogenic Ras^{V12} was sensitive to rapamycin treatment (Fig. 2B).

NPM mRNA is Unaffected by Serum, Ras^{V12}, or Rapamycin.

To investigate whether changes in NPM mRNA induction were responsible for the observed increases in NPM protein expression, low-passage wild-type MEFs were synchronized by serum starvation and subsequently induced to proliferate by serum addition. RNA was isolated post-stimulation and subjected to northern blot analysis. Staining of 18S and 28S rRNA was performed to ensure equal loading of total RNA (Fig. 3A). Surprisingly, although NPM protein levels increased upon serum stimulation (Fig. 1A), NPM mRNA levels remained constant (Fig. 3A). In addition to the northern blot, parallel cells at identical time points were harvested for western blot analysis of cyclin D1 to ensure successful synchronization and release into the cell cycle (Fig 3A) (29).

To determine whether NPM mRNA levels responded to oncogenic stimuli, wild-type MEFs were retrovirally infected with Ras^{V12}. Even though NPM protein levels were elevated at this time point (Fig. 1B), mRNA levels again remained unchanged (Fig. 3B). We next tested whether NPM mRNA levels were sensitive to rapamycin by treating Ras^{V12}-infected MEFs for 48 hours. Although our earlier results demonstrated that Ras^{V12}-induced NPM protein expression was sensitive to rapamycin treatment (Fig. 2B),

rapamycin had no effect on NPM mRNA expression in the presence of Ras^{V12} (Fig. 3B). Notably, addition of the proteasome inhibitor MG132 had no appreciable effect on NPM protein expression levels, indicating that protein stability was not a major cause for the observed increases in NPM protein levels (data not shown). Taken together, these data indicate that NPM mRNA levels remain constant regardless of stimulation or treatment, suggesting that overall regulation of NPM protein expression is regulated posttranscriptionally through a mechanism independent of protein stability.

TSC1 Regulates the Translation of NPM mRNAs.

Given our finding that NPM protein is positively regulated by growth factors and that this effect is abrogated upon treatment with rapamycin, we hypothesized that NPM levels would be elevated in cells with a hyperactive mTOR pathway. Recent studies in both *Drosophila* and mammalian systems have shown that the TSC1/TSC2 complex functions upstream of mTOR in the PI-3K pathway to suppress cell growth and proliferation (37-40). Primary MEFs lacking either component of the complex initially proliferate faster than their wild-type counterparts, but ultimately undergo premature senescence in a p53-dependent manner (28). Loss of p53 rescues the premature senescence, and MEFs lacking both *Tsc1* and *p53* exhibit greater growth rates than those lacking p53 alone (28). Consistent with these observations, we observed a 20-fold increase in NPM protein expression in $Tsc1^{-/-}/p53^{-/-}$ MEFs, compared to only modest increases in the absence of *p53* alone (Fig. 4A). The addition of rapamycin inhibited the increase in NPM protein expression observed in $Tsc1^{-/-}/p53^{-/-}$ cells (Fig. 4B, left panel), consistent with current models placing the TSC signaling complex upstream of mTOR. Re-expression of TSC1

in *Tsc1*$^{-/-}$/*p53*$^{-/-}$ cells reduced NPM protein expression below basal expression levels (Fig. 4B, right panel), indicating that TSC1 is a potent suppressor of NPM protein expression.

Inactivation of the TSC1/TSC2 complex results in mTOR activation and leads to phosphorylation of two main mTOR substrates, the eukaryotic initiation factor 4E binding protein-1 (4E-BP1) and the ribosomal S6 kinase (S6K). These two mTOR-dependent cascades stimulate mRNA translation through distinct mechanisms to coordinate overall protein synthesis in the cell (41, 42). To investigate whether these downstream mTOR targets regulate NPM protein expression, wild-type MEFs were transduced with constructs encoding wild-type eIF4E and S6K1. Western blot analysis demonstrated that NPM was induced upon overexpression of S6K1, but was unaltered by eIF4E transduction (Fig. 4C), implying that directed translation by S6K could provide a mechanism for NPM protein regulation. To follow up on this result, we performed a pulse-label analysis to assess the rates of NPM translation in wild-type cells versus those lacking *p53* or *Tsc1*$^{-/-}$/*p53*$^{-/-}$. Our results demonstrate that *p53*$^{-/-}$ cells exhibit a similar rate of NPM translation as wild-type cells, but that cells lacking *Tsc1*$^{-/-}$/*p53*$^{-/-}$ synthesize more NPM in the same time period and at an accelerated rate (Fig. 4D). Importantly, the increases in NPM translation seen in the absence of *Tsc1* were abolished with rapamycin (Fig. 4D). These data demonstrate that, in the absence of *Tsc1*, NPM mRNA translation is significantly increased, resulting in dramatic accumulation of NPM proteins.

MEFs Lacking *Tsc1* Have More Polysomes and a Higher Rate of Overall Protein Synthesis than Their Wild-type Counterparts.

Previous findings from our lab have shown that NPM is required for the nucleolar/nuclear export of 28S, 18S, 5.8S and 5S ribosomal RNAs (rRNA) in cells, and that NPM is rate-limiting in this process, with increases in NPM protein expression amplifying the amount of cytosolic ribosomes available for mRNA translation (19)(Maggi and Weber, unpublished observations). Given that NPM levels are higher in cells lacking *Tsc1*, we hypothesized that *Tsc1*$^{-/-}$ cells would also exhibit a larger pool of actively translating ribosomes. To test this, ribosomal profiles were generated for wild-type, *Tsc1*$^{-/-}$*/p53* $^{-/-}$, or *p53*$^{-/-}$ MEFs. mRNAs that are being actively translated have variable numbers of ribosomes associated with them, forming large structures called polysomes. These polysomes can be separated from inactive 40S, 60S, and 80S subunits by sucrose gradient densities and detected by RNA absorption at 254 nm. Our findings demonstrate that *Tsc1*$^{-/-}$*/p53*$^{-/-}$ MEFs have significantly more actively translating ribosomes than wild-type MEFs and that this difference is nearly 50% greater than *p53* loss alone (Fig. 5A). The larger polysomal fraction in MEFs expressing higher levels of NPM protein is consistent with our previous finding that overexpression of NPM causes a similar increase in polysomes (Maggi and Weber, unpublished observations).

In order to determine whether the increased polysomal fraction in MEFs lacking *Tsc1* exhibited increased overall protein synthesis, newly synthesized proteins were labeled over time to measure protein synthesis rates. The results from this experiment are consistent with our polysome profiles in that *Tsc1*$^{-/-}$*/p53*$^{-/-}$ cells exhibited the greatest amount of overall protein synthesis compared to equal numbers of *p53*$^{-/-}$ and wild-type MEFs (Fig. 5B).

Expression of a Dominant-Negative NPM Reverses the Effects of *Tsc1* Loss on Ribosome Biogenesis and Cell Proliferation.

To more directly test the hypothesis that higher levels of NPM protein expression caused the increased polysome fractions and greater rates of protein synthesis in MEFs lacking *Tsc1*, we employed a previously described mutant of NPM (NPMdL) that lacks the ability to shuttle ribosomes between the nucleus and cytoplasm and acts in a dominant negative fashion by forming hetero-oligomers with wild-type NPM molecules (19). As seen previously, the polysomal fraction was significantly larger in *Tsc1*$^{-/-}$*/p53*$^{-/-}$ MEFs relative to wild-type cells. However, retroviral introduction of NPMdL into *Tsc1*$^{-/-}$*/p53*$^{-/-}$ MEFs lowered the polysome peaks below the baseline of wild-type cells (Fig 6A), demonstrating that NPM function is a rate-limiting factor for the larger pool of actively translating ribosomes observed in MEFs lacking *Tsc1*.

To further investigate the mechanism behind the extremely low levels of 40S, 60S, 80S and polysomes in the cytoplasm of *Tsc1*$^{-/-}$*/p53*$^{-/-}$ MEFs overexpressing the NPMdL mutant, we decided to examine the ribosomal nuclear export rates in the presence or absence of the dominant negative NPM in wild-type and *Tsc1*$^{-/-}$*/p53*$^{-/-}$ MEFs. Consistent with our previous findings (19)(Maggi and Weber unpublished observations), expression of the NPMdL mutant prevented a majority of newly synthesized ribosomal RNAs from being exported into the cytoplasm in wild-type and MEFs (Figure 6B, lanes 1 and 3). In *Tsc1*$^{-/-}$*/p53*$^{-/-}$ MEFs, a tremendous increase was observed in rRNA export compared to wild-type cells (Figure 6B, lanes 1 and 5) and this increase was greatly diminished in the presence of the NPMdL mutant, indicating that increased rRNA nuclear export in the absence of *Tsc1* required functional NPM proteins.

To determine whether the loss of ribosome export had an effect on the hyperproliferative phenotype of *Tsc1*$^{-/-}$/*p53*$^{-/-}$ MEFs, cells were infected with retroviruses encoding NPMdL mutants and assayed for cell proliferation. Consistent with the correlation between increased NPM shuttling activity and loss of *Tsc1*, ectopic expression of NPMdL severely attenuated short-term (Fig. 6C, graph panel) and long-term (Fig. 6C, foci panel) proliferation of *Tsc1*$^{-/-}$/*p53*$^{-/-}$ MEFs. These data indicate a requirement for increased NPM nuclear export of newly synthesized ribosomes to maintain the proliferative advantage of cells lacking *Tsc1*. Additionally, reduction of NPM protein expression to nearly wild-type levels using siRNAs targeting NPM in *Tsc1*$^{-/-}$/*p53*$^{-/-}$ MEFs (Fig. 6D, inset) resulted in nearly identical reductions in *Tsc1*$^{-/-}$/*p53*$^{-/-}$ MEF short and long-term proliferation (Fig. 6D). Together, these findings imply a crucial role for both increased NPM protein expression levels and shuttling activity in setting the proliferative capacity of cells lacking *Tsc1*.

DISCUSSION

Nucleophosmin (NPM/B23) is a multifunctional nucleolar protein involved in the processes of ribosome assembly, nucleocytoplasmic shuttling, and cellular proliferation (2, 4-6, 10, 43-45). Consistent with NPM's role in promoting proliferation are the findings that reduced NPM protein expression in primary mouse embryonic fibroblasts or genetic ablation of *Npm1* in the mouse germline causes severe defects in cell cycle progression and cellular growth (6, 7). These findings point to an active role for NPM in promoting cell cycle progression and replace the adage that NPM protein levels are passive indicators of cell proliferation. NPM has positioned itself as a critical mediator of cell cycle progression and as an essential integrator of growth-promoting signals. Additionally, its nucleolar localization reinforces the idea that the nucleolus itself is a critical sensor of growth and proliferation (46). Here, we extend these findings and show that NPM protein expression is induced upon stimulation with mitogenic factors to demonstrate that NPM functions as a nucleolar growth factor sensor (47).

Given our observations that NPM protein expression is induced upon stimulation with growth factors, it was not surprising to find that NPM protein levels increased upon overexpression of oncogenic Ras^{V12} or loss of *Tsc1* (hyperactive mTOR signaling). However, increases in NPM protein in response to hyperactive mTOR signals were not the result of increased mRNA induction, but were instead the result of dramatic increases in protein translation. This suggests that NPM levels are tightly controlled by the cell: a pool of extremely stable mRNA exists whether serum is present or not and a direct, immediate mechanism is employed by the cell to induce high levels of NPM protein expression under either growth or hyperproliferative signals.

While much has been elucidated concerning mitogen-activated signaling pathways and their ability to stimulate cell cycle progression (through induction of cyclins), little is known about how these proliferative signals might also be interpreted by the nucleolus to appropriately couple pro-growth signals to the protein synthesis machinery. We found that induction of NPM, a nucleolar protein important for ribosome export, is sensitive to rapamycin, demonstrating mTOR regulation of NPM expression. Importantly, this finding now provides a mechanistic link between mTOR signaling and regulation of nucleolar processes capable of modulating protein synthesis. Increasing evidence in mice and humans points to a more direct role of aberrant mTOR signaling in promoting tumorigenesis, specifically, linking the disruption of mTOR-mediated translation to alterations in the cell cycle and cell growth (48). For example, the Tuberous Sclerosis Complex inherited cancer syndrome is caused by germline mutations in either the *Tsc1* or *Tsc2* gene (49). Interestingly, we have demonstrated that genetic ablation of *Tsc1* not only causes NPM protein to accumulate, but has the biological consequence of promoting nucleolar/nuclear export of maturing ribosomal subunits, increasing the cytoplasmic pool of translating ribosomes and elevating the overall levels of protein synthesis. Our findings imply participation of the mTOR pathway in determining the rate of ribosome export through its effects on NPM translation rates and place the TSC1/TSC2 complex in an important position to actively suppress ribosome biogenesis (through NPM downregulation). Interestingly, much work has shown that mTOR regulates ribosome biogenesis by controlling the transcription of Pol-I-dependent rRNA and Pol-II-dependent ribosomal protein genes (50). Here we demonstrate that

mTOR modulates ribosome biogenesis not only by regulating rRNA synthesis, but also by controlling NPM-induced ribosome nuclear export.

As an essential mediator of G1 progression, NPM functions as a key nucleolar growth factor sensor, one that readily responds to growth factor or oncogenic signals relayed by mTOR. NPM's responsiveness to mTOR activity places it in an ideal position to control mTOR-dependent increases in protein translation. Likewise, given its ability to increase proto-oncogenic NPM protein levels, mTOR then establishes a direct growth target that might help explain its ability to stimulate tumor formation. With ribosome processing and export originating in the nucleolus and being obvious targets in the transition from normal to tumorigenic cell states, it has been difficult to imagine how mTOR signals might gain access to this isolated subcellular compartment to stimulate increases in this process or how the TSC1/TSC2 complex might perform tumor suppressive functions. The ability of NPM to sense increased mTOR activity in the absence of TSC1/2 suppression provides a novel link between the growth signals that ultimately increase protein synthesis in proliferating cells and the trafficking protein that increases ribosome output from the nucleolus.

ACKNOWLEDGEMENTS

The authors would like to thank Sheila Stewart, Martine Roussel, Charles Sherr and Greg Longmore and for plasmid constructs and antibodies. We are extremely grateful to J. Alan Diehl, Joe Baldassare, Howard McLeod, Usha Andley, Greg Longmore and Ken Blumer for insightful discussions.

C.L.P. is supported by funds from The Lucille P. Markey Special Emphasis Pathway in Human Pathobiology. L.B.M. is supported by the Department of Defense Prostate Cancer Research Program under award number W81XWH-04-0909. D.K.S. is supported by a National Research Service Award (Medical Scientist 5 T32 GM07200). Views and opinions of, and endorsements by the author(s) do not reflect those of the US Army or the Department of Defense. This work is supported in part by a grant from the National Cancer Institute (U01-CA84314) to D.H.G. J.D.W. thanks the Pew Charitable Trusts and is a recipient of grants-in-aid from the Susan G. Komen Breast Cancer Foundation, and National Institutes of Health (GM066032).

REFERENCES

1. Wang D, Umekawa H, Olson MO. Expression and subcellular locations of two forms of nucleolar protein B23 in rat tissues and cells. Cell Mol Biol Res 1993;39:33-42.
2. Feuerstein N, Mond JJ. "Numatrin," a nuclear matrix protein associated with induction of proliferation in B lymphocytes. J Biol Chem 1987;262:11389-97.
3. Feuerstein N, Chan PK, Mond JJ. Identification of numatrin, the nuclear matrix protein associated with induction of mitogenesis, as the nucleolar protein B23. Implication for the role of the nucleolus in early transduction of mitogenic signals. J Biol Chem 1988;263:10608-12.
4. Chan WY, Liu QR, Borjigin J, et al. Characterization of the cDNA encoding human nucleophosmin and studies of its role in normal and abnormal growth. Biochemistry 1989;28:1033-9.
5. Jiang PS, Yung BY. Down-regulation of nucleophosmin/B23 mRNA delays the entry of cells into mitosis. Biochem Biophys Res Commun 1999;257:865-70.
6. Brady SN, Yu Y, Maggi LB, Jr., et al. ARF impedes NPM/B23 shuttling in an Mdm2-sensitive tumor suppressor pathway. Mol Cell Biol 2004;24:9327-38.
7. Grisendi S, Bernardi R, Rossi M, et al. Role of nucleophosmin in embryonic development and tumorigenesis. Nature 2005;437:147-53.
8. Colombo E, Bonetti P, Lazzerini Denchi E, et al. Nucleophosmin Is Required for DNA Integrity and p19Arf Protein Stability. Mol Cell Biol 2005;25:8874-86.
9. Okuwaki M, Matsumoto K, Tsujimoto M, et al. Function of nucleophosmin/B23, a nucleolar acidic protein, as a histone chaperone. FEBS Lett 2001;506:272-6.
10. Colombo E, Marine JC, Danovi D, et al. Nucleophosmin regulates the stability and transcriptional activity of p53. Nat Cell Biol 2002;4:529-33.
11. Okuda M, Horn HF, Tarapore P, et al. Nucleophosmin/B23 is a target of CDK2/cyclin E in centrosome duplication. Cell 2000;103:127-40.
12. Hingorani K, Szebeni A, Olson MO. Mapping the functional domains of nucleolar protein B23. J Biol Chem 2000;275:24451-7.
13. Feuerstein N, Mond JJ, Kinchington PR, et al. Evidence for DNA binding activity of numatrin (B23), a cell cycle-regulated nuclear matrix protein. Biochim Biophys Acta 1990;1087:127-36.
14. Wang D, Baumann A, Szebeni A, et al. The nucleic acid binding activity of nucleolar protein B23.1 resides in its carboxyl-terminal end. J Biol Chem 1994;269:30994-8.
15. Herrera JE, Savkur R, Olson MO. The ribonuclease activity of nucleolar protein B23. Nucleic Acids Res 1995;23:3974-9.
16. Okuwaki M, Tsujimoto M, Nagata K. The RNA binding activity of a ribosome biogenesis factor, nucleophosmin/B23, is modulated by phosphorylation with a cell cycle-dependent kinase and by association with its subtype. Mol Biol Cell 2002;13:2016-30.
17. Hadjiolov AA. The nucleolus and ribosome biogenesis. New York: Springer-Verlag;1984.
18. Johnson AW, Lund E, Dahlberg J. Nuclear export of ribosomal subunits. Trends Biochem Sci 2002;27:580-5.

19. Yu Y, Maggi LB, Brady SN, et al. Nucleophosmin is essential for ribosomal protein L5 nuclear export. Mol Cell Biol 2006;26:3798-809.
20. Fingar DC, Blenis J. Target of rapamycin (TOR): an integrator of nutrient and growth factor signals and coordinator of cell growth and cell cycle progression. Oncogene 2004;23:3151-71.
21. Brown EJ, Schreiber SL. A signaling pathway to translational control. Cell 1996;86:517-20.
22. Hashemolhosseini S, Nagamine Y, Morley SJ, et al. Rapamycin inhibition of the G1 to S transition is mediated by effects on cyclin D1 mRNA and protein stability. J Biol Chem 1998;273:14424-9.
23. Inoki K, Li Y, Xu T, et al. Rheb GTPase is a direct target of TSC2 GAP activity and regulates mTOR signaling. Genes Dev 2003;17:1829-34.
24. Garami A, Zwartkruis FJ, Nobukuni T, et al. Insulin activation of Rheb, a mediator of mTOR/S6K/4E-BP signaling, is inhibited by TSC1 and 2. Mol Cell 2003;11:1457-66.
25. Zhang Y, Gao X, Saucedo LJ, et al. Rheb is a direct target of the tuberous sclerosis tumour suppressor proteins. Nat Cell Biol 2003;5:578-81.
26. Tee AR, Manning BD, Roux PP, et al. Tuberous sclerosis complex gene products, Tuberin and Hamartin, control mTOR signaling by acting as a GTPase-activating protein complex toward Rheb. Curr Biol 2003;13:1259-68.
27. Kamijo T, Zindy F, Roussel MF, et al. Tumor suppression at the mouse INK4a locus mediated by the alternative reading frame product p19ARF. Cell 1997;91:649-59.
28. Kwiatkowski DJ, Zhang H, Bandura JL, et al. A mouse model of TSC1 reveals sex-dependent lethality from liver hemangiomas, and up-regulation of p70S6 kinase activity in Tsc1 null cells. Hum Mol Genet 2002;11:525-34.
29. Weber JD, Raben DM, Phillips PJ, et al. Sustained activation of extracellular-signal-regulated kinase 1 (ERK1) is required for the continued expression of cyclin D1 in G1 phase. Biochem J 1997;326:61-8.
30. Matsushime H, Roussel MF, Ashmun RA, et al. Colony-stimulating factor 1 regulates novel cyclins during the G1 phase of the cell cycle. Cell 1991;65:701-13.
31. Bar-Sagi D. Mechanisms of signal transduction by Ras. Semin Cell Biol 1992;3:93-8.
32. Ronnstrand L, Arvidsson AK, Kallin A, et al. SHP-2 binds to Tyr763 and Tyr1009 in the PDGF beta-receptor and mediates PDGF-induced activation of the Ras/MAP kinase pathway and chemotaxis. Oncogene 1999;18:3696-702.
33. Phillips-Mason PJ, Raben DM, Baldassare JJ. Phosphatidylinositol 3-kinase activity regulates alpha -thrombin-stimulated G1 progression by its effect on cyclin D1 expression and cyclin-dependent kinase 4 activity. J Biol Chem 2000;275:18046-53.
34. Chiosis G, Rosen N, Sepp-Lorenzino L. LY294002-geldanamycin heterodimers as selective inhibitors of the PI3K and PI3K-related family. Bioorg Med Chem Lett 2001;11:909-13.
35. Andjelkovic M, Alessi DR, Meier R, et al. Role of translocation in the activation and function of protein kinase B. J Biol Chem 1997;272:31515-24.

36. Chou MM, Blenis J. The 70 kDa S6 kinase: regulation of a kinase with multiple roles in mitogenic signalling. Curr Opin Cell Biol 1995;7:806-14.
37. Tapon N, Ito N, Dickson BJ, et al. The Drosophila tuberous sclerosis complex gene homologs restrict cell growth and cell proliferation. Cell 2001;105:345-55.
38. Shah OJ, Wang Z, Hunter T. Inappropriate activation of the TSC/Rheb/mTOR/S6K cassette induces IRS1/2 depletion, insulin resistance, and cell survival deficiencies. Curr Biol 2004;14:1650-6.
39. Potter CJ, Huang H, Xu T. Drosophila Tsc1 functions with Tsc2 to antagonize insulin signaling in regulating cell growth, cell proliferation, and organ size. Cell 2001;105:357-68.
40. Inoki K, Corradetti MN, Guan KL. Dysregulation of the TSC-mTOR pathway in human disease. Nat Genet 2005;37:19-24.
41. Holz MK, Ballif BA, Gygi SP, et al. mTOR and S6K1 mediate assembly of the translation preinitiation complex through dynamic protein interchange and ordered phosphorylation events. Cell 2005;123:569-80.
42. Fingar DC, Richardson CJ, Tee AR, et al. mTOR controls cell cycle progression through its cell growth effectors S6K1 and 4E-BP1/eukaryotic translation initiation factor 4E. Mol Cell Biol 2004;24:200-16.
43. Bertwistle D, Sugimoto M, Sherr CJ. Physical and functional interactions of the Arf tumor suppressor protein with nucleophosmin/B23. Mol Cell Biol 2004;24:985-96.
44. Kondo T, Minamino N, Nagamura-Inoue T, et al. Identification and characterization of nucleophosmin/B23/numatrin which binds the anti-oncogenic transcription factor IRF-1 and manifests oncogenic activity. Oncogene 1997;15:1275-81.
45. Pang Q, Christianson TA, Koretsky T, et al. Nucleophosmin interacts with and inhibits the catalytic function of eukaryotic initiation factor 2 kinase PKR. J Biol Chem 2003;278:41709-17.
46. Maggi LB, Weber JD. Nucleolar adaptation in human cancer. Cancer Investigation 2005;23:599-608.
47. Chan PK, Chan FY, Morris SW, et al. Isolation and characterization of the human nucleophosmin/B23 (NPM) gene: identification of the YY1 binding site at the 5' enhancer region. Nucleic Acids Res 1997;25:1225-32.
48. Holland EC, Sonenberg N, Pandolfi PP, et al. Signaling control of mRNA translation in cancer pathogenesis. Oncogene 2004;23:3138-44.
49. Nobukini T, Thomas G. The mTOR/S6K signaling pathway: the role of the TSC1/2 tumour suppressor complex and the proto-oncogene Rheb. Novartis Found Symp 2004;262:48-54.
50. Martin DE, Hall MN. The expanding TOR signaling network. Curr Opin Cell Biol 2005;17:158-66.

FIG. 1. NPM protein expression is induced by pro-growth signals and is sensitive to LY294002. (A) Serum-starved low passage wild-type MEFs were incubated with 10% serum or 200ng/mL PDGF for the durations indicated. Proteins were resolved by SDS-PAGE and immunoblotted with antibodies to γ-tubulin, NPM and cyclin D1. (B) MEFs were infected with retroviruses encoding β-galactosidase (EV) and Ras^{V12}, collected at the indicated times, and analyzed by western blot with the indicated antibodies. (C) MEFs were serum starved and pre-treated with 15μM LY294002 for one hour (+) before being stimulated with 10% serum for the indicated times. Proteins were separated by SDS-PAGE and immunoblotted with antibodies specific for NPM, AKT, and phospho-AKT. (D) Wild-type MEFs were transduced with the retroviruses encoding β-galactosidase (EV) and Ras^{V12}. LY294002 (15μM) was added 24 hours post-infection. All samples were collected 48 hours post-infection and lysates were immunoblotted with antibodies recognizing NPM, γ-tubulin and Ras.

FIG. 2. Effects of rapamycin on NPM expression. (A) Rapamycin (Rap, 100 nM) was added as indicated to asynchronous wild-type MEFs. Forty-eight hours after rapamycin treatment, cells were harvested and proteins were separated by SDS-PAGE and immunoblotted with antibodies specific for NPM, γ-tubulin and phospho-S6. (B) Wild-type MEFs were infected with retroviruses encoding β-galactosidase (EV) and Ras^{V12}. Rapamycin (100 nM) was added as indicated 24 hours post-infection. All samples were collected 48 hours post-infection and proteins were immunoblotted with antibodies against γ-tubulin, Ras and NPM.

FIG. 3. Effects of pro-growth signals and rapamycin on NPM mRNA levels. (A) Wild-type MEFs were serum-starved and subsequently incubated with 10% serum for the durations indicated. Proteins were resolved by SDS-PAGE and antibodies recognizing γ-tubulin and cyclin D1 were used as indicated. Total RNA was isolated at the indicated times and NPM mRNAs were visualized by Northern blot analysis (NB) with murine NPM probes. Ribosomal 28S and 18S rRNAs were visualized by methylene blue staining as a loading control. (B) Wild-type MEFs were infected with retroviruses encoding β-galactosidase (EV) and Ras^{V12}. Rapamycin (100 nM) was added as indicated 24 hours post-infection. All samples were collected 120 hours post-infection and analyzed by Northern blot with probes specific for murine NPM. Ribosomal 28S and 18S rRNAs were detected by methylene blue staining.

FIG. 4. NPM protein expression and rate of NPM mRNA translation is higher in MEFs lacking *Tsc1*. (A) Equal amounts of protein lysate from wild-type, $Tsc1^{-/-}/p53^{-/-}$, or $p53^{-/-}$ MEFs were resolved by SDS-PAGE and analyzed with antibodies specific for TSC1, γ-tubulin, and NPM. (B) $Tsc1^{-/-}/p53^{-/-}$ MEFs were treated with vehicle or rapamycin (100 nM) and harvested 24 hour later for western blot analysis. Proteins were resolved by SDS-PAGE and antibodies recognizing γ-tubulin, NPM and phospho-S6 were used as indicated. Wild-type and $Tsc1^{-/-}/p53^{-/-}$ MEFs were transduced with plasmids encoding β-galactosidase (+Vector) or TSC1 and harvested 24 hours later for western blot analysis. Proteins were resolved by SDS-PAGE and antibodies recognizing γ-tubulin, NPM and TSC1 were used as indicated. (C) Wild-type MEFs were transduced with pRK7 plasmids encoding HA-tagged S6K1 or eIF4E. Cells were harvested (48 hrs later) and proteins

were separated by SDS-PAGE and immunoblotted with antibodies specific for HA, γ-tubulin and NPM. (D) Wild-type, *Tsc1*$^{-/-}$/*p53*$^{-/-}$, or *p53*$^{-/-}$MEFs were starved of methionine and ^{35}S-methionine was subsequently added for the indicated time periods prior to harvesting to allow for incorporation of label into newly translated proteins in the absence or presence of rapamycin (100 nM). Immunoprecipitated NPM proteins were separated by SDS-PAGE and detected by autoradiography.

FIG. 5. Loss of *Tsc1* results in greater polysomes and increased rates of protein synthesis. (A) 3x10^6 cells for each genotype were lysed and fractionated over a 10-45% sucrose gradient. Gradients were fractionated and ribosomal subunits were detected by measuring RNA absorbance at 254nm. Percentages are given for differences in calculated areas under each polysome peak. (B) ^{35}S-methionine was added to methionine-starved cells of each genotype for the indicated time periods. Cells were immediately lysed and total protein was precipitated with TCA, pelleted, and subjected to liquid scintillation counting to measure incorporated cpm.

FIG. 6. Expression of NPM export mutant suppresses polysome formation and abrogates enhanced export of newly synthesized RNAs caused by *Tsc1* loss. (A) Wild-type and *Tsc1*$^{-/-}$/*p53*$^{-/-}$ MEFs were infected with retroviruses encoding β-galactosidase or His-tagged NPMdL, an NPM shuttling mutant. Cells (3x10^6) for each condition were lysed and fractionated over a 10-45% sucrose gradient. Gradients were fractionated and ribosomal subunits were detected by measuring RNA absorbance at 254nm. Inset shows western blot analysis of proteins harvested from each condition. Separated proteins were

immunoblotted with antibodies recognizing γ-tubulin and the His epitope. (B) Wild-type and *Tsc1*$^{-/-}$/*p53*$^{-/-}$ MEFs were infected with retroviruses encoding β-galactosidase (Control) His-NPM or His-NPMdL. Cells were labeled with [methyl-^{3}H] methionine and chased. Equal numbers of cells were subjected to nuclear and cytoplasmic fractionation. Total RNA extracted from each fraction was separated, transferred to membranes and subjected to autoradiography. Ethidium bromide staining of total rRNA loaded from each sample condition is given to ensure equal rRNA loading from identical sample cell numbers (lower panel). (C) *Tsc1*$^{-/-}$/*p53*$^{-/-}$ MEFs were infected with retroviruses encoding pSRα (Empty Vector) or His-NPMdL and selected in G418. Cells (1.5 x 10^{3}) were seeded on 100 mm dishes to assess foci formation (lower panel). Cells grew for 12 days in complete medium, were fixed with MeOH and stained with Giemsa. Proliferation rates were measured by seeding cells (1 x 10^{4}) in triplicate and counting total cell numbers daily over the course of 6 days (upper panel). Inset shows western blot analysis of proteins harvested from each condition. Separated proteins were immunoblotted with antibodies recognizing γ-tubulin and the His epitope. (D) *Tsc1*$^{-/-}$/*p53*$^{-/-}$ MEFs were infected with lentiviruses encoding siRNAs designed to knock-down expression of Luciferase or NPM and selected in puromycin. 96 hours post-infection, the ability to form foci and proliferation rates were assessed as described in (C). Efficient knock-down of NPM is shown by western blot analysis.

Figure 1- Pelletier

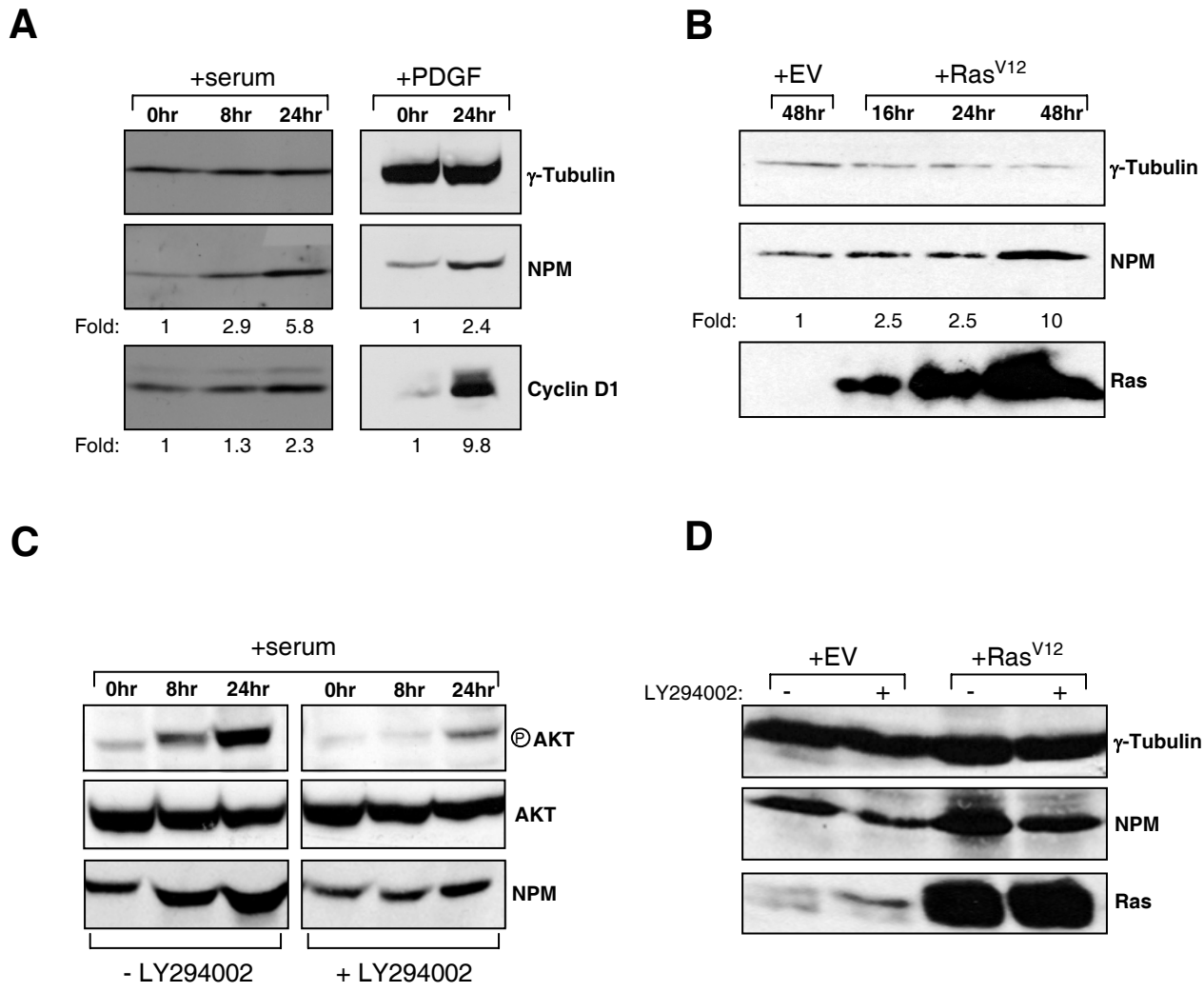

Figure 2- Pelletier

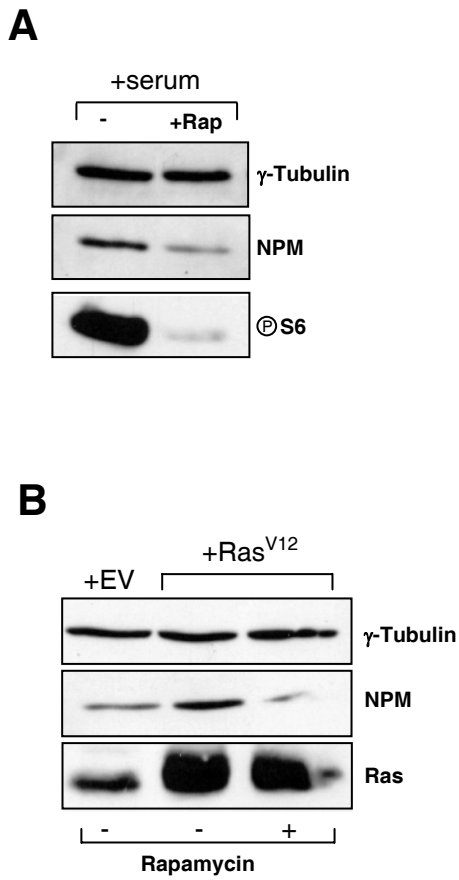

Figure 3- Pelletier

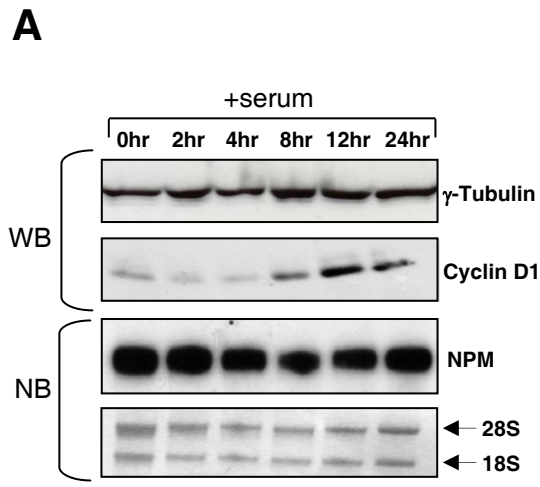

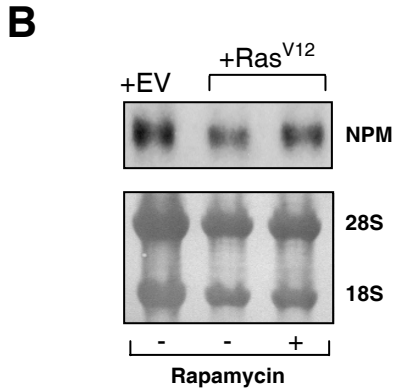

Figure 4- Pelletier

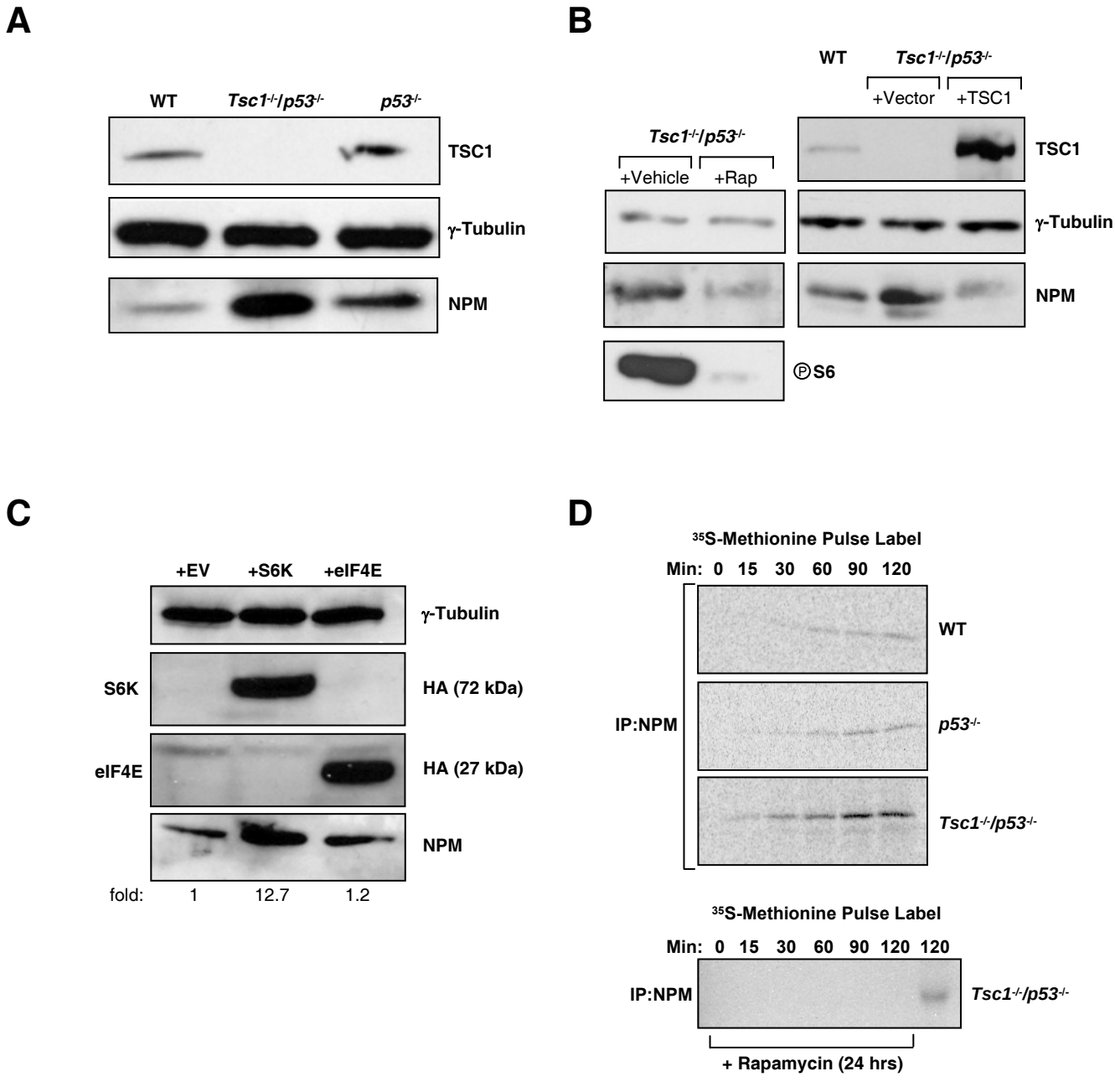

Figure 5- Pelletier

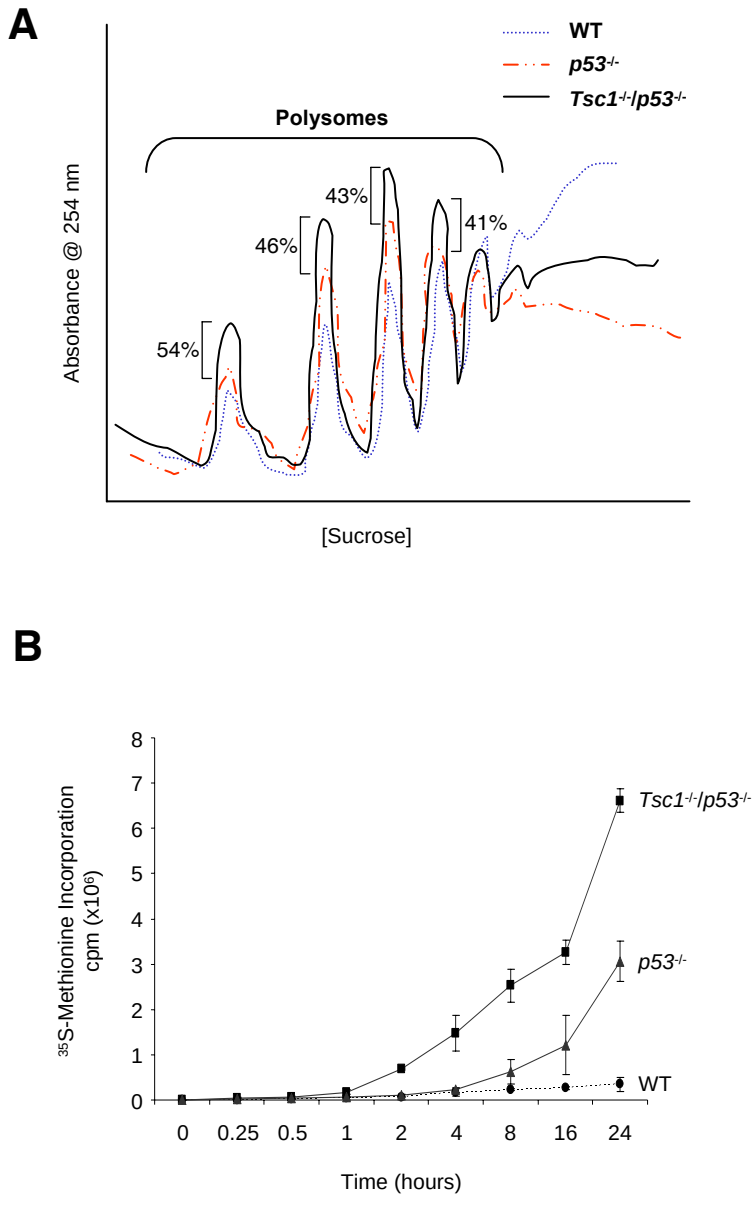

Figure 6- Pelletier

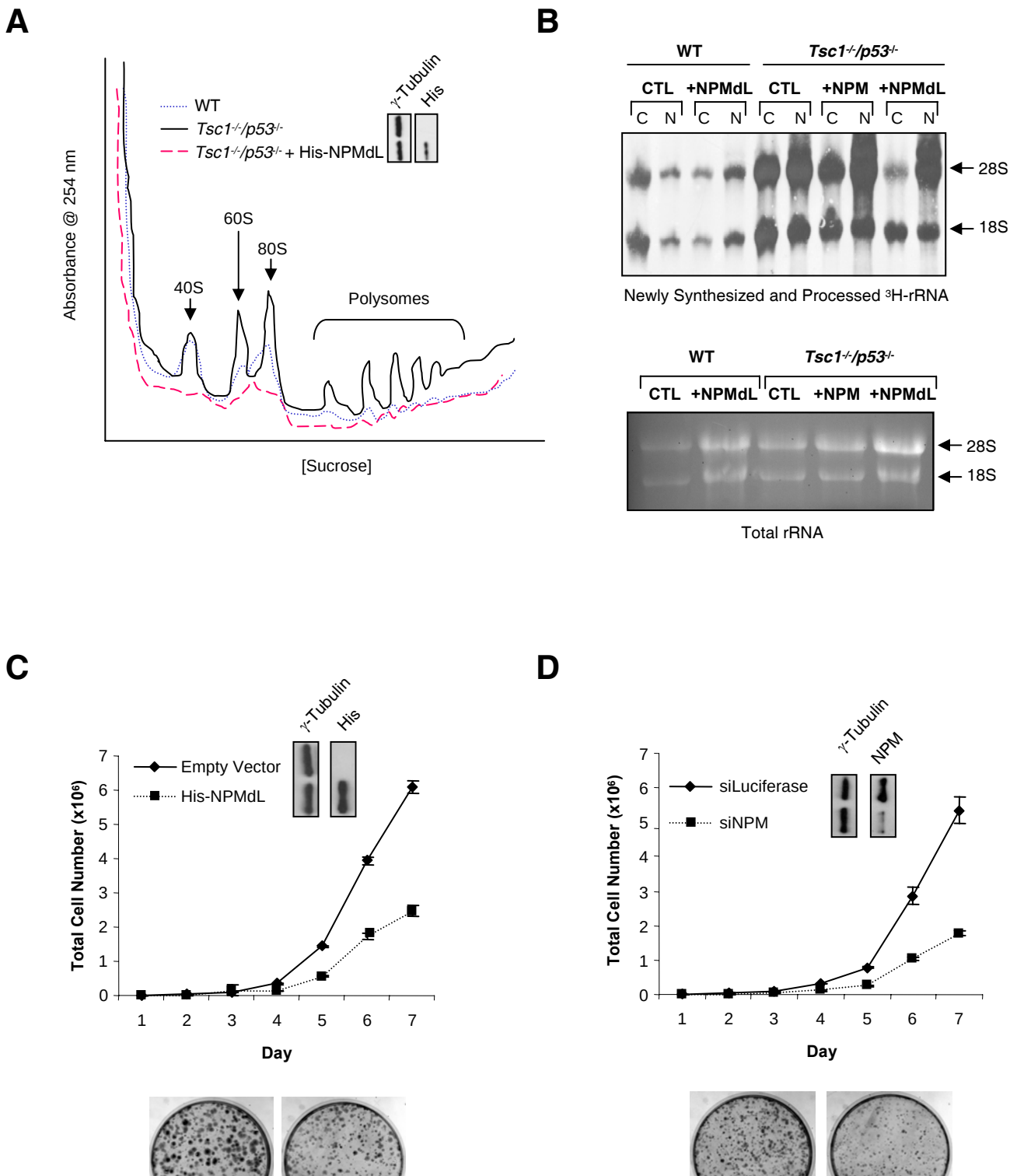

MOLECULAR AND CELLULAR BIOLOGY, May 2006, p. 3798–3809 Vol. 26, No. 10
0270-7306/06/$08.00+0 doi:10.1128/MCB.26.10.3798–3809.2006

Nucleophosmin Is Essential for Ribosomal Protein L5 Nuclear Export

Yue Yu,[1] Leonard B. Maggi, Jr.,[1] Suzanne N. Brady,[1] Anthony J. Apicelli,[1] Mu-Shui Dai,[2] Hua Lu,[2] and Jason D. Weber[1]*

Department of Internal Medicine, Division of Molecular Oncology, Siteman Cancer Center, Washington University School of Medicine, St. Louis, Missouri 63110,[1] and Department of Biochemistry and Molecular Biology, School of Medicine, Oregon Health Science University, Portland, Oregon 97201[2]

Received 20 October 2005/Returned for modification 7 December 2005/Accepted 24 February 2006

Nucleophosmin (NPM/B23) is a key regulator in the regulation of a number of processes including centrosome duplication, maintenance of genomic integrity, and ribosome biogenesis. While the mechanisms underlying NPM function are largely uncharacterized, NPM loss results in severe dysregulation of developmental and growth-related events. We show that NPM utilizes a conserved CRM1-dependent nuclear export sequence in its amino terminus to enable its shuttling between the nucleolus/nucleus and cytoplasm. In search of NPM trafficking targets, we biochemically purified NPM-bound protein complexes from HeLa cell lysates. Consistent with NPM's proposed role in ribosome biogenesis, we isolated ribosomal protein L5 (rpL5), a known chaperone for the 5S rRNA. Direct interaction of NPM with rpL5 mediated the colocalization of NPM with maturing nuclear 60S ribosomal subunits, as well as newly exported and assembled 80S ribosomes and polysomes. Inhibition of NPM shuttling or loss of *NPM* blocked the nuclear export of rpL5 and 5S rRNA, resulting in cell cycle arrest and demonstrating that NPM and its nuclear export provide a unique and necessary chaperoning activity to rpL5/5S.

As the most prominent of subnuclear structures, the nucleolus has long been recognized as the site of active transcription of rRNA and ribosome assembly (8). Various nucleolar proteins, RNAs, and other factors have been implicated in the complex process of ribosome production and maturation (18). Recently, several groups reported the successful isolation and mapping of the mammalian nucleolar proteome (1, 2, 44). While these studies clearly identified proteins and ribonucleoproteins with purported roles in ribosome biogenesis, a surprising number of proteins within the nucleolar proteome (>100) have no known function. In previous decades, it was assumed that all nucleolar proteins must somehow contribute to static ribosome biogenesis simply by virtue of their localization. However, more-recent findings have demonstrated that the nucleolus is a dynamic subnuclear organelle which regulates numerous cellular processes, prompting a broadened view of the potential functions of nucleolar proteins (28).

Nucleophosmin (NPM/B23) is an abundant phosphoprotein that resides within the granular regions of the nucleolus (46). Proliferating cells express NPM at high levels (9, 13), and NPM has been associated with a variety of cellular events, including ribosomal biogenesis, protein chaperoning, and centrosome duplication (13, 23, 35, 36). Structurally, NPM is present in both monomeric and multimeric states, although NPM multimers appear predominant in the nucleolus and may be crucial for the assembly of maturing ribosomes (33, 34, 53). Furthermore, NPM, along with other nucleolar proteins, is believed (or has been shown) to actively mobilize into distinct subcellular pools, supporting the notion that NPM trafficking may be essential for its (proper) function (6). Indeed, NPM's transit from the nucleolus/nucleus is an essential event in S phase progression; when NPM export was inhibited by the nucleolar tumor suppressor ARF, cells arrested in G_1 (7). Moreover, loss of NPM expression results in severe attenuation of cellular proliferation and increased apoptosis (5, 7, 16, 19), underscoring NPM's indispensable role within the cell.

Given that nuclear export of NPM promotes cell growth, we aimed to further elucidate the crucial roles of NPM's trafficking. While numerous proteins, such as Mdm2, cdc14p, and telomerase reverse transcriptase, are topologically restrained in the nucleolus following receipt of defined cellular cues, newly synthesized ribosomal subunits must be exported from the nucleolus to promote proper protein translation in the cytosol (45). Recent work with *Xenopus laevis* and *Saccharomyces cerevisiae* has shown that nuclear export of ribosomes utilizes the CRM1-RanGTP export receptor pathway (20) as well as the conserved nuclear adaptor protein NMD3 (51). While investigating the critical nature of NPM trafficking, we noted that NPM's exit from the nucleus also involved the classical CRM1-dependent nuclear export pathway. In search of proteins that are targeted for NPM-mediated nuclear export, we observed that nuclear and cytosolic NPM proteins directly bound to the ribosomal L5 protein (rpL5), a 60S subunit protein that chaperones the 5S rRNA into the nucleolus and out into the cytosol (31). Here we report that NPM mediates rpL5/5S nuclear export through a CRM1-dependent mechanism, allowing NPM to directly access the maturing ribosome and potentially regulate the protein translational machinery.

* Corresponding author. Mailing address: Department of Medicine, Division of Molecular Oncology, Washington University School of Medicine, Campus Box 8069, 660 South Euclid Avenue, St. Louis, MO 63110. Phone: (314) 747-3896. Fax: (314) 747-2797. E-mail: jweber@im.wustl.edu.

MATERIALS AND METHODS

Cell culture. HeLa and NIH 3T3 cells and wild-type (WT) mouse embryonic fibroblasts (MEFs) (ArtisOptimus, Carlsbad, CA) were maintained in Dulbecco's

modified Eagle's medium with 10% fetal bovine serum, 2 mM glutamine, 0.1 mM nonessential amino acids, and 100 U penicillin and streptomycin.

Plasmid constructs. Vectors encoding full-length His-tagged murine NPM are described elsewhere (7). The His epitope-tagged NPM coding sequence was subcloned into pcDNA3.1 (Invitrogen) and pEGFP (Clontech) vectors. His-$NPM_{\Delta 42-61}$, His-$NPM_{\Delta 62-83}$, or His-NPMdL mutants were generated using the primers 5′-GAAAATGAGCACCAGGCAGAAGCAATGAAC-3′ (sense) and 5′-GTTCATTGCTTCTGCCTGGTGCTCATTTTC-3′ (antisense), 5′-GTTAC ACATCGTAGAGCAACCAACAGTTTCC-3′ (sense) and 5′-GGAAACTGTT GGTTGCTCTACGATGTGTAAC-3′ (antisense), or 5′-GAAAATGAGCACC AGGCGTCAGCAAGAACGGTC-3′ (sense) and 5′-CTAAACTGACCGTTCTT GCTGACGCCTGGTGCTCATTTTC-3′ (antisense), respectively, by QuikChange mutagenesis (Stratagene). A myc-tagged NPC-M9 (40) in pcDNA3 and a green fluorescent protein (GFP)-tagged rpL5 plasmid (41) were generous gifts from Alan Diehl (University of Pennsylvania) and Joachim Hauber (Universitat Erlangen-Nurnberg).

Heterokaryon assay. HeLa cells (2×10^5) were seeded onto glass coverslips and transfected with plasmids. NIH 3T3 cells (6×10^5) were seeded onto the HeLa cells 24 h posttransfection. Cocultures were then incubated for 30 min with cycloheximide (100 μg/ml), followed by incubation with 50% polyethylene glycol in phosphate-buffered saline for 105 s. Cocultures were incubated with Dulbecco's modified Eagle's medium containing cycloheximide (100 μg/ml) for an additional 4 h. Heterokaryons were fixed and stained with a rabbit anti-His antibody (Santa Cruz) or mouse anti-myc antibody (Zymed), followed by either fluorescein isothiocyanate-conjugated or rhodamine X-conjugated anti-rabbit or anti-mouse immunoglobulin (Pierce) as described previously (7). Nuclei were stained with Hoechst (Sigma). Fluorescent signals were detected using a Nikon epifluorescence compound microscope (×100) fitted with a Nikon FDX-35 camera.

Immunoprecipitation and Western blot analysis. Cells were transduced as recommended by the manufacturer (Amaxa) with vectors encoding His-NPM, His-NPMdL, and GFP-rpL5 and lysed in binding buffer (25 mM Tris-HCl, pH 8, 150 mM NaCl, 1 mM EDTA, 0.1% NP-40) 48 h after the Nucleofector process. Primary antibody to the NPM N terminus (custom rabbit; Sigma Genosys), GFP (Santa Cruz), His (Santa Cruz), rpL5 (12), or nonimmune rabbit serum (NRS) was added to the binding reaction mixtures. Immune complexes were precipitated with protein A-Sepharose (Amersham). The precipitated proteins were separated by sodium dodecyl sulfate-polyacrylamide gel electrophoresis (SDS-PAGE) and transferred to polyvinylidene difluoride (PVDF) membranes. NPM, His-tagged proteins, and GFP-tagged proteins were visualized by direct immunoblotting with NPM (Zymed), His (Santa Cruz), and rpL5 and GFP (Santa Cruz) antibodies, respectively.

Fluid phase liquid chromatography. For affinity chromatography, a rabbit polyclonal antibody recognizing the N terminus of NPM (Sigma) was coupled to *N*-hydroxysuccinimide-activated Sepharose (Amersham). HeLa cells were lysed in 20 mM Tris, pH 7.4, and 0.1% Tween 20 and sonicated. Lysates (600 μg) were injected onto the NPM affinity column, washed with 20 mM Tris, and eluted with an increasing NaCl gradient (0.1 to 1 M) using BioLogic fluid phase liquid affinity chromatography and HR software (Bio-Rad). Fractions were precipitated with trichloroacetic acid (TCA). Proteins were resuspended in 1 M Tris-HCl (pH 7.4), separated by SDS-PAGE, and visualized with Coomassie blue stain (Sigma).

Proteomic analysis. Proteins from fluid phase liquid affinity chromatography fractions were precipitated with TCA and resuspended in Laemmli buffer. SDS-PAGE-separated proteins were stained with SYPRO-Ruby (Bio-Rad). Bands of interest were excised and processed for trypsin digestion. Tryptic peptides were calibrated with Sequazyme peptide mass standard kit (PE Biosystem) and analyzed by matrix-assisted laser desorption ionization–time of flight (MALDI-TOF) mass spectrometry (Voyager DE Pro; Applied Biosystems). Identification of proteins was performed using MS-Fit software (http://prospector.ucsf.edu/ucsfhtml4.0/msfit.htm). MALDI-TOF spectra and sequences were verified using a 4700 Proteomics tandem mass spectrometry system (Applied Biosystems). Identified proteins were additionally verified by direct Western blot analysis.

Bacterial protein purification. BL21 cells were transformed with pET28a vectors encoding NPM, NPMdL, rpL5, and p27kip1 proteins. Protein production was induced for 3 h with 1 mM IPTG (isopropyl-β-D-thiogalactopyranoside). Harvested cells were lysed in phosphate-buffered saline containing protease inhibitors and 1% Triton X-100 with sonication. Cleared lysates were subjected to affinity purification using Ni-nitrilotriacetic acid columns as described by the manufacturer (Sigma). Purified proteins were separated by SDS-PAGE and visualized for purity using Coomassie blue stain.

Subcellular fractionation. HeLa cells were subjected to the Nucleofector process with scrambled or small interfering NPM RNAs or control vector, His-NPM, and His-NPMdL and harvested. Pellets containing equal cell numbers were resuspended in HEPES buffer (10 mM HEPES, pH 7.4, with 4 mM $MgCl_2$, 1 mM phenylmethylsulfonyl fluoride [PMSF], 10 μg/ml leupeptin, 10 μg/ml aprotinin, 1 μg/ml pepstatin) and lysed with a syringe. Lysates were pelleted, and the supernatant was saved as the cytoplasmic fraction. The pellet was resuspended in fractionation buffer (10 mM Tris, pH 7.5, 10 mM NaCl, 1 mM EDTA, 0.5 mM EGTA, 4 mM $MgCl_2$, 1 mM PMSF, 10 μg/ml leupeptin, 10 μg/ml aprotinin, 1 μg/ml pepstatin), subjected to Dounce homogenization, layered over a cushion of sucrose (45%, wt/vol, in fractionation buffer), and centrifuged. The pellet was washed and resuspended in EBC buffer (50 mM Tris-HCl, pH 7.4, 120 mM NaCl, 1 mM EDTA, 0.5% NP-40, 1 mM PMSF, 10 μg/ml leupeptin, 10 μg/ml aprotinin, 1 μg/ml pepstatin, 1 mM NaF, 10 mM $NaVO_4$, β-glycerophosphate). Nuclear or cytoplasmic protein was subjected to SDS-PAGE. Superoxide dismutase (SOD; Cu/Zn-specific form), lamin A/C, and rpL5 proteins were visualized by direct immunoblotting with anti-SOD (Calbiochem), anti-lamin A/C (Santa Cruz), and anti-rpL5 antibodies (12), respectively. Similarly, total RNA was isolated from the fractions obtained above and separated on formaldehyde-agarose gels. Separated RNA from each nuclear and cytoplasmic fraction was analyzed by Northern blotting using a probe specific for the 5S rRNA. The 5S rRNA probe was obtained by PCR using HeLa cell genomic DNA as the template and the following primers: sense, 5′-CCTTCAGCGTCTACGGCCATACC-3′; antisense, 5′-GCCAAGAAA AAGCCTACAGCAGG-3′. The PCR product was cloned and confirmed by sequencing.

RNA FISH. HeLa cells were subjected to the Nucleofector process with pcDNA3.1 His, His-tagged NPM, or His-NPMdL and plated on coverslips. Cells were subjected to RNA fluorescence in situ hybridization (FISH) as described previously (3) using a tetramethyl rhodamine isocyanate (TRITC)-labeled 5S rRNA probe (Genedetect). DNA was counterstained with DAPI (4′,6′-diamidino-2-phenylindole).

Ribosome fractionation. Cells were subjected to cytosolic and nuclear ribosome fractionation, and lysates were separated on sucrose gradients as previously described (48). RNA was continuously monitored over the gradient by measuring UV absorbance at 254 nm. Fractions were collected, and proteins were precipitated with TCA. Proteins were separated by SDS-PAGE and immunoblotted with antibodies recognizing NPM (Zymed) and rpL5.

RESULTS

NPM nuclear export requires a CRM1-dependent nuclear export signal involving leucines 42 and 44. NPM is a ubiquitously expressed nucleolar phosphoprotein capable of regulated nuclear import (6). When NPM is transiently expressed in mammalian cells, it localizes predominantly to the nucleolus. Moreover, using in vivo heterokaryon shuttling assays (50), we have previously shown that NPM readily shuttles between the nucleolus/nucleus and cytoplasm (7). NPC-M9, a nuclear hnRNP protein that readily mobilizes to the cytoplasm, serves as a shuttling control (40). To distinguish between human donor and murine acceptor nuclei, chromosomal DNA was stained with Hoechst, clearly demarcating greater heterochromatin foci of NIH 3T3 mouse cells (speckled pattern, Fig. 1, Hoechst). As shown in Fig. 1A, NPM readily shuttles out of the human nucleolus, into the fused cytoplasm, and back into the mouse acceptor nucleus/nucleolus.

Given that a wide range of shuttling proteins utilize the CRM1 transport protein for their nuclear export, we further investigated the underlying export mechanism of NPM both in the presence and absence of leptomycin B (LMB), a potent inhibitor of CRM1-mediated nuclear export (24). In the absence of LMB, NPM readily migrated from human nucleoli to mouse nucleoli (Fig. 1A). However, in the presence of LMB, NPM failed to shuttle and was restricted to human nucleoli within heterokaryons (92% inhibition; Fig. 1B). The addition of LMB did not hinder the nucleocytoplasmic trafficking of Myc-NPC-M9, an hnRNP that readily shuttles in a CRM1-independent nuclear export pathway (38).

A sequence alignment of NPM residues with known CRM1-dependent shuttling proteins revealed two motifs containing

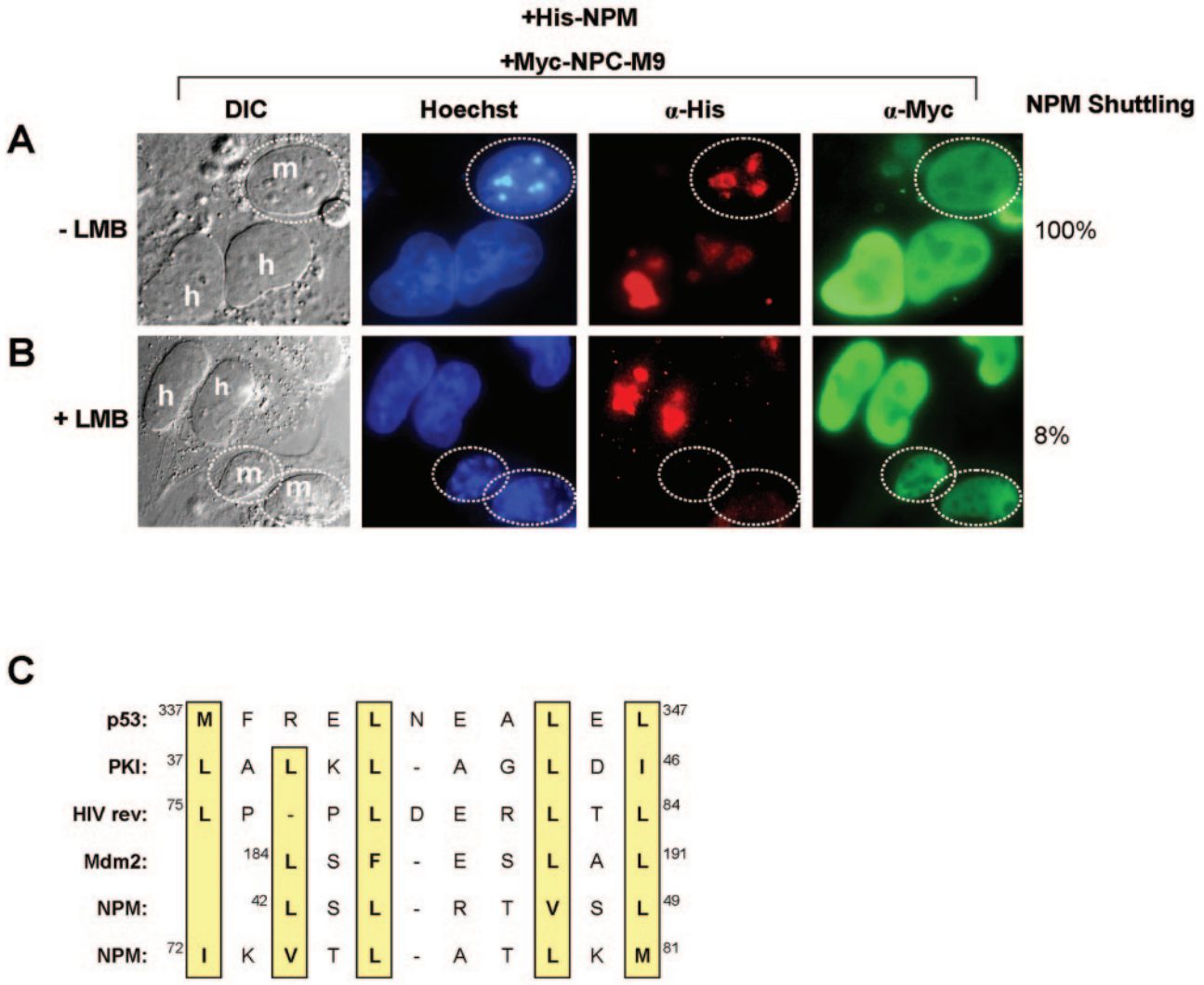

FIG. 1. Nuclear export of NPM is CRM1 dependent. NIH 3T3 cells were seeded onto HeLa cells that had been transfected with His-NPM in combination with Myc-NPC-M9 (shuttling control) in the (A) absence or (B) presence of LMB. Heterokaryons were incubated in media containing cycloheximide for an additional 4 h before fixation. Heterokaryon formation was verified by phase-contrast microscopy, while His-NPM and Myc-NPC-M9 proteins were visualized with antibodies against His (red) and Myc (green), respectively. DNA was stained with Hoechst. Mouse nuclei are demarcated with dotted circles. Human and mouse nuclei are labeled h and m, respectively. These data are representative of at least five independent heterokaryons formed for each transfection condition in three independent experiments. The percentages of His-NPM shuttling in heterokaryons are given. DIC, differential interference contrast; α, anti. (C) Sequence alignment of putative NPM NESs with known NESs of CRM1-dependent nuclear export proteins (p53, protein kinase inhibitor [PKI], rev, and Mdm2). Critical hydrophobic residues are indicated in yellow.

short leucine-rich hydrophobic stretches of amino acids characteristic of CRM1-dependent nuclear export sequences (NESs) (Fig. 1C) (14, 15). In order to identify which region(s) of NPM contains its NES, we generated deletion mutants of NPM lacking either of the two potential NESs ($NPM_{\Delta 42–61}$ and $NPM_{\Delta 62–83}$). Using these NPM constructs, we again conducted interspecies heterokaryon assays. As shown in Fig. 2A, deletion of amino acids 42 to 61 of NPM (His-$NPM_{\Delta 42–61}$) prevented its shuttling (100% inhibition) to mouse nucleoli. Importantly, a myc-tagged NPC-M9 shuttling control readily shuttled in the same human-mouse heterokaryon, indicating that these heterokaryons were not impaired for nucleocytoplasmic shuttling in general. In contrast, deletion of amino acids 62 to 83 of NPM (His-$NPM_{\Delta 62–83}$) did not prevent NPM from shuttling between human and mouse nucleoli (6% inhibition; Fig. 2B), revealing that the putative NES resides within amino acids 42 to 61 of the NPM protein.

Since the type of NES recognized and bound by the CRM1 export receptor is dependent on closely spaced hydrophobic amino acids (particularly leucines) (14, 15), we introduced point mutations into the corresponding leucine residues within the NES of NPM (Leu-42 and Leu-44 to Ala-42 and Ala-44). First, we tested this NPM mutant (designated NPMdL for *d*ouble-*l*eucine mutant) with Myc-NPC-M9 as a shuttling control. As expected, NPMdL was unable to transit from a human nucleus to the cytoplasm and into a murine nucleus (100%

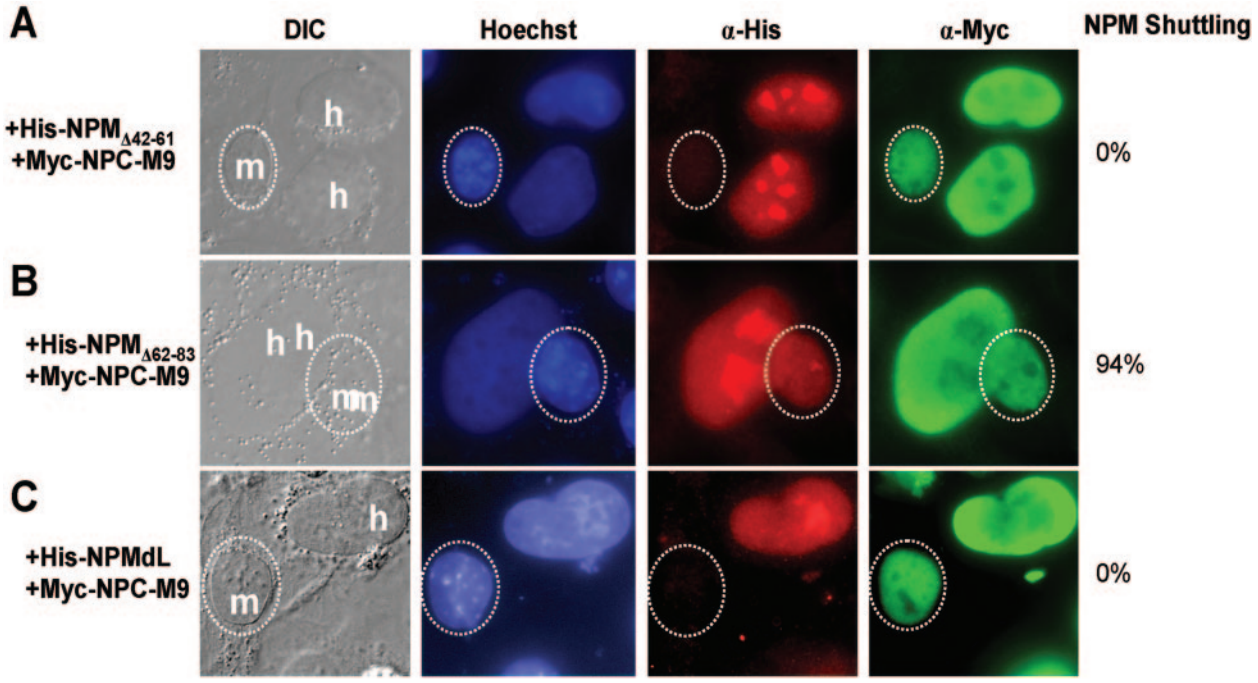

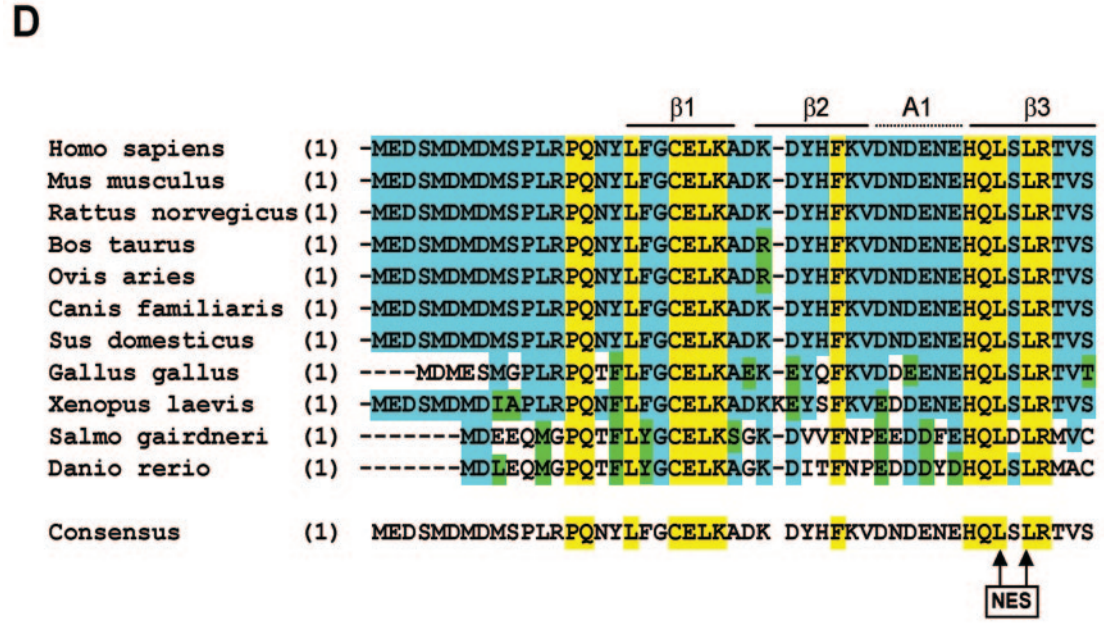

FIG. 2. Leucine 42 and leucine 44 are identified as critical nuclear export residues. NIH 3T3 cells were seeded onto HeLa cells that had been transfected with (A) His-NPM$_{\Delta 42-61}$, (B) His-NPM$_{\Delta 62-83}$, or (C) NPMdL in combination with Myc-NPC-M9. Ectopic NPM proteins and Myc-NPC-M9 proteins were visualized with antibodies against His (red) and Myc (green), respectively. DNA was stained with Hoechst. Mouse nuclei are demarcated with dotted circles. Human and mouse nuclei are labeled h and m, respectively. These data are representative of at least five independent heterokaryons formed for each transfection condition in three independent experiments. The percentages of His-NPM shuttling in heterokaryons are given. DIC, differential interference contrast; α, anti. (D) Sequence alignment of NPM homologues throughout evolution. Identical residues in all species are marked yellow, identical residues in at least seven species are highlighted blue, and conserved residues are marked green. Crystal structure features are identified above the sequences. The consensus NPM sequence for all 11 identified homologues is given, with conserved nuclear export leucines 42 and 44 marked with arrows (NES).

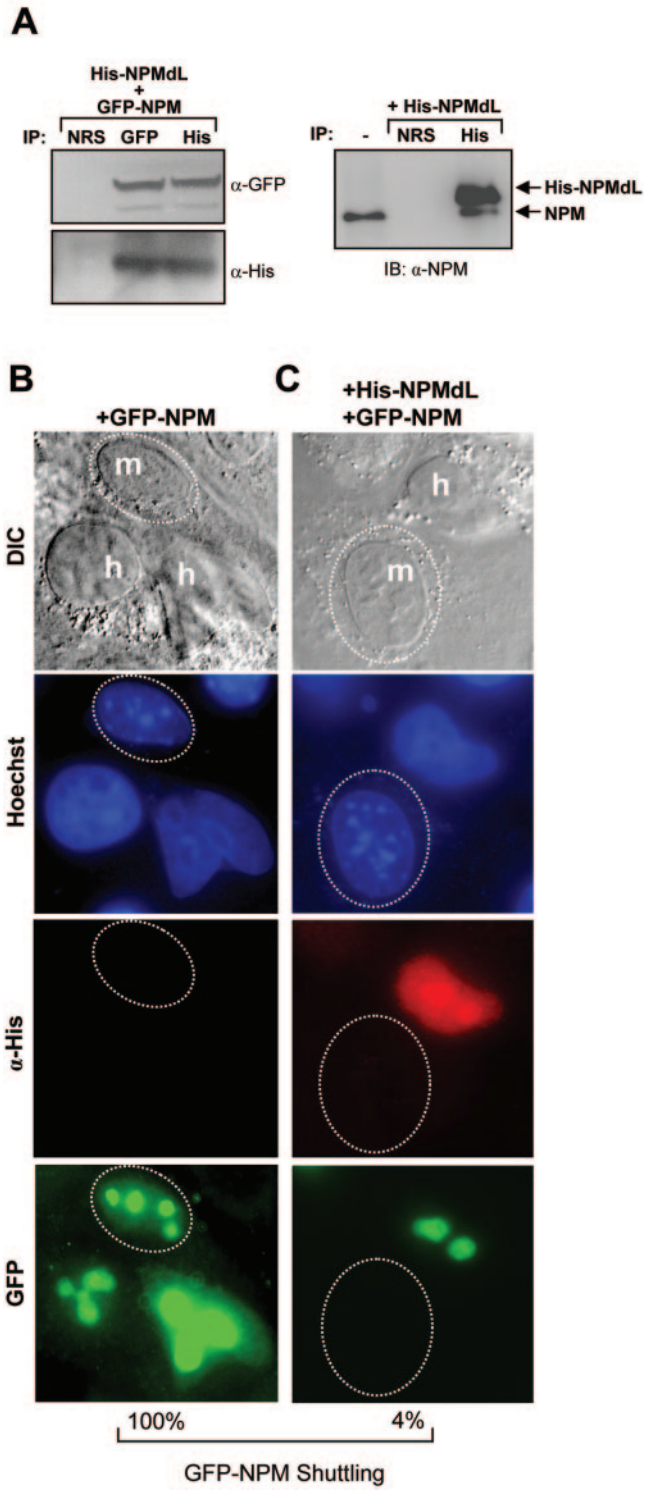

FIG. 3. NPM shuttling mutants act as dominant negative inhibitors of NPM nuclear export. (A, left) HeLa cells transduced with His-NPMdL and GFP-NPM were lysed, and the whole-cell lysate was subjected to immunoprecipitation (IP) with NRS or antibodies recognizing His and GFP epitopes. Precipitated protein complexes were separated by SDS-PAGE, and ectopic NPM proteins were visualized with antibodies against GFP and His epitopes. (A, right) HeLa cells transfected with His-NPMdL were lysed, and the whole-cell lysate was subjected to immunoprecipitation with NRS or antibodies recognizing His epitopes. Precipitated protein complexes were separated by SDS-PAGE, and ectopic mutant and endogenous wild-type NPM proteins were visualized with antibodies against NPM. Untransfected HeLa whole-cell lysate was loaded as a marker for endogenous NPM expression (lane 1). IB, immunoblot; α, anti; DIC, differential interference contrast. NIH 3T3 cells were seeded onto HeLa cells that had been transfected with GFP-NPM (B) alone or (C) in combination with His-NPMdL. Heterokaryon assays were performed, and His-NPMdL and GFP-NPM proteins were visualized with antibodies against His (red) or naturally emitting GFP spectra (green). DNA was stained with Hoechst. Mouse nuclei are demarcated with dotted circles. Human and mouse nuclei are labeled h and m, respectively. These data are representative of at least five independent heterokaryons formed for each transfection condition in three independent experiments. The percentages of GFP-NPM shuttling in heterokaryons are given.

inhibition), indicating that these two leucine residues are critical for nuclear export of the NPM protein (Fig. 2C). Sequence alignment of numerous nucleophosmin homologues underscores the evolutionary importance of this amino-terminal export motif as it is nearly identical from zebra fish to humans (Fig. 2D).

Heterogeneous complexes containing NPM NES mutants and wild-type NPM fail to shuttle. Because NPM readily self-oligomerizes (32, 33, 34, 53), we considered the possibility that mutant NPM molecules could form hetero-oligomers with wild-type NPM proteins. To test this hypothesis, HeLa cells were transduced with His-tagged NPMdL expression vectors. Immunoprecipitation of His-NPMdL proteins revealed the coprecipitation of wild-type endogenous NPM proteins, demonstrating the formation of mutant–wild-type hetero-oligomers in cells (Fig. 3A, right). Additionally, cells transduced with His-NPMdL and GFP-NPM displayed formation of hetero-oligomers, as observed by coprecipitation of both proteins using antibodies directed at either epitope tag (His or GFP; Fig. 3A, left). Given our finding that mutant NPM forms oligomers with wild-type NPM, we next examined whether the NPM shuttling mutant NPMdL could also block wild-type NPM from shuttling. In the absence of the shuttling mutant, GFP-tagged NPM readily shuttled from human to mouse nucleoli (Fig. 3C). However, in the presence of His-tagged NPMdL, GFP-NPM was retained in human nuclei (Fig. 3D; 96% inhibition). Although we were unable to determine the exact stoichiometry between mutant proteins and wild-type proteins in the NPM oligomer, it is clear that overexpression of NPMdL severely impaired the shuttling activity of nearly all NPM oligomers.

NPM associates with cytoplasmic and nuclear rpL5 ribosome complexes. Previous studies have indicated that NPM might function as an integral component of ribosome maturation through its RNA binding activities (36). However, most hypotheses in this regard are largely based on the fact that NPM is nucleolar and, thus, most likely to be involved in the major process in the nucleolus: ribosome biogenesis. To formally test the nucleolar function of NPM, we examined the composition of in vivo NPM protein complexes in HeLa cell lysates. We generated a custom NPM polyclonal antibody affinity column and used a control nonimmune immunoglobulin column to preclear protein lysates. NPM complexes were eluted with increasing salt concentrations and visualized following SDS-PAGE and SYPRO-Ruby staining. As seen in Fig. 4A, we observed very little protein bound to our non-

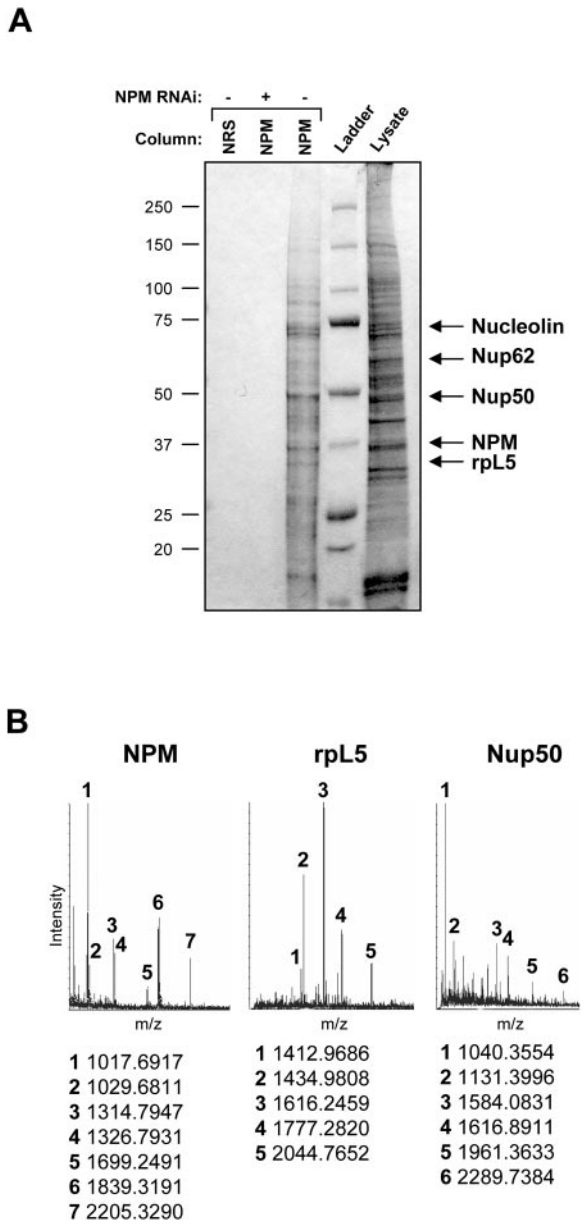

FIG. 4. Isolation of endogenous NPM protein complexes. (A) HeLa cell lysates (600 μg) transduced with control (−) or NPM-directed RNA interference (RNAi) constructs (+) were injected onto either an NRS column or custom NPM polyclonal antibody affinity columns and eluted with an increasing NaCl gradient (0.1 to 1.0 M). Eluted proteins were separated by SDS-PAGE and visualized with Coomassie blue stain. Identified bands are labeled. (B) Representative MALDI-TOF spectra of labeled protein bands from panel A are shown with labeled matching peptide masses.

immune rabbit serum column (lane 1). However, some proteins (~18) were specifically eluted from the NPM antibody column (lane 3), including NPM and the previously known binding protein nucleolin. To determine whether the eluted proteins were in fact bound to the column through their interaction with NPM, we depleted NPM from HeLa cells using NPM-targeted RNA interference. Knockdown of NPM resulted in a loss of specific proteins bound and eluted from the NPM antibody column, demonstrating that our identified NPM protein complex is specific for NPM (lane 2). Protein bands were excised and identified using MALDI-TOF and tandem mass spectrometry analyses. Among those proteins bound to NPM, a cluster of proteins associated with ribosome biogenesis, including rpL5 and nucleolin, as well as the nuclear pore complex proteins Nup50 and Nup62, were identified (Fig. 4A and B), with nucleolin (C23) being the only known NPM binding protein (26, 27). Western blot analysis of NPM protein complexes verified the presence of these proteins in salt-eluted fractions (data not shown).

Given the novelty and potentially significant ribosome biology of finding rpL5 in the NPM complex, we focused on verifying the NPM-rpL5 interaction. Purified recombinant NPM, NPMdL, and rpL5 proteins (Fig. 5A, left panels) mixed overnight were coprecipitated (Fig. 5A, middle panels), demonstrating that the NPM-rpL5 interaction is direct and independent of the NPM nuclear export signal. To show that the interaction of recombinant proteins was specific, NPM and rpL5 were mixed overnight with recombinant p27kip1 proteins (equally charged proteins not bound to the NPM antibody column). Precipitated proteins exhibited no complex formation between NPM and p27kip1 or rpL5 and p27kip1 (Fig. 5A, right panels). Both NPM and rpL5 readily interact with RNAs through conserved nucleic acid binding domains. To determine whether RNA binding is required for the NPM-rpL5 interaction, HeLa lysates were subjected to RNase A treatment prior to coprecipitation of NPM-rpL5 complexes. Even in the presence of RNase A, NPM and rpL5 visibly formed in vivo protein complexes (Fig. 5B) indistinguishable from those from untreated cells and consistent with our earlier finding that the interaction can be recapitulated with purified recombinant proteins (Fig. 5A). While NPM and rpL5 formed complexes in vivo, serial immunoprecipitation of NPM proteins from HeLa lysates showed that NPM and rpL5 are not exclusive partners. We failed to detect rpL5 in some NPM complexes (Fig. 5C, 3° and 4°), and we also noted that there was a significant amount of rpL5 free from NPM complexes in the remaining supernatant (Fig. 5C, Sup), indicating that both NPM and rpL5 can exist in complexes independent of one another.

Having identified a critical member of the 60S ribosomal subunit, namely, rpL5, in NPM complexes, we wanted to evaluate the colocalization of NPM with ribosomes in vivo. In order to follow the spatial control of NPM-rpL5 complexes in vivo, we utilized the UV absorbance of the ribosome. Ribosomal protein L5 is known to supply the maturing 60S ribosomal subunit with 5S rRNA prior to nucleolar/nuclear export of the 60S subunit (47), providing NPM an ideal time to form nucleolar complexes with rpL5. Cytoplasmic and nuclear extracts of HeLa cells were subjected to sucrose gradient centrifugation, and the gradients were fractionated with continuous UV monitoring. As shown in Fig. 6, NPM associates with the 40S, 60S, 80S, and polysome fractions in the cytoplasm while nuclear pools of NPM associate with the 40S/pre-60S and 60S fractions in the nucleus. Consistent with previous reports (30), we found rpL5 associated with the 60S, 80S, and polysome fractions in the cytoplasm and the 40S/pre-60S and 60S fractions in the nucleus (Fig. 6). These data demonstrate that NPM and rpL5 are localized with the maturing 60S ribosomal subunits in the nucleus and are maintained in the mature ribo-

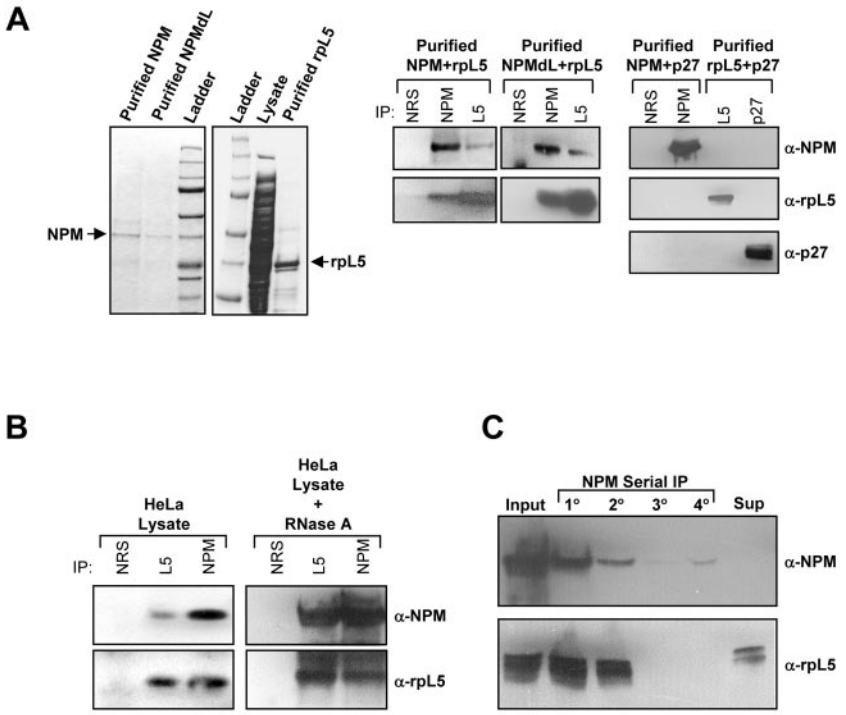

FIG. 5. NPM interacts directly with rpL5. (A, left) Recombinant NPM, NPMdL, and rpL5 were purified from bacterial lysates using Ni-nitrilotriacetic acid affinity chromatography. Purified proteins were separated by SDS-PAGE and detected with Coomassie blue stain. (A, middle) Purified NPM or NPMdL proteins were incubated overnight with rpL5 and immunoprecipitated (IP) with NRS or antibodies recognizing NPM or rpL5. Precipitated proteins were separated by SDS-PAGE, transferred to PVDF membranes, and immunoblotted with NPM and rpL5 antibodies. (A, left) Purified NPM or rpL5 proteins were incubated overnight with recombinant p27 and immunoprecipitated with NRS or antibodies recognizing NPM, rpL5, or p27. Precipitated proteins were separated by SDS-PAGE, transferred to PVDF membranes, and immunoblotted with NPM, rpL5, and p27 antibodies. α, anti. (B) Proteins from HeLa cell lysates were immunoprecipitated with NRS, rpL5 antibody, or NPM antibodies. Precipitated proteins were separated by SDS-PAGE, transferred to PVDF membranes, and immunoblotted with NPM and rpL5 antibodies. Alternatively, HeLa lysates were pretreated for 1 h with RNase A prior to immunoprecipitation as described above. (C) HeLa lysates were subjected to serial immunoprecipitation with NPM antibodies (lanes 1° to 4°). Precipitated proteins and proteins in the final supernatant (unbound) were separated by SDS-PAGE, transferred to PVDF membranes, and immunoblotted with antibodies recognizing NPM and rpL5.

some once it reaches the cytosol. They also indicate that NPM also associates with the 40S subunit, which is devoid of rpL5 (Fig. 6) (30).

Transduction of HeLa cells with His-NPMdL resulted in a dramatic redistribution of rpL5 in cytosolic ribosomes; rpL5 was maintained in the 60S subunits but severely reduced in 80S ribosomes (Fig. 6, middle left panels). Given these findings, we cannot rule out the possibility that rpL5 proteins are still capable of some NPM-independent shuttling. However, it is more likely that rpL5 association with cytosolic ribosomes in the presence of NPMdL is a result of preexisting, stable cytosolic rpL5 complexes. This notion is further substantiated by treatment of HeLa cells with LMB. LMB treatment yielded results that were consistent with NPMdL overexpression (Fig. 6, lower panel). Both NPM and rpL5 proteins were found in the cytosol of LMB-treated cells (at reduced levels), even though the nuclear export of both proteins is LMB sensitive. This finding suggests that some preexisting cytosolic NPM and rpL5 ribosome complexes are fairly stable (~24 h) and that, if either protein utilizes CRM1-independent export, it is minimal.

NPM is required for rpL5 nuclear export. Having demonstrated a reduction of rpL5 associated with cytosolic ribosome subunits in the absence of NPM nuclear export signals, we next

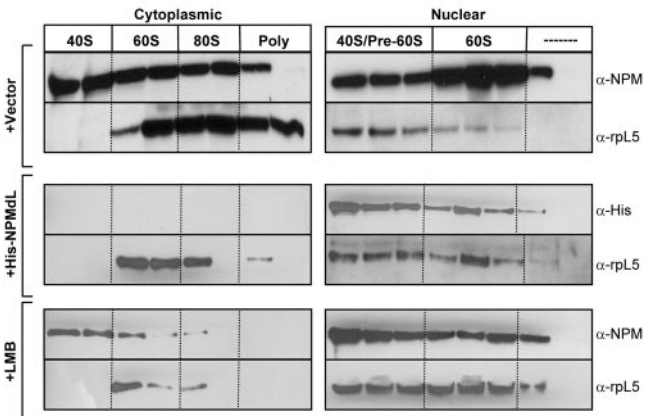

FIG. 6. NPM and rpL5 colocalize with nuclear and cytosolic ribosome subunits. HeLa cells transduced with vector (top panels) or His-NPMdL (middle panels) or treated with LMB (bottom panels) were divided into cytoplasmic and nuclear fractions and subjected to sucrose gradient centrifugation. Absorbance was monitored at 254 nm, and fractions containing 40S, 60S, 80S, and polysome units were collected. Proteins from each fraction were separated by SDS-PAGE, transferred to PVDF membranes, and immunoblotted with antibodies recognizing NPM, the His epitope, and rpL5. α, anti.

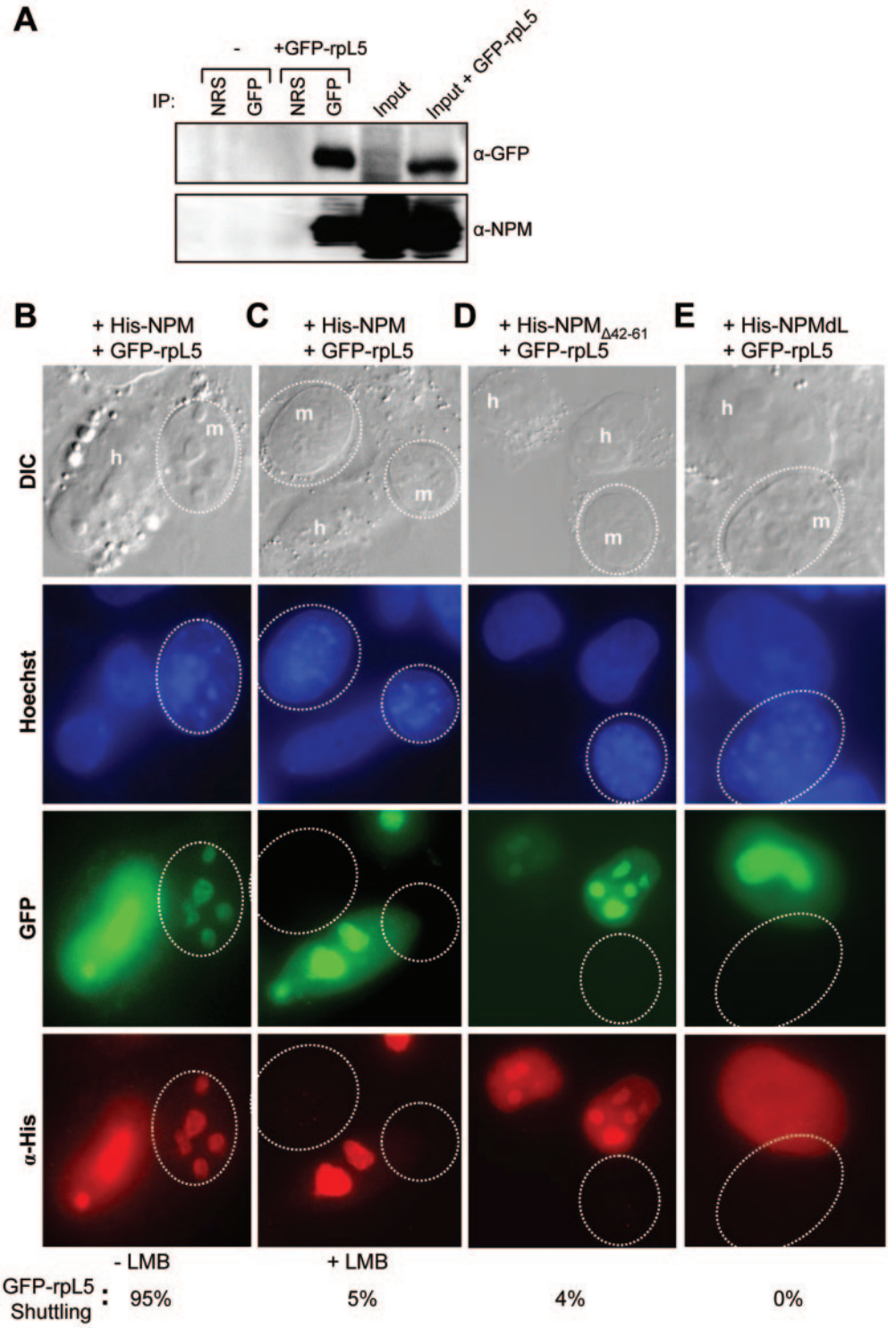

FIG. 7. NPM nuclear export signals are required for the efficient export of GFP-rpL5. (A) HeLa cells either untransfected or transfected with GFP-tagged L5 for 48 h were harvested and lysed. Proteins were immunoprecipitated (IP) with NRS or a rabbit GFP antibody. Precipitated proteins were separated by SDS-PAGE, transferred to PVDF membranes, and immunoblotted with GFP and NPM antibodies. α, anti; DIC, differential interference contrast. Loading inputs are indicated. (B to E) NIH 3T3 cells were seeded onto HeLa cells that had been transfected with GFP-rpL5 in combination with (B and C) His-NPM, (D) His-NPM$_{\Delta 42-61}$, and (E) His-NPMdL. Additionally, HeLa cells in panel C were treated with LMB for 18 h prior to fusion. Heterokaryon assays were performed with NPM and GFP-rpL5 proteins being visualized with antibodies against His (red) and naturally emitting GFP spectra (green), respectively. DNA was stained with Hoechst. Mouse nuclei are demarcated with dotted circles. Human and mouse nuclei are labeled h and m, respectively. These data are representative of at least five independent heterokaryons formed in three independent experiments. The percentages of heterokaryons exhibiting GFP-rpL5 shuttling are given.

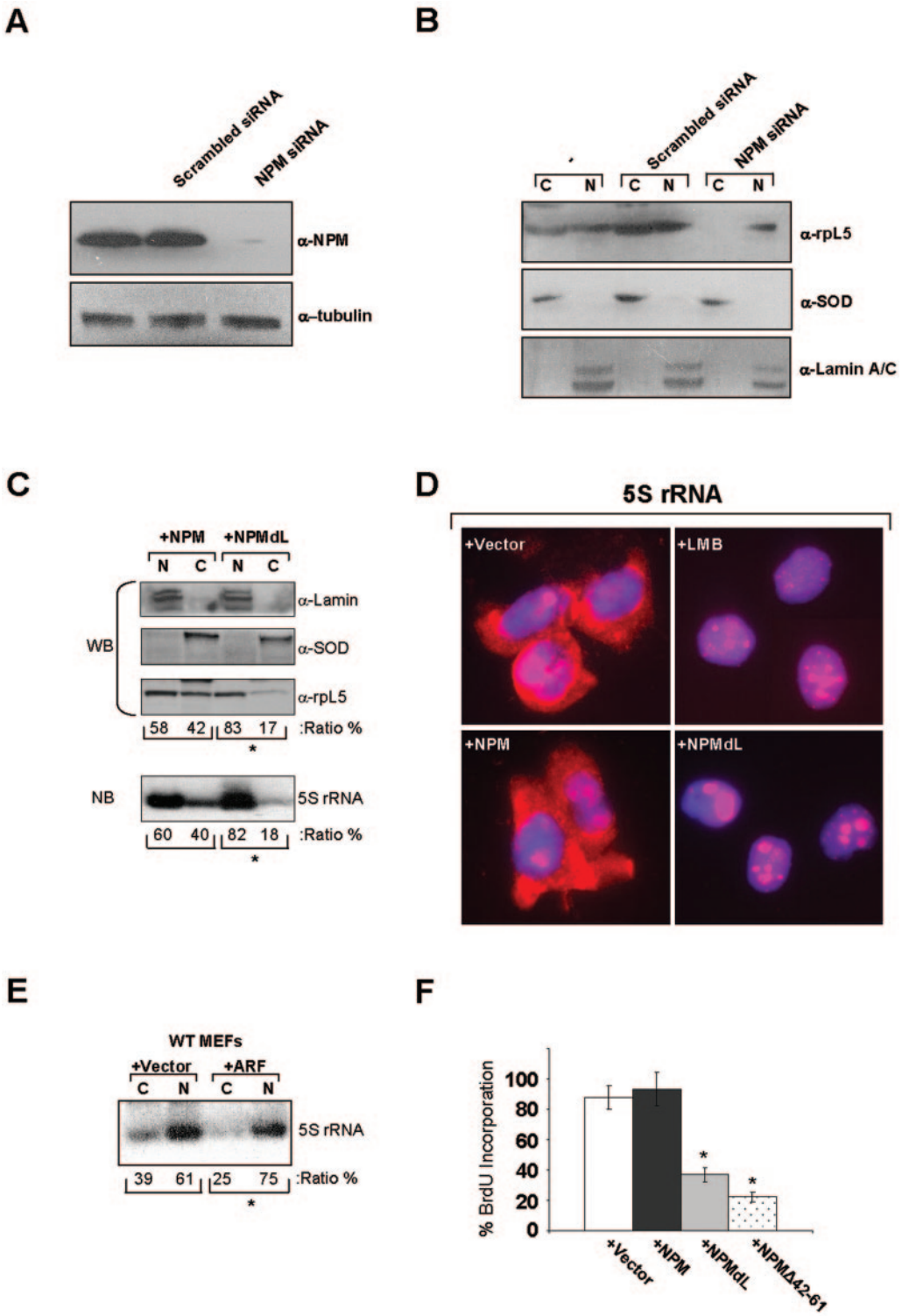

FIG. 8. NPM is essential for rpL5 nuclear export. (A) HeLa cells (−) or cells transduced with siRNAs encoding either scrambled control or NPM-specific sequences were harvested 72 h posttransduction for Western blot analysis. Proteins separated by SDS-PAGE were transferred to PVDF membranes and immunoblotted with antibodies recognizing NPM and γ-tubulin. α, anti. (B) HeLa cells (−) or cells transduced with siRNAs encoding either scrambled control or NPM-specific sequences were harvested 72 h posttransduction for cellular fractionation. Proteins from nuclear (N) and cytosolic (C) fractions were analyzed by SDS-PAGE and immunoblotted with antibodies recognizing rpL5, SOD (cytoplasm control), and lamin A/C (nuclear control). (C) HeLa cells were transfected with His-NPM or His-NPMdL, and 24 h later equal numbers of cells were subjected to fractionation into cytoplasmic (C) and nuclear (N) extracts. L5 protein was detected by Western blot analysis (top panels; WB). Lamin A/C and SOD are shown as nuclear and cytoplasmic fractionation controls, respectively (top panels; WB). 5S rRNA was detected by Northern blot analysis of total RNA extracted from the nuclear and cytosolic fractions (bottom panel; NB). The ratios of nuclear to cytoplasmic

examined the direct influence of NPM shuttling mutants on rpL5 nuclear export using a previously characterized GFP-tagged rpL5 protein (41). To confirm that GFP-rpL5 retained the NPM-binding properties of the endogenous rpL5 protein, we transiently overexpressed GFP-rpL5 in HeLa cells and performed Western blot analysis of GFP-immunoprecipitated complexes. As shown in Fig. 7A, precipitated GFP-rpL5 complexes contained endogenous NPM, confirming that the GFP moiety does not adversely affect the formation of NPM-rpL5 complexes in vivo. GFP-rpL5 and His-NPM readily migrated from human nucleoli to mouse nucleoli, as visualized in interspecies heterokaryons (Fig. 7B). However, in the presence of LMB, both GFP-rpL5 and His-NPM failed to shuttle (95% inhibition; Fig. 7C). Introduction of NPM shuttling mutant $NPM_{\Delta 42-61}$ or NPMdL inhibited GFP-rpL5 shuttling into mouse nucleoli, restricting its expression to human nuclei (Fig. 7D and E; 96% and 100% inhibition, respectively), establishing that NPM nuclear export is required for the export of rpL5. To more definitively show that NPM is required for rpL5 nuclear export, we knocked down NPM expression in HeLa cells (Fig. 8A). Cells lacking NPM protein expression failed to accumulate rpL5 in the cytoplasm, while cells transduced with scrambled small interfering RNA (siRNA) as a control exhibited an equal distribution of rpL5 between the nucleus and cytoplasm (Fig. 8B). These data underscore the necessity of NPM proteins for the efficient transport of rpL5 out of the nucleus and into the cytoplasm.

Ribosomal protein L5 is known to bind specifically to the mature 5S rRNA and aid in its nucleocytoplasmic transport (31, 37, 47). We hypothesized that NPM export, through its influence on rpL5, is the critical determinant for 5S rRNA nuclear export. To test this hypothesis, we performed Northern blot analysis of similar cellular fractions in the presence and absence of NPM shuttling. Indeed, in the presence of dominant negative NPM shuttling mutants, 5S rRNA failed to accumulate in the cytosol and instead was retained in the nucleus in a ratio similar to that for rpL5 (Fig. 8C). In addition to our fractionation studies, we performed RNA FISH to visualize the localization of steady-state levels of 5S rRNA. As shown in Fig. 8D, 5S rRNA was distributed throughout the nucleoli/nuclei and cytoplasm of HeLa cells transduced with empty vector as well as with wild-type NPM. Consistent with our fractionation data, inhibition of NPM and rpL5 nuclear export with LMB or NPMdL resulted in a severe attenuation of 5S rRNA export to the cytosol (Fig. 8D).

To further expand on this theme, we transduced wild-type MEFs with ARF, a known inhibitor of NPM nuclear export (7). Again, in the presence of the ARF tumor suppressor, 5S rRNA failed to transit to the cytosol and instead was retained the nucleoplasm (Fig. 8E). These data imply that ARF and NPM mutants defective in shuttling act similarly to prevent rpL5-5S rRNA nuclear export. To determine whether NPM shuttling mutants also prevent cell cycle progression, HeLa cells transduced with NPM expression constructs were labeled with 5-bromodeoxyuridine (BrdU) to measure active DNA synthesis. Similar to ARF's known cell cycle arrest properties (7), cells expressing NPMdL or $NPM_{\Delta 42-61}$ failed to enter S phase (Fig. 8F). Thus, NPM shuttling activity is not only required for the nuclear export of the rpL5-5S rRNA complex but also necessary for continued cell proliferation.

DISCUSSION

The nucleolus, a highly specialized and structured organelle, has been described as the cell's control center for ribosomal synthesis, maturation, and assembly, with a host of proteins, RNAs, and other factors being implicated in these processes (8). Recently, numerous proteins (cdc14, NPM, cyclin E, Mybbp1a, telomerase reverse transcriptase, and others) have been shown to continuously shuttle from the nucleolus to various subcellular compartments in a regulated manner, providing evidence that the nucleolus is a dynamic site of multiple cellular events (4, 7, 21, 22, 52).

One such protein, NPM/B23, has been linked to a variety of important cellular processes, both in and out of the nucleolus, including ribosome processing, molecular chaperoning, maintenance of genomic integrity, centrosome duplication, and transcriptional regulation (9, 10, 13, 16, 23, 35). Initially, NPM which was imported into the nucleolus from the cytoplasm was presumed to move about the various compartments of the nucleus (6), a feature shared by many critical cell cycle regulators. This shuttling of proteins between the nucleus and cytoplasm is now recognized as a key mechanism for ensuring proper cell cycle progression (39, 43). In previous reports, we and others identified NPM as a novel p53-independent target of the ARF tumor suppressor protein (5, 7, 19). We have since shown that, in response to hyperproliferative signals, nucleolar ARF directly binds NPM, effectively inhibiting NPM's nucleocytoplasmic shuttling. Here, we have further explored the mechanism and significance of NPM intracellular trafficking. First, we have described the CRM1-dependent nuclear export of NPM, identifying the two leucine residues (42 and 44) that are critical to this process. In addition, we have shown that alteration of the NPM NES resulted in the failure of wild-type NPM to be exported out of the nucleolus, providing evidence that these mutations function in a dominant-negative fashion,

accumulation of rpL5 and 5S rRNA are given as percentages of totals (*, $P > 0.001$). (D) HeLa cells were transfected with vector, His-NPM, or His-NPMdL, and cells were plated on glass coverslips. Twenty-four hours later, cells were subjected to RNA FISH with a TRITC-labeled 5S rRNA probe. Nuclei were stained with DAPI. Untransfected HeLa cells were treated with LMB for 18 h prior to RNA FISH analysis. Results of 5S rRNA localization are each representative of three independent experiments. (E) Wild-type (WT) MEFs were infected with control retroviruses or those encoding ARF, and 48 h later equal numbers of cells were subjected to fractionation into cytoplasmic (C) and nuclear (N) extracts. 5S rRNA was detected by Northern blot analysis of total RNA extracted from the nuclear and cytosolic fractions (*, $P > 0.005$). (F) HeLa cells were transfected with vector, His-NPM, His-NPMdL, or His-$NPM_{\Delta 42-61}$ and plated on glass coverslips. Cells were incubated with BrdU 72 h posttransfection and fixed 20 h later. Fixed cells were stained with antibodies recognizing BrdU and His epitopes and visualized by immunofluorescence using fluorescein isothiocyanate- and TRITC-labeled secondary antibodies, respectively. Cells (100) were counted for each condition in triplicate. Standard deviations are reported as error bars (*, $P > 0.005$).

through the formation of NPM-NPMdL heteromultimers. Thus, NPMdL mimics the effects of ARF induction by directly impeding the nucleocytoplasmic shuttling of NPM through direct interaction, further demonstrating that NPM must exit the nucleolus/nucleus to maintain and promote cell growth.

We have previously proposed that targets of nucleolar sequestration might in fact "ride the ribosome" from the nucleolus to the cytoplasm to engage in growth-promoting events (45). In agreement with this hypothesis, our findings reveal a direct interaction between NPM and rpL5, providing the first physical link between NPM and ribosomal subunits. Much of the field's focus has been on the putative role of rpL5 in delivering 5S rRNA to the nucleolus, following the initial transcription of 5S rRNA by RNA polymerase III in the nucleoplasm (31, 37, 47). However, it is also possible that rpL5 is a critical player in the export of the large ribosomal subunit (60S), containing 5S rRNA, from the nucleolus/nucleus to the cytoplasm after its assembly. Clearly, the latter events would render themselves sensitive to NPM regulation, given that NPM provides the necessary export signals and chaperoning capabilities (via rpL5) required to transport components of the ribosome to the cytosol. Indeed, inhibition of NPM nuclear export via deletion or mutation of its NES prevented the trafficking of rpL5, an integral component of the 60S ribosomal subunit. Moreover, reduction of NPM expression through RNA interference completely abolished the cytosolic stores of rpL5, underscoring the absolute requirement for NPM in rpL5 nuclear export. Thus, our initial hypothesis of "riding the ribosome" should be revised to "taking the ribosome for a ride."

While many components of the ribosome, including rpL5, encode their own NESs, it is clear that a single NES forms a relatively weak interaction with CRM1 (25), suggesting a requirement for additional NESs in the efficient export of complexes. Consequently, proteins like NPM and NMD3 may have evolved to serve this purpose. Additionally, NPM and rpL5 were found, in reduced amounts, in cytosolic 40S and 60S complexes, respectively, after LMB treatment, implying either that these particular protein-ribosome complexes are fairly stable or that minor fractions of NPM and rpL5 utilize CRM1-independent modes of transport from the nucleus. Considering that the predominant function of rpL5 is to bind and mobilize 5S rRNA molecules, it was not surprising that 5S transport was also NPM sensitive, and thus NPM contributes to the efficient nuclear export of rpL5-5S rRNA complexes. However, NPM was present in 40S, 60S, 80S, and polysomes in the cytoplasm, implying that NPM, free (within the 40S subunit) or bound to rpL5, remains associated with the mature ribosome as it assembles and forms actively translating polysomes in the cytosol. Taken together, these findings open up the possibility that NPM might transmit additional cues (beyond nuclear export) to cytosolic ribosomes during translation, consistent with nucleolus's proposed role in dictating translation rates (28).

While it has been appreciated for several decades that changes in nucleolar structure are reliable markers of cellular transformation, experiments that provide a direct link between nucleolar dysfunction and tumorigenesis remain to be conducted. In fact, the nucleolus has largely been dismissed as a static organelle, having little to no impact on the overall well-being of the cell. However, this "nucleolar stigma" recently has been challenged with the discovery that tumor suppressors, such as p53 and ARF, play a direct role in regulating nucleolar processes (5, 7, 42, 49). Interestingly, rpL5 is also a binding partner of Mdm2 and p53 (12, 17, 29), suggesting that rpL5 may provide an intriguing mechanistic link between ARF and ARF-binding partners. Clearly, through its interaction with NPM, ARF is capable of inhibiting nuclear export of rpL5-5S rRNA complexes. Inhibition of NPM-directed rpL5-5S nuclear export by ARF or NPM mutants defective in shuttling results in cell cycle arrest, demonstrating the importance of rpL5-5S export in maintaining cell proliferation. Moreover, NPM itself is a unique player in both the p53 and ARF responses (10, 11), providing us with a glimpse of how this network of protein interactions may inevitably become sensitive to oncogenic and tumor-suppressive signals in determining tumorigenic cell fates.

ACKNOWLEDGMENTS

We thank J. Alan Diehl and Joachim Hauber for plasmid constructs as well as Loryn Rikimaru, Yijun Yi, and Myla Ashfaq for their excellent technical assistance. We are extremely grateful to Alan Diehl, Chuck Sherr, Greg Longmore, Helen Piwnica-Worms, David Gutmann, and Joseph Baldassare for insightful discussions.

Y.Y. and A.J.A. are recipients of a grant-in-aid from the Department of Defense Breast Cancer Research Program (BC030793). L.B.M. is supported by the Department of Defense Prostate Cancer Research Program under award number PC040009. H.L. is supported by a grant from the National Cancer Institute (CA-095441). J.D.W. thanks the Pew Charitable Trusts and is a recipient of grant-in-aid from the National Institutes of Health (GM-066032).

Views and opinions of, and endorsements by, the author(s) do not reflect those of the U.S. Army or the Department of Defense.

REFERENCES

1. **Andersen, J. S., Y. W. Lam, A. K. Leung, S. E. Ong, C. E. Lyon, A. I. Lamond, and M. Mann.** 2005. Nucleolar proteome dynamics. Nature **433:**77–83.
2. **Andersen, J. S., C. E. Lyon, A. H. Fox, A. K. Leung, Y. W. Lam, H. Steen, M. Mann, and A. I. Lamond.** 2002. Directed proteomic analysis of the human nucleolus. Curr. Biol. **12:**1–11.
3. **Ashe, H. L., J. Monks, M. Wijgerde, P. Fraser, and N. J. Proudfoot.** 1997. Intergenic transcription and transinduction of the human beta-globin locus. Genes Dev. **11:**2494–2509.
4. **Azzam, R., S. L. Chen, W. Shou, A. S. Mah, G. Alexandru, K. Nasmyth, R. S. Annan, S. A. Carr, and R. J. Deshaies.** 2004. Phosphorylation by cyclin B-Cdk underlies release of mitotic exit activator Cdc14 from the nucleolus. Science **305:**516–519.
5. **Bertwistle, D., M. Sugimoto, and C. J. Sherr.** 2004. Physical and functional interactions of the Arf tumor suppressor protein with nucleophosmin/B23. Mol. Cell. Biol. **24:**985–996.
6. **Borer, R. A., C. F. Lehner, H. M. Eppenberger, and E. A. Nigg.** 1989. Major nucleolar proteins shuttle between nucleus and cytoplasm. Cell **56:**379–390.
7. **Brady, S. N., Y. Yu, L. B. Maggi, Jr., and J. D. Weber.** 2004. ARF impedes NPM/B23 shuttling in an Mdm2-sensitive tumor suppressor pathway. Mol. Cell. Biol. **24:**9327–9338.
8. **Busch, H., and K. Smetana.** 1970. The nucleolus. Academic Press, New York, N.Y.
9. **Chan, W. Y., Q. R. Liu, J. Borjigin, H. Busch, O. M. Rennert, L. A. Tease, and P. K. Chan.** 1989. Characterization of the cDNA encoding human nucleophosmin and studies of its role in normal and abnormal growth. Biochemistry **28:**1033–1039.
10. **Colombo, E., P. Bonetti, E. Lazzerini Denchi, P. Martinelli, R. Zamponi, J. C. Marine, K. Helin, B. Falini, and P. G. Pelicci.** 2005. Nucleophosmin is required for DNA integrity and p19Arf protein stability. Mol. Cell. Biol. **25:**8874–8886.
11. **Colombo, E., J. C. Marine, D. Danovi, B. Falini, and P. G. Pelicci.** 2002. Nucleophosmin regulates the stability and transcriptional activity of p53. Nat. Cell Biol. **4:**529–533.
12. **Dai, M. S., and H. Lu.** 2004. Inhibition of MDM2-mediated p53 ubiquitination and degradation by ribosomal protein L5. J. Biol. Chem. **279:**44475–44482.
13. **Feuerstein, N., S. Spiegel, and J. J. Mond.** 1988. The nuclear matrix protein, numatrin (B23), is associated with growth factor-induced mitogenesis in Swiss 3T3 fibroblasts and with T lymphocyte proliferation stimulated by lectins and anti-T cell antigen receptor antibody. J. Cell Biol. **107:**1629–1642.
14. **Fornerod, M., M. Ohno, M. Yoshida, and I. W. Mattaj.** 1997. CRM1 is an export receptor for leucine-rich nuclear export signals. Cell **90:**1051–1060.

15. **Fukuda, M., S. Asano, T. Nakamura, M. Adachi, M. Yoshida, M. Yanagida, and E. Nishida.** 1997. CRM1 is responsible for intracellular transport mediated by the nuclear export signal. Nature **390:**308–311.
16. **Grisendi, S., R. Bernardi, M. Rossi, K. Cheng, L. Khandker, K. Manova, and P. P. Pandolfi.** 2005. Role of nucleophosmin in embryonic development and tumorigenesis. Nature **437:**147–153.
17. **Guerra, B., and O. G. Issinger.** 1998. p53 and the ribosomal protein L5 participate in high molecular mass complex formation with protein kinase CK2 in murine teratocarcinoma cell line F9 after serum stimulation and cisplatin treatment. FEBS Lett. **434:**115–120.
18. **Hadjiolov, A. A.** 1984. The nucleolus and ribosome biogenesis. Springer-Verlag, New York, N.Y.
19. **Itahana, K., K. P. Bhat, A. Jin, Y. Itahana, D. Hawke, R. Kobayashi, and Y. Zhang.** 2003. Tumor suppressor ARF degrades B23, a nucleolar protein involved in ribosome biogenesis and cell proliferation. Mol. Cell **12:**1151–1164.
20. **Johnson, A. W., E. Lund, and J. Dahlberg.** 2002. Nuclear export of ribosomal subunits. Trends Biochem. Sci. **27:**580–585.
21. **Juan, G., and C. Cordon-Cardo.** 2001. Intranuclear compartmentalization of cyclin E during the cell cycle: disruption of the nucleoplasm-nucleolar shuttling of cyclin E in bladder cancer. Cancer Res. **61:**1220–1226.
22. **Keough, R. A., E. M. Macmillan, J. K. Lutwyche, J. M. Gardner, F. J. Tavner, D. A. Jans, B. R. Henderson, and T. J. Gonda.** 2003. Myb-binding protein 1a is a nucleocytoplasmic shuttling protein that utilizes CRM1-dependent and independent nuclear export pathways. Exp. Cell Res. **289:**108–123.
23. **Kondo, T., N. Minamino, T. Nagamura-Inoue, M. Matsumoto, T. Taniguchi, and N. Tanaka.** 1997. Identification and characterization of nucleophosmin/B23/numatrin which binds the anti-oncogenic transcription factor IRF-1 and manifests oncogenic activity. Oncogene **15:**1275–1281.
24. **Kudo, N., B. Wolff, T. Sekimoto, E. P. Schreiner, Y. Yoneda, M. Yanagida, S. Horinouchi, and M. Yoshida.** 1998. Leptomycin B inhibition of signal-mediated nuclear export by direct binding to CRM1. Exp. Cell Res. **242:**540–547.
25. **Kutay, U., and S. Guttinger.** 2005. Leucine-rich nuclear-export signals: born to be weak. Trends Cell Biol. **15:**121–124.
26. **Li, Y. P., R. K. Busch, B. C. Valdez, and H. Busch.** 1996. C23 interacts with B23, a putative nucleolar-localization-signal-binding protein. Eur. J. Biochem. **237:**153–158.
27. **Liu, H. T., and B. Y. Yung.** 1999. In vivo interaction of nucleophosmin/B23 and protein C23 during cell cycle progression in HeLa cells. Cancer Lett. **144:**45–54.
28. **Maggi, L. B., Jr., and J. D. Weber.** 2005. Nucleolar adaptation in human cancer. Cancer Investig. **23:**599–608.
29. **Marechal, V., B. Elenbaas, J. Piette, J. C. Nicolas, and A. J. Levine.** 1994. The ribosomal L5 protein is associated with mdm-2 and mdm-2-p53 complexes. Mol. Cell. Biol. **14:**7414–7420.
30. **Marion, M. J., and C. Marion.** 1987. Localization of ribosomal proteins on the surface of mammalian 60S ribosomal subunits by means of immobilized enzymes. Correlation with chemical cross-linking data. Biochem. Biophys. Res. Commun. **149:**1077–1083.
31. **Michael, W. M., and G. Dreyfuss.** 1996. Distinct domains in ribosomal protein L5 mediate 5 S rRNA binding and nucleolar localization. J. Biol. Chem. **271:**11571–11574.
32. **Namboodiri, V. M., I. V. Akey, M. S. Schmidt-Zachmann, J. F. Head, and C. W. Akey.** 2004. The structure and function of *Xenopus* NO38-core, a histone chaperone in the nucleolus. Structure **12:**2149–2160.
33. **Namboodiri, V. M., S. Dutta, I. V. Akey, J. F. Head, and C. W. Akey.** 2003. The crystal structure of *Drosophila* NLP-core provides insight into pentamer formation and histone binding. Structure (Cambridge) **11:**175–186.
34. **Namboodiri, V. M., M. S. Schmidt-Zachmann, J. F. Head, and C. W. Akey.** 2004. Purification, crystallization and preliminary X-ray analysis of the N-terminal domain of NO38, a nucleolar protein from *Xenopus laevis*. Acta Crystallogr. Sect. D Biol. Crystallogr. **60:**2325–2327.
35. **Okuda, M., H. F. Horn, P. Tarapore, Y. Tokuyama, A. G. Smulian, P. K. Chan, E. S. Knudsen, I. A. Hofmann, J. D. Snyder, K. E. Bove, and K. Fukasawa.** 2000. Nucleophosmin/B23 is a target of CDK2/cyclin E in centrosome duplication. Cell **103:**127–140.
36. **Okuwaki, M., K. Matsumoto, M. Tsujimoto, and K. Nagata.** 2001. Function of nucleophosmin/B23, a nucleolar acidic protein, as a histone chaperone. FEBS Lett. **506:**272–276.
37. **Pieler, T., and F. Rudt.** 1997. Nucleocytoplasmic transport of 5S ribosomal RNA. Semin. Cell Dev. Biol. **8:**79–82.
38. **Pinol-Roma, S.** 1997. HnRNP proteins and the nuclear export of mRNA. Semin. Cell Dev. Biol. **8:**57–63.
39. **Piwnica-Worms, H.** 1999. Cell cycle. Fools rush in. Nature **401:**535, 537.
40. **Pollard, V. W., W. M. Michael, S. Nakielny, M. C. Siomi, F. Wang, and G. Dreyfuss.** 1996. A novel receptor-mediated nuclear protein import pathway. Cell **86:**985–994.
41. **Rosorius, O., B. Fries, R. H. Stauber, N. Hirschmann, D. Bevec, and J. Hauber.** 2000. Human ribosomal protein L5 contains defined nuclear localization and export signals. J. Biol. Chem. **275:**12061–12068.
42. **Rubbi, C. P., and J. Milner.** 2003. Disruption of the nucleolus mediates stabilization of p53 in response to DNA damage and other stresses. EMBO J. **22:**6068–6077.
43. **Ryan, K. M., A. C. Phillips, and K. H. Vousden.** 2001. Regulation and function of the p53 tumor suppressor protein. Curr. Opin. Cell Biol. **13:**332–337.
44. **Scherl, A., Y. Coute, C. Deon, A. Calle, K. Kindbeiter, J. C. Sanchez, A. Greco, D. Hochstrasser, and J. J. Diaz.** 2002. Functional proteomic analysis of human nucleolus. Mol. Biol. Cell **13:**4100–4109.
45. **Sherr, C. J., and J. D. Weber.** 2000. The ARF/p53 pathway. Curr. Opin. Genet. Dev. **10:**94–99.
46. **Spector, D. L., R. L. Ochs, and H. Busch.** 1984. Silver staining, immunofluorescence, and immunoelectron microscopic localization of nucleolar phosphoproteins B23 and C23. Chromosoma **90:**139–148.
47. **Steitz, J. A., C. Berg, J. P. Hendrick, H. La Branche-Chabot, A. Metspalu, J. Rinke, and T. Yario.** 1988. A 5S rRNA/L5 complex is a precursor to ribosome assembly in mammalian cells. J. Cell Biol. **106:**545–556.
48. **Strezoska, Z., D. G. Pestov, and L. F. Lau.** 2000. Bop1 is a mouse WD40 repeat nucleolar protein involved in 28S and 5.8S rRNA processing and 60S ribosome biogenesis. Mol. Cell. Biol. **20:**5516–5528.
49. **Sugimoto, M., M. L. Kuo, M. F. Roussel, and C. J. Sherr.** 2003. Nucleolar Arf tumor suppressor inhibits ribosomal RNA processing. Mol. Cell **11:**415–424.
50. **Tao, W., and A. J. Levine.** 1999. Nucleocytoplasmic shuttling of oncoprotein Hdm2 is required for Hdm2-mediated degradation of p53. Proc. Natl. Acad. Sci. USA **96:**3077–3080.
51. **Trotta, C. R., E. Lund, L. Kahan, A. W. Johnson, and J. E. Dahlberg.** 2003. Coordinated nuclear export of 60S ribosomal subunits and NMD3 in vertebrates. EMBO J. **22:**2841–2851.
52. **Wong, J. M., L. Kusdra, and K. Collins.** 2002. Subnuclear shuttling of human telomerase induced by transformation and DNA damage. Nat. Cell Biol. **4:**731–736.
53. **Yung, B. Y., and P. K. Chan.** 1987. Identification and characterization of a hexameric form of nucleolar phosphoprotein B23. Biochim. Biophys. Acta **925:**74–82.

Nucleophosmin directs ribosome nuclear export and cell growth

Leonard B. Maggi, Jr.[1], Yue Yu[1], Silvia Grisendi[2], Wanghai Zhang[1], R. Reid Townsend[3], Howard L. McLeod[1], Pier Paolo Pandolfi[2], and Jason D. Weber[1*]

[1]Department of Medicine, Division of Molecular Oncology, Siteman Cancer Center, Washington University School of Medicine, St. Louis, MO 63110, USA

[2]Cancer Biology and Genetics Program, Department of Pathology, Sloan-Kettering Institute, Memorial Sloan-Kettering Cancer Center, New York, NY 10021, USA

[3]Department of Medicine, Division of Metabolism and Proteomics Center, Siteman Cancer Center, Washington University School of Medicine, St. Louis, MO 63110, USA

Running Title: *NPM directs ribosome export*

Key Words: Nucleolus/Ribosome/Nucleophosmin/Export/Transformation

[*] Please address correspondence to:
Jason D. Weber, Ph.D.
Department of Medicine
Division of Molecular Oncology
Washington University School of Medicine
Campus Box 8069
660 South Euclid Avenue
St. Louis, MO 63110, USA
Tel: (314) 747-3896
Fax: (314) 747-2797
jweber@im.wustl.edu

Abstract

Nucleophosmin (NPM/B23) is an essential protein in mouse development and cell growth. NPM is a critical target of ARF tumor suppression while, in the absence of *ARF*, NPM is capable of transforming cells. Here, we present the first reported mechanism for NPM's regulation of cell growth; NPM directs the nuclear export of both 40S and 60S ribosomal subunits. Transduction of NPM shuttling-defective mutants or loss of *Npm*, inhibited nuclear export of both the 40S and 60S ribosomal subunits, reduced the available pool of cytoplasmic polysomes, and diminished overall protein synthesis without affecting ribosomal RNA processing. Modest increases in NPM expression amplified the export of newly synthesized ribosomal RNAs, resulting in increased rates of protein synthesis and indicating that NPM is rate-limiting in this pathway. These results support the idea that NPM-regulated ribosome export is a fundamental process in growth and cellular transformation.

Introduction

The nucleolus is a dynamic subnuclear organelle that contains proteins not only involved in ribosome production but also oncogenesis and tumor suppression (Maggi and Weber 2005). As the site for ribosome biogenesis, a cell's nucleoli are centered around ribosomal DNA (rDNA) genes which are transcribed to produce ribosomal RNAs (rRNAs) (Warner 1990). A host of proteins are involved in the intricate processing and assembly steps required to produce the small, 40S, and large, 60S, ribosomal subunits (Warner 1990; Eichler and Craig 1994; Moss and Stefanovsky 2002). Once exported from the nucleus, the 40S and 60S subunits are combined in the cytoplasm to form functional 80S subunits (Johnson et al. 2002; Moss and Stefanovsky 2002). While the steps involved in the transcription and processing of rRNAs within the nucleolus are beginning to be understood, little is known about how ribosomal subunits are exported to the cytosol in mammalian cells. Studies from *Saccharomyces cerevisiae* and *Xenopus laevis* oocytes have shown that the process is dependent on the CRM1-RanGTP export receptor pathway (Johnson et al. 2002). Additionally, NMD3, a highly conserved adapter protein, assists in the nuclear export of the 60S subunit in yeast (Ho and Johnson 1999). However, experiments in mammalian cells demonstrated that nuclear export of rRNAs was not completely dependent on NMD3, with some rRNAs not affected at all (Trotta et al. 2003). Thus other nucleolar proteins must be involved in the nuclear export of ribosomes.

The difficulty in assessing nucleolar protein function stems from early assumptions that all nucleolar proteins must be involved, in some way, with rDNA transcription or rRNA processing by virtue of their unique subnuclear localization. However, a more contemporary view of the nucleolus as a dynamic nuclear organelle capable of regulating numerous cellular processes, apart from rDNA transcription and rRNA processing, has led to a re-evaluation of

nucleolar protein function(s). Nucleophosmin (NPM) is an abundant nucleolar phospho-protein that is highly expressed in proliferating cells (Feuerstein et al. 1988). Our lab and others have shown that NPM is a target of the nucleolar tumor suppressor, p19ARF (Itahana et al. 2003; Bertwistle et al. 2004; Brady et al. 2004). We have shown that NPM can shuttle from the nucleolus/nucleus to the cytoplasm, but upregulation of ARF can block its nucleolar/cytoplasmic trafficking (Brady et al. 2004). NPM shuttling requires a conserved CRM1 binding site and mutation of two critical leucine residues blocks NPM's ability to leave the nucleus (Yu et al. 2006). Additionally, NPM is an essential nucleolar protein with acute loss of expression resulting in severe attenuation of cellular proliferation and increased apoptosis (Itahana et al. 2003; Bertwistle et al. 2004; Brady et al. 2004). In agreement with these *in vitro* findings, two recent reports have shown that *Npm* is required for embryonic development and that fibroblasts derived from *Npm*-deficient embryos have a reduced capacity to proliferate (Colombo et al. 2005; Grisendi et al. 2005). Given NPM's reported involvement in numerous cellular processes as diverse as ribosome biogenesis (Okuwaki et al. 2002), centrosome duplication (Okuda et al. 2000), chaperoning (Okuwaki et al. 2001), and transcriptional control (Colombo et al. 2002), the underlying mechanism behind NPM's requirement for cellular proliferation has remained elusive.

In an effort to uncover this mechanism, we observed a consistent increase in cell size and proliferative capacity of fibroblasts overexpressing NPM that was dependent on the nuclear export activities of NPM. Furthermore, NPM trafficking led to amplified protein synthesis rates, underscoring the ability of NPM to drive growth and proliferation. Here, we describe the mechanism behind this observation, revealing a prominent role for NPM in driving ribosome nuclear export and thereby controlling cell growth.

Results

NPM is a Potent Oncogene in the Absence of ARF

NPM is induced upon mitogenic stimulation and is a direct transcriptional target of the *Myc* oncogene, providing the first evidence that NPM might be involved in cell cycle progression (Guo et al. 2000; Zeller et al. 2001; Menssen and Hermeking 2002; Watson et al. 2002). In order to further assess the role of NPM in promoting cell proliferation and transformation, we examined the effects of NPM overexpression on cell growth, S phase entry, and cellular transformation in immortalized *ARF*$^{-/-}$ mouse embryonic fibroblasts (MEFs) (Kamijo et al. 1997). As shown in Figure 1A, NPM overexpression induced a significant increase in cell size as measured by flow cytometry forward and side scatter, to a slightly greater extent than oncogenic Ras^{V12}. *Arf*$^{-/-}$ MEFs transduced with either vector control or wild-type NPM readily enter S phase, as evidenced by incorporation of BrdU into replicating DNA (Figure 1B). In contrast, an NPM shuttling mutant, NPMdL (Yu et al. 2006), significantly attenuated S phase entry (Figure 1B), implying that NPM nuclear export is required for S phase entry. We next assessed the ability of NPM to transform immortalized *Arf*$^{-/-}$ MEFs in colony formation assays. Overexpression of NPM resulted in increased colony size in soft agar over control (Figure 1D, upper panels) although not as large as Ras^{V12} colonies, as well as an increase in foci number (lower panels). Again, expression of the NPM shuttling mutant blocked colony growth in soft agar as well as foci formation, supporting the role of NPM nuclear export in these processes.

In order to further assess the role of NPM in promoting cell proliferation and transformation, we analyzed 60 carcinoma samples from breast, prostate and colon cancers. Approximately 10-18 % of the actively proliferating tumor samples (Ki-67 positive) stained negative for NPM (Figure 1B, left panels), indicating that not all highly proliferative tumor cells

engage in NPM overexpression as a readout of active cell cycle progression. The remainder of the samples stained positive for NPM (82-90%) with nearly 50% of the NPM-positive tumor samples, irregardless of tumor type, exhibiting particularly strong nuclear/nucleolar NPM staining (Figure 1D, right panels).

Arf$^{-/-}$ MEFs, although immortal, remain diploid (Kamijo et al. 1997) and retain normal centrosome numbers throughout cellular passaging *in vitro* (see below). Given previous findings that NPM plays a key role in centrosome duplication, we next sought to determine whether introduction of exogenous NPM altered the ploidy of *Arf*$^{-/-}$ cells through centrosome amplification. Additionally, Grisendi and colleagues recently showed that *Npm* loss results in multiple centrosome formation accompanied by genome instability, suggesting that NPM is a key regulator in maintaining proper centrosome duplication (Grisendi et al. 2005). As shown in Figure 1E, NPM overexpression did not alter centrosome number compared to control cells nor did it alter the overall chromosome number in *Arf*$^{-/-}$ MEFs (Figure 1F). Taken together these data demonstrate that the transforming properties of NPM are not coupled to its ability to regulate or dysregulate centrosome numbers and DNA ploidy.

Endogenous NPM Protein Complexes Contain Ribosomal Proteins

In an effort to conduct an unbiased assessment of NPM function in promoting growth and proliferation, we examined the composition of *in vivo* NPM protein complexes isolated from HeLa cells. Gel filtration and anion exchange chromatography of HeLa cell lysates revealed numerous distinct endogenous NPM complexes (Figure 3A and data not shown). Using native gel analysis of the sizing column fractions, we were able to determine that oligomeric NPM was present in protein complexes greater than 440 kDa (Figure 3A and data not shown). In an

attempt to identify the protein components of the NPM complex, we generated an NPM polyclonal antibody affinity column. Pooled NPM complexes eluted from the sizing column were cleared over an IgG column prior to passage over the NPM affinity column and eluted with increasing salt concentrations. Further separation of NPM protein complexes by two-dimensional electrophoresis aided in the positive identification of various NPM-associated proteins via mass spectrometry analysis (Figure 3B). Among those proteins bound to NPM, a cluster of proteins associated with ribosome biogenesis, as well as the nuclear pore complex proteins, Nup50 and Nup62, were identified (Figure 3B and Table 1). A complete list of NPM complex proteins is shown in Table 1. Notably, rpL5, nucleolin and Brca1 proteins identified from our isolated NPM complexes have previously been shown to interact with NPM, demonstrating the effectiveness of our approach to identifying NPM components (Liu and Yung 1999; Sato et al. 2004; Yu et al. 2006). Of the fifteen known proteins identified in our NPM complex, nine constitute integral components of the 40S and 60S ribosomal subunits. Additionally, six of the remaining nine NPM binding proteins are involved in translational regulation. Although we could not determine the exact stoichiometry of these complexes to one another, it was apparent that NPM protein complexes involved in some facet of ribosome biogenesis predominated.

NPM Nuclear Export is Required for Protein Synthesis

Testing the hypothesis that NPM-ribosomal protein complexes play a role in promoting cell growth, we next investigated the potential function of NPM in protein synthesis. HeLa cells transduced with empty vector, wild-type NPM or NPMdL, were labeled with ^{35}S-Methionine for the indicated times and total trichloroacetic acid-precipitable proteins were counted for label

incorporation. Addition of the shuttling defective mutant, NPMdL, significantly attenuated the rate of total protein synthesis. Interestingly, slight overexpression of wild-type NPM (Figure 4A inset) resulted in a significant increase in the rate of protein synthesis. This was not a result of simple acceleration of cell cycle progression as HeLa cells expressing exogenous NPM proliferated at a rate similar to control cells (data not shown).

We next examined NPM's ability to influence cytosolic ribosome profiles. Cytosolic ribosomes were isolated via sucrose gradient centrifugation from equal numbers of HeLa cells transduced with empty vector, wild-type NPM or NPMdL. Continuous evaluation of the gradient by ultraviolet absorbance for the presence of rRNAs indicated that in the absence of NPM shuttling (NPMdL), formation of cytosolic 40S and 60S ribosome subunits was dramatically impaired (Figure 4B, green line) while mild overexpression of NPM (Figure 4B, inset) resulted in enhanced formation of cytosolic 40S and 60S subunits (Figure 4B, blue line). Notably, NPM overexpression amplified (~30%) the amount of cytosolic ribosomes engaged in active mRNA translation (Figure 4B, blue line) in a mechanism that was dependent on the nuclear export activities of NPM molecules (Figure 4B, green line).

NPM is the Rate-limiting Factor for rRNA Nuclear Export and Cytosolic Ribosome Accumulation

We have presented data here that NPM nuclear export is required for the enhanced accumulation of cytosolic ribosomes and polysomes (Figure 4). To understand the mechanism behind this observed increase in cytosolic ribosomes, we examined the effects of NPM on the nuclear export of newly synthesized rRNAs. HeLa cells transduced with control vector, wild-type NPM, or the shuttling mutant, NPMdL, were pulsed with [methyl-^{3}H] methionine to label

newly synthesized and processed rRNAs (Sugimoto et al. 2003). Importantly, ectopic expression of wild-type NPM or NPMdL shuttling mutants had no affect on HeLa cell proliferation at the 24h time point used for these experiments (data not shown), allowing us to separate cell cycle progression from ribosomal biogenesis.

Consistent with our earlier findings for protein synthesis and ribosome profiles, NPMdL significantly attenuated (>12-fold) the cytoplasmic accumulation of all rRNAs to nearly undetectable levels (Figure 5A). In contrast, cells overexpressing wild-type NPM exhibited a significant increase (>7-fold) in the cytoplasmic accumulation of rRNAs (Figure 5A). We observed similar effects of NPM overexpression in $Arf^{-/-}$ MEFs (Figure 5B), indicating that these effects of NPM overexpression are not cell type specific and corroborate our initial growth and transformation findings in $Arf^{-/-}$ cells. Importantly, overexpression of NPM did not alter rRNA processing of newly transcribed 47S rRNA into 28S, 18S, and 5.8S rRNA species (Figure 5C), implying that increased accumulation of rRNAs in the cytosol was not simply due to enhanced rRNA processing in the nucleolus.

To determine the distribution of newly exported rRNAs into cytosolic ribosomes and polysomes, we pulse-labeled cells with [methyl-^{3}H] methionine and measured the amount of incorporated label in each sucrose gradient fraction containing 40S, 60S, 80S and polysomes. While NPM overexpression appeared to affect the steady-state levels of polysome production (~30%, Figure 4B), transduction of cells with wild-type NPM greatly increased (~3-fold) the amounts of newly exported cytosolic ribosomal subunits, including the 40S, 60S, 80S and polysomes available for protein synthesis (Figure 5D), underscoring the ability of NPM to not only enhance the export of ribosomal subunits, but also to provide more ribosomes for polysome-directed protein synthesis.

Loss of NPM Blocks rRNA Export *in vitro* and *in vivo*

Inhibition of NPM shuttling activity using the dominant negative mutant, NPMdL, indicates that NPM nuclear export is required for rRNA export to the cytoplasm. However, we cannot rule out the possibility that the NPMdL mutant prevents ribosome export in an indirect and passive manner. To confirm that NPM is required for the nuclear export of rRNAs, we examined the effects of loss of NPM on export of newly synthesized rRNAs. HeLa cells transduced with scrambled control or NPM-specific short interfering RNAs (siRNAs) (Yu et al. 2006) were pulsed with [methyl-^{3}H] methionine to label newly synthesized and processed rRNAs. Specific knockdown of endogenous NPM was confirmed (Figure 6A, bottom panel). Dramatic reduction of NPM protein expression significantly attenuated the cytoplasmic accumulation of all rRNAs to nearly undetectable levels (Figure 6A, top panel). In addition, transduction of HeLa cells with NPM siRNAs significantly decreased the steady state levels of all cytosolic ribosomal subunits (40S, 60S, 80S and polysomes) compared to scramble control (Figure 6B), providing strong evidence that NPM is an essential component in the nuclear export of ribosomal subunits and maintenance of sufficient pools of cytosolic polysomes. Similarly, MEFs carrying hypomorphic NPM alleles ($Npm^{hy/hy}$), which express nearly undetectable levels of NPM ((Grisendi et al. 2005) and Figure 6C, bottom panel), show a striking decrease in nuclear export of 28S and 18S rRNA compared to littermate matched wild-type MEFs (Figure 6C).

Embryos nullizygous for *Npm* fail to develop properly and die *in utero* between days 11.5 and 16.5 (Grisendi et al. 2005). To determine whether a defect in rRNA nuclear export might be responsible for the growth retardation observed in these *Npm*-null embryos, we examined *in vivo* 5S rRNA export. Utilizing a biotinylated 5S rRNA probe, we performed RNA *in situ*

hybridization on day E10.5 wild-type and *Npm*$^{-/-}$ embryos. Littermate matched wild-type embryos readily exported 5S rRNA (purple stain) out of the nucleus (pink stain) and into the cytoplasm in numerous embryonic cell compartments (Figure 7A-D). In contrast *Npm*$^{-/-}$ embryos did not export 5S rRNA in any of the embryonic cells as evidenced by the accumulation of dark nuclear 5S RNA stain (purple) and lack of cytoplasmic stain (Figure 7E-H). Taken together these data indicate that NPM is absolutely required for export of rRNAs *in vivo*.

Discussion

The nucleolus is a dynamic subnuclear organelle tasked with producing the core of the protein translation machinery of a cell: the ribosome (Warner 1990; Moss and Stefanovsky 2002). Historic models of nucleolar function have depicted ribosome biogenesis as a passive, reactionary process in the cell where growth signals are relayed to the nucleolus to increase ribosomal RNA (rRNA) synthesis, resulting in higher rates of ribosome production to meet the demands of increased proliferation rates. However, a more current view of the nucleolus as a sensor of both stress and growth has emerged. In challenge of this "static ribosome factory" model, numerous proteins originally thought to solely reside in the nucleolus have been recently shown to continuously shuttle from the nucleolus to various subcellular compartments in a regulated manner, providing evidence that the nucleolus is a dynamic site of numerous cellular events (Juan and Cordon-Cardo 2001; Keough et al. 2003; Azzam et al. 2004; Brady et al. 2004; Yu et al. 2006). One of these nucleolar proteins, NPM, has been suggested to be involved in a variety of important cellular processes in and out of the nucleolus including ribosome processing, molecular chaperoning, centrosome duplication, and transcriptional regulation (Feuerstein et al. 1988; Chan et al. 1989; Kondo et al. 1997; Okuda et al. 2000; Okuwaki et al. 2001; Okuwaki et al. 2002). Our current study offers data which integrates many of these seemingly disconnected functions of NPM.

One of the conundrums surrounding NPM is its apparent ability to perform functions that are in stark contrast to one another. Specifically, NPM has been reported to interact with all three components of the ARF-p53-Mdm2 pathway to both activate and suppress this cascade (Szebeni and Olson 1999; Colombo et al. 2002; Itahana et al. 2003; Bertwistle et al. 2004; Brady et al. 2004; Kuo et al. 2004; Kurki et al. 2004; Li et al. 2004). However, the overarching theme

of this pathway is the regulation of growth and proliferation. In this regards, we have shown that NPM can transform immortalized *Arf*$^{-/-}$ MEFs through increased protein synthesis rates, indicating, at the very least, that NPM is a growth promoter. Taken as single observations, numerous conflicting views of NPM function can be readily made. However, when placed together with our current findings, a more unified outlook on NPM function emerges as we will discuss below.

The mechanism of NPM's growth promoting properties is thought to be mandated through alterations in rRNA processing (Savkur and Olson 1998). We have clearly shown that NPM does not alter processing. In fact, we have presented evidence that NPM serves as a nuclear export chaperone for the ribosome, drawing similarities to earlier studies that showed an *in vitro* propensity for NPM to serve as a protein chaperone (Szebeni and Olson 1999; Okuwaki et al. 2001). Even modest increases in NPM protein expression amplified ribosome export resulting in increased rates of protein synthesis and ultimately cell growth, demonstrating that NPM is rate-limiting in its capacity to shuttle ribosomes to the cytosol. Under this model, NPM would serve as an adaptor, analogous to NMD3, bridging the ribosome with CRM1 prior to export through the nuclear pore (Trotta et al. 2003). In fact, we were able to co-purify nuclear pore proteins Nup50 and Nup62 with NPM demonstrating that these export complexes exist *in vivo*.

The similarities between NPM and NMD3 are intriguing, but there are enough measurable differences to suggest that they do not perform identical functions and rather most likely, complement one another in their ability to act as nuclear export chaperones. Unlike NMD3, we found NPM in complexes with ribosomal proteins from both the small and large ribosome subunits. Additionally, mutation of the NMD3 NES results in only an attenuation of

the 28S rRNA (Trotta et al. 2003), whereas NPMdL readily inhibits the nuclear export of all newly synthesized 28S, 18S and 5S rRNAs, suggesting that NPM may reside upstream of NMD3 in regulating the nuclear export of all ribosomal subunits. Moreover, overexpression of NPM was capable of dramatically increasing ribosome nuclear export, a finding that has not been produced for NMD3. The dramatic sequestration of the entire ribosome in the nucleus by mutant NPM molecules is underscored further by the rapid depletion of newly assembled polysomes in cells unable to shuttle NPM protein complexes. Thus, we propose that NPM serves as a "growth thermostat" in the nucleolus, ready to respond to changes in the cell that might require more or less ribosome output for protein synthesis. Loss of *Npm* confirms this hypothesis, with $Npm^{hy/hy}$ and $Npm^{-/-}$ cells displaying severe attenuation of all rRNA export.

Given NPM's role in the nucleolar growth promoting pathway through regulating ribosome export, it is not surprising that several groups including our own have shown NPM to be a p53-independent target of the nucleolar tumor suppressor ARF (Itahana et al. 2003; Bertwistle et al. 2004; Brady et al. 2004). The fact that NPM promotes ribosome export in *Arf*-null cells leading to increased protein synthesis and cellular transformation, suggests that ARF itself is not the critical target of NPM as has been recently postulated (Korgaonkar et al. 2005). Instead, in order to maintain proper nucleolar function, ARF must be sensitive to abrupt changes in ribosome output, constantly monitoring the rate of ribosome synthesis and export by NPM. We tend to think of ARF as a sensor of hyperproliferative signals, such as those emanating from Myc and Ras (Palmero et al. 1998; Zindy et al. 1998; Groth et al. 2000), but both of these oncoproteins are quite capable of eliciting hyper-growth signals as well. Indeed, recent evidence has demonstrated that oncogenic myc translocates to the nucleolus in order to greatly increase ribosomal DNA synthesis (Arabi et al. 2005; Grandori et al. 2005), and under some settings,

ARF can act to antagonize nucleolar myc oncoproteins (Qi et al. 2004; Gregory et al. 2005). In order to maintain nucleolar integrity in the face of myc-induced increases in ribosomal RNAs, the cell would also require NPM to enhance the rate of ribosome nuclear export. In support of this notion, *Npm* is a direct transcriptional target of myc (Guo et al. 2000; Zeller et al. 2001; Menssen and Hermeking 2002; Watson et al. 2002). Accordingly, nucleolar ARF has evolved to monitor this process, and as such, is also a target of myc induction (Zindy et al. 1998). In human cancers, it then becomes advantageous to disrupt the normal regulation of this process. Under normal conditions, NPM is devoted to ribosome nuclear export and protein synthesis is maintained at a constant rate. We would predict that this nucleolar homeostasis is interrupted by two different signals. First, stress signals that alter nucleolar structures (Rubbi and Milner 2003) and de-localize NPM to the nucleoplasm where it binds to p53 or Mdm2 (Colombo et al. 2002; Kurki et al. 2004) would serve to not only activate the p53 pathway but also to divert NPM from its normal role in rRNA export. Dramatic decreases in protein synthesis rates are hallmarks of cellular stress outcomes (Pyronnet and Sonenberg 2001). Second, oncogenic growth signals that up-regulate NPM protein expression would also trigger the ARF checkpoint with accumulated nucleolar ARF proteins preventing the nuclear export of NPM-ribosome complexes. Thus, in the absence of an intact ARF checkpoint, NPM proteins are capable of amplifying the rate of rRNA export, resulting in dramatic unopposed increases in protein translation and eventual cell transformation recorded in this report.

Materials and methods

Cell Culture, Virus Production, and Nucleofection

HeLa cells and *Arf*$^{-/-}$ MEFs were maintained in Dulbecco's modified Eagle's medium (DMEM) with 10% fetal bovine serum, 2 mM glutamine, 0.1 mM non-essential amino acids, and 100 U penicillin and streptomycin. *Npm*$^{+/+}$ and *Npm*$^{hy/hy}$ litter matched MEFs were maintained in identical media with gentimycin. Virus production and infection of MEFs were carried out using retroviral helper and vector plasmids provided by Charles Sawyers (UCLA). HeLa cells ($2x10^6$) were nucleofected with 2 μg of the indicated plasmids according to manufacturer's instructions (Amaxa Inc.).

Plasmid Constructs

Retroviral vectors encoding full-length His-tagged murine NPM, NPMdL, and H-Ras^{V12} are described elsewhere (Groth et al. 2000; Brady et al. 2004; Yu et al. 2006) . His-epitope tagged NPM and His-NPMdL in pcDNA3.1 expression vectors have been previously described (Yu et al. 2006). Short-interfering RNAs against NPM and a scrambled control siRNA have been previously described (Yu et al. 2006).

FACS Analysis

Arf$^{-/-}$ MEFS infected with control, His-NPM, His-NPMdL, or Ras^{V12} retroviruses were harvested 72 h post-infection. Cells were fixed in 95% ethanol, washed and resuspended in 1X PBS/1% FBS, and filtered prior to cell size analysis using a FACSCalibur flow cytometer (Becton Dickson).

Western Blot Analysis

Cells were lysed by sonication in EBC buffer (25 mM Tris-HCl pH 8, 150 mM NaCl, 1 mM EDTA, 0.1% NP-40) at the indicated times. NPM, Lamin A/C, SOD, and His-tagged proteins were visualized by direct immunoblotting with NPM (Zymed), Lamin A/C (Santa Cruz), SOD (Santa Cruz), and His (Santa Cruz) antibodies, respectively. As a loading control, blots were probed with γ-tubulin antibody (Santa Cruz) as indicated.

Foci formation assay

Arf$^{-/-}$ MEFS were infected with control, His-NPM, His-NPMdL, or Ras^{V12} retroviruses and seeded (2 x 10^3) onto 100 mm dishes. Cells were grown for 14 days in complete medium, fixed in 100% MeOH and stained for 30 min with 50% Giemsa (vol:vol in H_2O).

Soft Agar Colony formation assay

Arf$^{-/-}$ MEFS were infected with control, His-NPM, His-NPMdL, or Ras^{V12} retroviruses and seeded (1 x 10^3) in quadruplicate wells of a 24 well plate. Colonies were allowed to grow for 14 days in complete media supplemented with FBS and Noble Agar.

Common Cancer Tissue Array

The TARP4 tissue array was purchased from NCI Tissue Array Research Project. The tissues used to construct arrays were obtained from the Cooperative Human Tissue Network (CHTN). Tissue array slides were mounted on siliconized glass slides and purchased ready for use in immunohistochemistry.

Immunohistochemistry

Immunohistochemistry was performed using the SABC method on a BioGenex i6000^{TM} automated staining system (BioGenex, San Ramon, CA). Briefly, de-paraffinized tissue sections were first treated with 3% H_2O_2 for 30 min to inhibit endogenous peroxidase followed by antigen retrieval by microwave heating in citra plus solution (BioGenex) for 15 min. After subjecting to avidin block, biotin block and power block for 15 min, respectively, the sections were incubated with mouse anti-NPM (Zymed) primary antibodies as described above for 1 h at room temperature with an antibody dilution of 1:50. After further incubation with biotinylated multi-link antibody for 45 min and peroxidase-labeled strepavadin for 30 min, the staining was developed by reaction with 3,3'-diaminobenzidine tetrahydrochloride substrate-chromogen solution for 3 min followed by counterstaining with hematoxylin for 10 sec.

Semi-quantitative assessment of NPM expression in human tumors

NPM signal was localized to the nucleolus and nucleus. The final staining scores were according to the extent of positive cells. 0-5% was scored as negative (-), 6-25% (+), 26-50% (++), 51-75% (+++). Cells exhibiting NPM staining (-) or (+++) are shown in the representative figure panel.

Fluid Phase Liquid Chromatography

HeLa cells were lysed in Tween-20 lysis buffer (10 mM Tris-HCl, pH 7.4; 150 mM NaCl; 0.1% Tween-20; 1 μM $NaVO_4$; 10 μM NaF; 1 mM PMSF; 1 μg/ml Aprotinin) by sonication. Lysates (600 μg) were injected on to a HiPrep 16/60 Sephacryl S-300 Column (Amersham). Proteins were eluted with 150 mM NaCl, 50 mM NaH_2PO_4 pH 7.2 using BioLogic fluid phase liquid chromatography (FPLC) and HR software (Bio-Rad). Fractions were precipitated with

trichloroacetic acid (TCA), re-suspended in 1 M Tris-HCl (pH 7.4), separated by SDS-PAGE, transferred to PVDF membranes and immunoblotted with antibodies recognizing NPM (Zymed). For affinity chromatography, a rabbit polyclonal antibody recognizing the N-terminus of NPM (Sigma) was bound to NHS-activated Sepharose (Amersham). HeLa cells were lysed in 20 mM Tris pH 7.4, 0.1% Tween-20 and sonicated. Lysates (600 μg) were injected first over the sizing column and subsequent NPM pools were loaded onto the NPM affinity column, washed with 20 mM Tris and eluted with an increasing NaCl gradient (0.1-1M). Collected fractions were pooled, precipitated, and subjected to proteomic analysis as described below.

Proteomic Analysis

Proteins from FPLC fractions were precipitated with TCA and resuspended in re-hydration buffer (BioRad). 500 μg of proteins and 12.5 μL of 200 mM tributylphosphine (BioRad) were mixed and loaded by passive in-gel re-hydration. IPG strips (BioRad, pH 3-10) were focused according to standard protocols. Separated proteins were stained with SYPRO-Ruby (BioRad). Tryptic peptides were calibrated with Sequazyme peptide mass standards kit (PE Biosystem) and analyzed by MALDI-TOF mass spectrometry (Voyager DE Pro, Applied Biosystems). Identification of proteins was performed using MS-Fit software (http://prospector.ucsf.edu/ucsfhtml4.0/msfit.htm) and verified using tandem MS/MS techniques.

^{35}S-Methionine labeling of newly synthesized proteins

HeLa cells were nucleofected with the indicated plasmids and 24 h later were labeled with 150 μCi ^{35}S-Methionine in 5 ml methionine-free media for the indicated times. Cells were harvested,

counted and equal numbers of cells were lysed. Total protein was precipitated with TCA, and ^{35}S-CPM was measured for each time point.

rRNA [methyl-^{3}H] Methionine and [^{3}H]Uridine Labeling

HeLa cells ($2x10^6$) were nucleofected with pcDNA3.1-His, His-tagged NPM or His-NPMdL. Cells were methionine starved for 15 min and labeled with 50 μCi/ml L-[methyl-^{3}H] methionine (Amersham) for 30 min followed by a 2 h ten-fold excess cold methionine chase. Cells were harvested, counted, and equal numbers were fractionated into cytoplasm and nuclei as described (Yu et al., 2006). Total RNA was isolated from the cytosolic and nuclear fractions with TRIZOL (Invitrogen), and fractionated by gel electrophoresis. *Arf*$^{-/-}$ MEFs infected with retroviruses encoding control, His-NPM, or Ras^{V12} were labeled with 50 μCi/ml [^{3}H]Uridine (Amersham) for 45 min followed by a 1 h chase in cold media. Total RNA was isolated from equal numbers of cells ($1.5x10^6$) with TRIZOL (Invitrogen), and fractionated by gel electrophoresis. RNA was transferred to Hybond-NX Membrane (Amersham), cross-linked, sprayed with EN^{3}HANCE (Perkin Elmer), and subjected to autoradiography.

Ribosome Fractionation

HeLa cells ($2x10^6$) were nucleofected with pcDNA3.1-His, His-tagged NPM or His-NPMdL. Cells were treated with 50 μg/ml cycloheximide prior to harvesting and counting. Cells ($3x10^6$) were subjected to cytoplasmic or nuclear ribosome fractionation as previously described (Strezoska et al. 2000). For radiolabeling of newly synthesized rRNAs, cells were labeled and fractionated as above. Fractions were collected, RNA extracted with TRIZOL, and ^{3}H-CPM was measured for each fraction and graphed for the 40S, 60S, 80S, and polysome peaks.

5S rRNA in situ hybridization

Sections from day E10.5 wild-type and *Npm*$^{-/-}$ embryos were mounted on glass slides as previously described (Grisendi et al. 2005). *In situ* RNA FISH analysis was performed using a biotin-labeled probe recognizing the 5S rRNA (GeneDetect.com) according to manufacturer's instructions. Biotin was detected using an in situ hybridization biotin detection kit from DakoCytomation (purple). Nuclear Fast Red (DakoCytomation) counterstaining was used to demarcate nuclei (pink). Whole embryos were visualized at 2X (WT) and 4X (*Npm*$^{-/-}$), respectively and cell images were observed at 60X magnification using a Nikon DIC compound microscope fitted with a Nikon FDX-35 charge-coupled device camera.

Densitometry and Image Analysis

Autoradiograms were scanned using a FlourChem8900 (Alpha Innotech), and densities were determined using NIH ImageJ version 1.33 software.

Acknowledgements

We are grateful to Loryn Rikimaru and Myla Ashfaq for excellent technical assistance and Alan Diehl, Joe Baldassare, Helen Piwnica-Worms, John Cleveland, Sheila Stewart and other members of the J.D.W. lab for discussion, critical reading of the manuscript and support. This work was funded by grants from the National Institutes of Health to P.P.P. and J.D.W and the Pew Scholars Program in Biomedical Sciences to J.D.W. Y.Y. is a recipient of grant-in-aid from the Department of Defense Breast Cancer Research Program (BC030793). L.B.M. is supported by the Department of Defense Prostate Cancer Research Program (PC040009). Views and opinions of, and endorsements by the author(s) do not reflect those of the US Army or the Department of Defense.

References

Arabi, A., S. Wu, K. Ridderstrale, H. Bierhoff, C. Shiue, K. Fatyol, S. Fahlen, P. Hydbring, O. Soderberg, I. Grummt, L.G. Larsson, and A.P. Wright. 2005. c-Myc associates with ribosomal DNA and activates RNA polymerase I transcription. *Nat Cell Biol* **7**: 303-10.

Azzam, R., S.L. Chen, W. Shou, A.S. Mah, G. Alexandru, K. Nasmyth, R.S. Annan, S.A. Carr, and R.J. Deshaies. 2004. Phosphorylation by cyclin B-Cdk underlies release of mitotic exit activator Cdc14 from the nucleolus. *Science* **305**: 516-9.

Bertwistle, D., M. Sugimoto, and C.J. Sherr. 2004. Physical and functional interactions of the Arf tumor suppressor protein with nucleophosmin/B23. *Mol Cell Biol* **24**: 985-96.

Brady, S.N., Y. Yu, L.B. Maggi, Jr., and J.D. Weber. 2004. ARF impedes NPM/B23 shuttling in an Mdm2-sensitive tumor suppressor pathway. *Mol Cell Biol* **24**: 9327-38.

Chan, W.Y., Q.R. Liu, J. Borjigin, H. Busch, O.M. Rennert, L.A. Tease, and P.K. Chan. 1989. Characterization of the cDNA encoding human nucleophosmin and studies of its role in normal and abnormal growth. *Biochemistry* **28**: 1033-9.

Colombo, E., P. Bonetti, E. Lazzerini Denchi, P. Martinelli, R. Zamponi, J.C. Marine, K. Helin, B. Falini, and P.G. Pelicci. 2005. Nucleophosmin Is Required for DNA Integrity and p19Arf Protein Stability. *Mol Cell Biol* **25**: 8874-86.

Colombo, E., J.C. Marine, D. Danovi, B. Falini, and P.G. Pelicci. 2002. Nucleophosmin regulates the stability and transcriptional activity of p53. *Nat Cell Biol* **4**: 529-33.

Eichler, D.C. and N. Craig. 1994. Processing of eukaryotic ribosomal RNA. *Prog Nucleic Acid Res Mol Biol* **49**: 197-239.

Feuerstein, N., S. Spiegel, and J.J. Mond. 1988. The nuclear matrix protein, numatrin (B23), is associated with growth factor-induced mitogenesis in Swiss 3T3 fibroblasts and with T lymphocyte proliferation stimulated by lectins and anti-T cell antigen receptor antibody. *J Cell Biol* **107**: 1629-42.

Grandori, C., N. Gomez-Roman, Z.A. Felton-Edkins, C. Ngouenet, D.A. Galloway, R.N. Eisenman, and R.J. White. 2005. c-Myc binds to human ribosomal DNA and stimulates transcription of rRNA genes by RNA polymerase I. *Nat Cell Biol* **7**: 311-8.

Gregory, M.A., Y. Qi, and S.R. Hann. 2005. The ARF tumor suppressor: keeping Myc on a leash. *Cell Cycle* **4**: 249-52.

Grisendi, S., R. Bernardi, M. Rossi, K. Cheng, L. Khandker, K. Manova, and P.P. Pandolfi. 2005. Role of nucleophosmin in embryonic development and tumorigenesis. *Nature* **437**: 147-53.

Groth, A., J.D. Weber, B.M. Willumsen, C.J. Sherr, and M.F. Roussel. 2000. Oncogenic Ras induces p19ARF and growth arrest in mouse embryo fibroblasts lacking p21Cip1 and p27Kip1 without activating cyclin D-dependent kinases. *J Biol Chem* **275**: 27473-80.

Guo, Q.M., R.L. Malek, S. Kim, C. Chiao, M. He, M. Ruffy, K. Sanka, N.H. Lee, C.V. Dang, and E.T. Liu. 2000. Identification of c-myc responsive genes using rat cDNA microarray. *Cancer Res* **60**: 5922-8.

Ho, J.H. and A.W. Johnson. 1999. NMD3 encodes an essential cytoplasmic protein required for stable 60S ribosomal subunits in Saccharomyces cerevisiae. *Mol Cell Biol* **19**: 2389-99.

Itahana, K., K.P. Bhat, A. Jin, Y. Itahana, D. Hawke, R. Kobayashi, and Y. Zhang. 2003. Tumor suppressor ARF degrades B23, a nucleolar protein involved in ribosome biogenesis and cell proliferation. *Mol Cell* **12**: 1151-64.

Johnson, A.W., E. Lund, and J. Dahlberg. 2002. Nuclear export of ribosomal subunits. *Trends Biochem Sci* **27**: 580-5.

Juan, G. and C. Cordon-Cardo. 2001. Intranuclear compartmentalization of cyclin E during the cell cycle: disruption of the nucleoplasm-nucleolar shuttling of cyclin E in bladder cancer. *Cancer Res* **61**: 1220-6.

Kamijo, T., F. Zindy, M.F. Roussel, D.E. Quelle, J.R. Downing, R.A. Ashmun, G. Grosveld, and C.J. Sherr. 1997. Tumor suppression at the mouse INK4a locus mediated by the alternative reading frame product p19ARF. *Cell* **91**: 649-59.

Keough, R.A., E.M. Macmillan, J.K. Lutwyche, J.M. Gardner, F.J. Tavner, D.A. Jans, B.R. Henderson, and T.J. Gonda. 2003. Myb-binding protein 1a is a nucleocytoplasmic shuttling protein that utilizes CRM1-dependent and independent nuclear export pathways. *Exp Cell Res* **289**: 108-23.

Kondo, T., N. Minamino, T. Nagamura-Inoue, M. Matsumoto, T. Taniguchi, and N. Tanaka. 1997. Identification and characterization of nucleophosmin/B23/numatrin which binds the anti-oncogenic transcription factor IRF-1 and manifests oncogenic activity. *Oncogene* **15**: 1275-81.

Korgaonkar, C., J. Hagen, V. Tompkins, A.A. Frazier, C. Allamargot, F.W. Quelle, and D.E. Quelle. 2005. Nucleophosmin (B23) targets ARF to nucleoli and inhibits its function. *Mol Cell Biol* **25**: 1258-71.

Kuo, M.L., W. den Besten, D. Bertwistle, M.F. Roussel, and C.J. Sherr. 2004. N-terminal polyubiquitination and degradation of the Arf tumor suppressor. *Genes Dev* **18**: 1862-74.

Kurki, S., K. Peltonen, L. Latonen, T.M. Kiviharju, P.M. Ojala, D. Meek, and M. Laiho. 2004. Nucleolar protein NPM interacts with HDM2 and protects tumor suppressor protein p53 from HDM2-mediated degradation. *Cancer Cell* **5**: 465-75.

Li, J., X. Zhang, D.P. Sejas, G.C. Bagby, and Q. Pang. 2004. Hypoxia-induced nucleophosmin protects cell death through inhibition of p53. *J Biol Chem* **279**: 41275-9.

Liu, H.T. and B.Y. Yung. 1999. In vivo interaction of nucleophosmin/B23 and protein C23 during cell cycle progression in HeLa cells. *Cancer Lett* **144**: 45-54.

Maggi, L.B., Jr. and J.D. Weber. 2005. Nucleolar adaptation in human cancer. *Cancer Investigation* **23**: 599-608.

Menssen, A. and H. Hermeking. 2002. Characterization of the c-MYC-regulated transcriptome by SAGE: identification and analysis of c-MYC target genes. *Proc Natl Acad Sci U S A* **99**: 6274-9.

Moss, T. and V.Y. Stefanovsky. 2002. At the center of eukaryotic life. *Cell* **109**: 545-8.

Okuda, M., H.F. Horn, P. Tarapore, Y. Tokuyama, A.G. Smulian, P.K. Chan, E.S. Knudsen, I.A. Hofmann, J.D. Snyder, K.E. Bove, and K. Fukasawa. 2000. Nucleophosmin/B23 is a target of CDK2/cyclin E in centrosome duplication. *Cell* **103**: 127-40.

Okuwaki, M., K. Matsumoto, M. Tsujimoto, and K. Nagata. 2001. Function of nucleophosmin/B23, a nucleolar acidic protein, as a histone chaperone. *FEBS Lett* **506**: 272-6.

Okuwaki, M., M. Tsujimoto, and K. Nagata. 2002. The RNA binding activity of a ribosome biogenesis factor, nucleophosmin/B23, is modulated by phosphorylation with a cell cycle-dependent kinase and by association with its subtype. *Mol Biol Cell* **13**: 2016-30.

Palmero, I., C. Pantoja, and M. Serrano. 1998. p19ARF links the tumour suppressor p53 to Ras. *Nature* **395**: 125-6.

Pyronnet, S. and N. Sonenberg. 2001. Cell-cycle-dependent translational control. *Curr Opin Genet Dev* **11**: 13-8.

Qi, Y., M.A. Gregory, Z. Li, J.P. Brousal, K. West, and S.R. Hann. 2004. p19ARF directly and differentially controls the functions of c-Myc independently of p53. *Nature* **431**: 712-7.

Rubbi, C.P. and J. Milner. 2003. Disruption of the nucleolus mediates stabilization of p53 in response to DNA damage and other stresses. *Embo J* **22**: 6068-77.

Sato, K., R. Hayami, W. Wu, T. Nishikawa, H. Nishikawa, Y. Okuda, H. Ogata, M. Fukuda, and T. Ohta. 2004. Nucleophosmin/B23 is a candidate substrate for the BRCA1-BARD1 ubiquitin ligase. *J Biol Chem* **279**: 30919-22.

Savkur, R.S. and M.O. Olson. 1998. Preferential cleavage in pre-ribosomal RNA byprotein B23 endoribonuclease. *Nucleic Acids Res* **26**: 4508-15.

Strezoska, Z., D.G. Pestov, and L.F. Lau. 2000. Bop1 is a mouse WD40 repeat nucleolar protein involved in 28S and 5. 8S RRNA processing and 60S ribosome biogenesis. *Mol Cell Biol* **20**: 5516-28.

Sugimoto, M., M.L. Kuo, M.F. Roussel, and C.J. Sherr. 2003. Nucleolar Arf tumor suppressor inhibits ribosomal RNA processing. *Mol Cell* **11**: 415-24.

Szebeni, A. and M.O. Olson. 1999. Nucleolar protein B23 has molecular chaperone activities. *Protein Sci* **8**: 905-12.

Trotta, C.R., E. Lund, L. Kahan, A.W. Johnson, and J.E. Dahlberg. 2003. Coordinated nuclear export of 60S ribosomal subunits and NMD3 in vertebrates. *Embo J* **22**: 2841-51.

Warner, J.R. 1990. The nucleolus and ribosome formation. *Curr Opin Cell Biol* **2**: 521-7.

Watson, J.D., S.K. Oster, M. Shago, F. Khosravi, and L.Z. Penn. 2002. Identifying genes regulated in a Myc-dependent manner. *J Biol Chem* **277**: 36921-30.

Yu, Y., L.B. Maggi, S.N. Brady, A.J. Apicelli, M. Dai, H. Lu, and J.D. Weber. 2006. Nucleophosmin is essential for ribosomal protein L5 nuclear export. *Molecular and Cellular Biology* **In press**.

Zeller, K.I., T.J. Haggerty, J.F. Barrett, Q. Guo, D.R. Wonsey, and C.V. Dang. 2001. Characterization of nucleophosmin (B23) as a Myc target by scanning chromatin immunoprecipitation. *J Biol Chem* **276**: 48285-91.

Zindy, F., C.M. Eischen, D.H. Randle, T. Kamijo, J.L. Cleveland, C.J. Sherr, and M.F. Roussel. 1998. Myc signaling via the ARF tumor suppressor regulates p53-dependent apoptosis and immortalization. *Genes Dev* **12**: 2424-33.

Table 1. Components of the Nucleophosmin Protein Complex [a]

Protein	Function
rpL4	60S Ribosome subunit
rpL5[b]	Molecular chaperone for 5S rRNA (Steitz et al., 1998)
rpL13a	60S Ribosome subunit
rpL22	60S Ribosome subunit
rpL27	60S Ribosome subunit
rpS3a	40S Ribosome subunit
rpS5	40S Ribosome subunit
rpS6	40S Ribosome subunit
rpS7	40S Ribosome subunit
Nucleolin[b]	Repress p53 translation (Takagi et al., 2005)
Bop1	Required for rRNA processing (Strezoska et al., 2000)
CPSF6	mRNA processing (Dettwiler et al., 2004)
hnRNP A1	mRNA processing and transport (Dreyfuss et al., 1993)
hnRNP H2	mRNA processing (Dreyfuss et al., 1993)
EF-2	Translational regulation (Carlberg et al., 1990)
Nup50	Nuclear pore complex (Guan et al., 2000)
Nup62	Nuclear pore complex (Radu et al., 1993)
Brca1[b]	E3 ubiquitin ligase for NPM (Sato et al, 2004)

[a] Isolated by nucleophosmin affinity chromatography and identified by MALDI-TOF or tandem mass spectrometry.
[b] Known NPM binding proteins

Figure Legends

Figure 1. NPM is a potent oncogene in the absence of ARF

A *Arf*$^{-/-}$ MEFs infected with retroviruses encoding His-tagged NPM or H-Ras^{V12} were fixed and subjected to forward and side scatter analysis by flow cytometry. The upper right quadrant represents the cell population with increased size.

B *Arf*$^{-/-}$ MEFs infected with retroviruses encoding His-tagged NPM or NPMdL were labeled with BrdU for 24 hours prior to fixation and staining with antibodies recognizing BrdU incorporated into replicating DNA. DAPI was used to demarcate cell nuclei. n=3 with the reported standard deviations (*, P>0.01, **, P>0.005).

C *Arf*$^{-/-}$ MEFs infected with retroviruses encoding Ras^{V12}, His-tagged NPM or NPMdL were seeded ($3x10^3$ cells) in media containing soft agar and assayed colony formation fourteen days later. Additionally, *Arf*$^{-/-}$ MEFs infected with retroviruses encoding His-tagged NPM or NPMdL were seeded in media containing G418 and assayed for foci formation twelve days later.

D Primary human breast, prostate, and colon carcinoma tissue microarrays were obtained and stained for NPM protein expression, with representative cancerous tissues staining negative for NPM shown on the left panels, and those staining extremely positive for NPM shown on the right panels. Statistics of NPM protein expression in all three carcinomas are indicated in the insets (% of total slides exhibiting the pattern of staining).

E *Arf*$^{-/-}$ MEFs infected with retroviruses encoding His-tagged NPM were fixed and stained with antibodies recognizing γ-tubulin. Nuclei were demarcated with DAPI. Centrosomes from over 200 cells were counted for each condition and plotted as a representative experiment (n=3).

F *Arf*$^{-/-}$ MEFs infected with retroviruses encoding His-tagged NPM were treated with colcemid and fixed. Chromosomes from each condition were prepared and visualized with DAPI.

Expression of His-tagged NPM protein was confirmed by western blot analysis using antibodies recognizing the His moiety.

Figure 2. Isolation of endogenous NPM protein complexes

A HeLa cell lysates (600 μg) were injected onto a Sephacryl 300 gel filtration column and fractions were collected as indicated. Proteins were separated by SDS-PAGE and immunoblotted with antibodies recognizing NPM. Gel filtration sizes are indicated above the fractions and the presence of NPM oligomers and monomers is indicated below.

B Pooled sizing column fractions (2-16) containing NPM (600 μg) were injected onto an NPM polyclonal antibody affinity column and eluted with an increasing NaCl gradient (0.1-1.0M). Eluted proteins were separated by two-dimensional electrophoresis and visualized with SYPRO-Ruby dye (2D). Spots were excised and digested with trypsin. Tryptic peptides were analyzed by mass spectrometry. Representative MALDI-TOF spectra of labeled spots from above are presented with corresponding identified peptide sequences.

Figure 3. NPM nuclear export is required for Protein Synthesis

A HeLa cells were transduced with pcDNA3.1-His (red line), His-NPM (blue line), or His-NPMdL (green line) and incubated for 24 hours. Cells were labeled with ^{35}S-Methionine for the indicated times. Equal numbers of cells ($3x10^6$) were lysed, and TCA-precipitated counts were measured. His-tagged NPM protein expression was measured by anti-His immunoblot to confirm transduction (inset).

B HeLa cells were transduced with pcDNA3.1-His (red line), His-NPM (blue line), or His-NPMdL (green line) and incubated for 24 hours. Equal numbers of transduced cells ($3x10^6$)

were lysed and separated on sucrose gradients with constant UV (254 nm) monitoring for ribosome and polysome detection. His-tagged NPM protein expression was measured by anti-His immunoblot to confirm transduction (inset).

Figure 4. NPM is the rating-limiting factor for rRNA export

A HeLa cells were transduced with pcDNA3.1-His (CTL), His-NPM, or His-NPMdL. Cells were labeled with [methyl-^{3}H] methionine and chased. Equal numbers of labeled cells ($2x10^{6}$) were subjected to fractionation into cytoplasmic (C) and nuclear (N) extracts. Total RNA extracted from each fraction was separated, transferred to membranes and subjected to autoradiography. Newly synthesized and labeled 28S, 18S and 5.8/5S rRNAs are indicated by arrows. The bottom 5.8S/5S panel is a longer exposure of the same autoradiograph as shown above.

B *Arf*$^{-/-}$ MEFs infected with retroviruses encoding His-NPM were labeled with [methyl-^{3}H] methionine and chased. Equal numbers of labeled cells ($3x10^{6}$) were subjected to fractionation into cytoplasmic (C) and nuclear (N) extracts. Total RNA extracted from each fraction was separated, transferred to membranes and subjected to autoradiography. Newly synthesized and labeled 28S, 18S and 5.8/5S rRNAs are indicated by arrows.

C *Arf*$^{-/-}$ MEFs infected with retroviruses encoding His-NPM or Ras^{V12} were labeled with [^{3}H] uridine and chased. Total RNA extracted from equal numbers of labeled cells ($3x10^{6}$) was separated, transferred to membranes and subjected to autoradiography. Newly synthesized and labeled 28S, 18S and 5.8/5S rRNAs are indicated by arrows.

D HeLa cells were transduced with pcDNA3.1-His (Control) or His-NPM and incubated for 24 hours. Cells were labeled with [methyl-^{3}H] methionine and $3x10^{6}$ cells were subjected to polysome fractionation. Fractions from the sucrose gradient were isolated and counted for

[methyl-^{3}H] methionine incorporation into newly synthesized rRNAs and assembled cytosolic ribosomes. ^{3}H-counts were normalized for the efficiency of label incorporation into total RNA for each condition (*, P>0.005).

Figure 5. NPM is an essential mediator of ribosome nuclear export

A HeLa cells were nucleofected with scrambled or NPM siRNAs and incubated for 72 hours prior to labeling with [methyl-^{3}H] methionine. Equal numbers of cells ($2x10^{6}$) were subjected to fractionation into cytoplasmic (C) and nuclear (N) extracts. Total RNA extracted from each fraction was separated, transferred to membranes and subjected to autoradiography. Newly synthesized and labeled 28S, 18S and 5.8/5S rRNAs are indicated by arrows. Western blot analysis using antibodies recognizing NPM was used to visualize efficient knockdown.

B HeLa cells were nucleofected with scrambled (solid line) or NPM (dashed line) siRNAs and incubated for 72 hours. Equal numbers of cells ($3x10^{6}$) were separated on sucrose gradients with constant UV (254 nm) monitoring for ribosome and polysome detection.

C Wild-type (WT) and *Npm*$^{hy/hy}$ MEFs were labeled with [methyl-^{3}H] methionine and equal numbers of cells ($3x10^{6}$) were subjected to fractionation into cytoplasmic (C) and nuclear (N) extracts. Total RNA extracted from each fraction was separated, transferred to membranes and subjected to autoradiography. Newly synthesized and labeled 28S, 18S and 5.8/5S rRNAs are indicated by arrows. Lack of NPM protein expression in *Npm*$^{hy/hy}$ cells was monitored via western blot analysis using antibodies recognizing NPM.

Figure 6. Loss of *Npm* prevents 5S rRNA export *in vivo*

In situ RNA FISH analysis was performed on wild-type **(A-D)** and *Npm*$^{-/-}$ **(E-H)** day E10.5 embryos using a probe recognizing the 5S rRNA (purple). Nuclear Fast Red counterstaining was used to demarcate nuclei (pink). Whole embryos were visualized at 2X (WT) and 4X (*Npm*$^{-/-}$), respectively. Cell images (**A-D** and **E-H**) were observed at 60X magnification.

Figure 1- Maggi

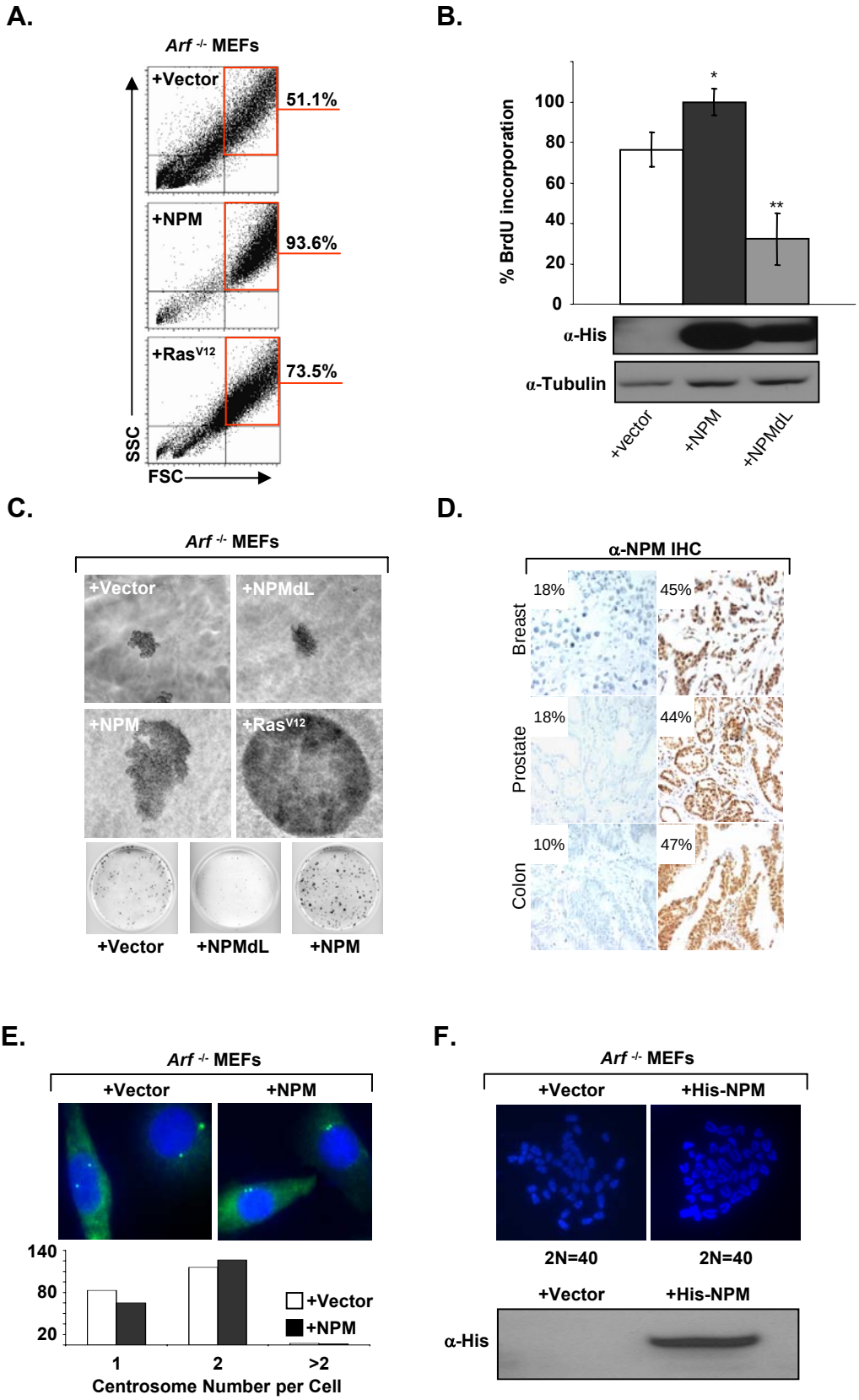

Figure 2- Maggi

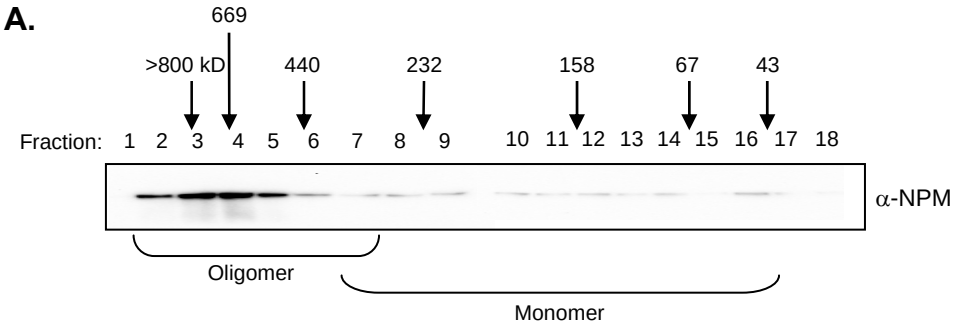

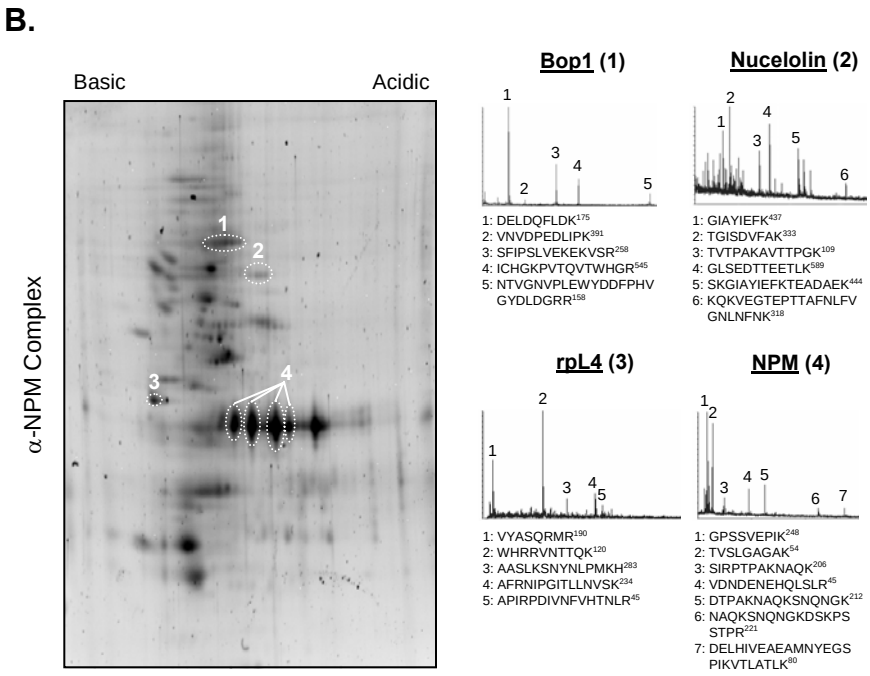

Figure 3- Maggi

A.

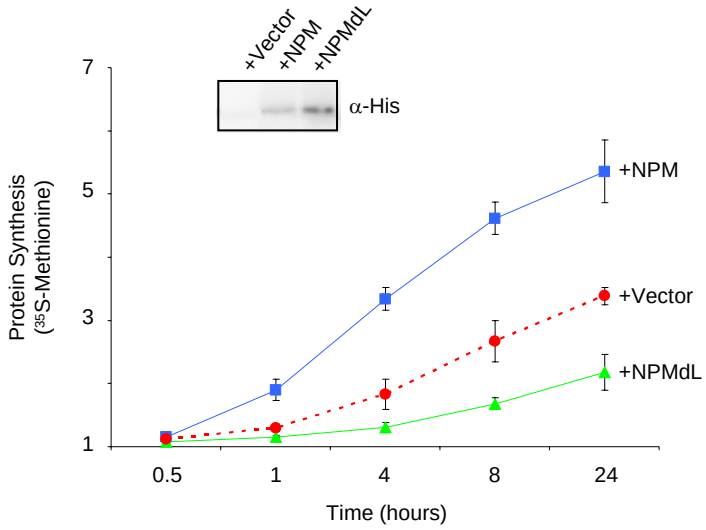

B.

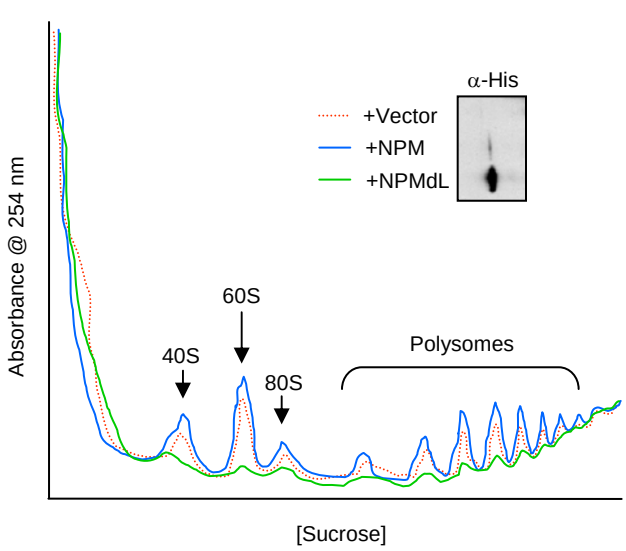

Figure 4- Maggi

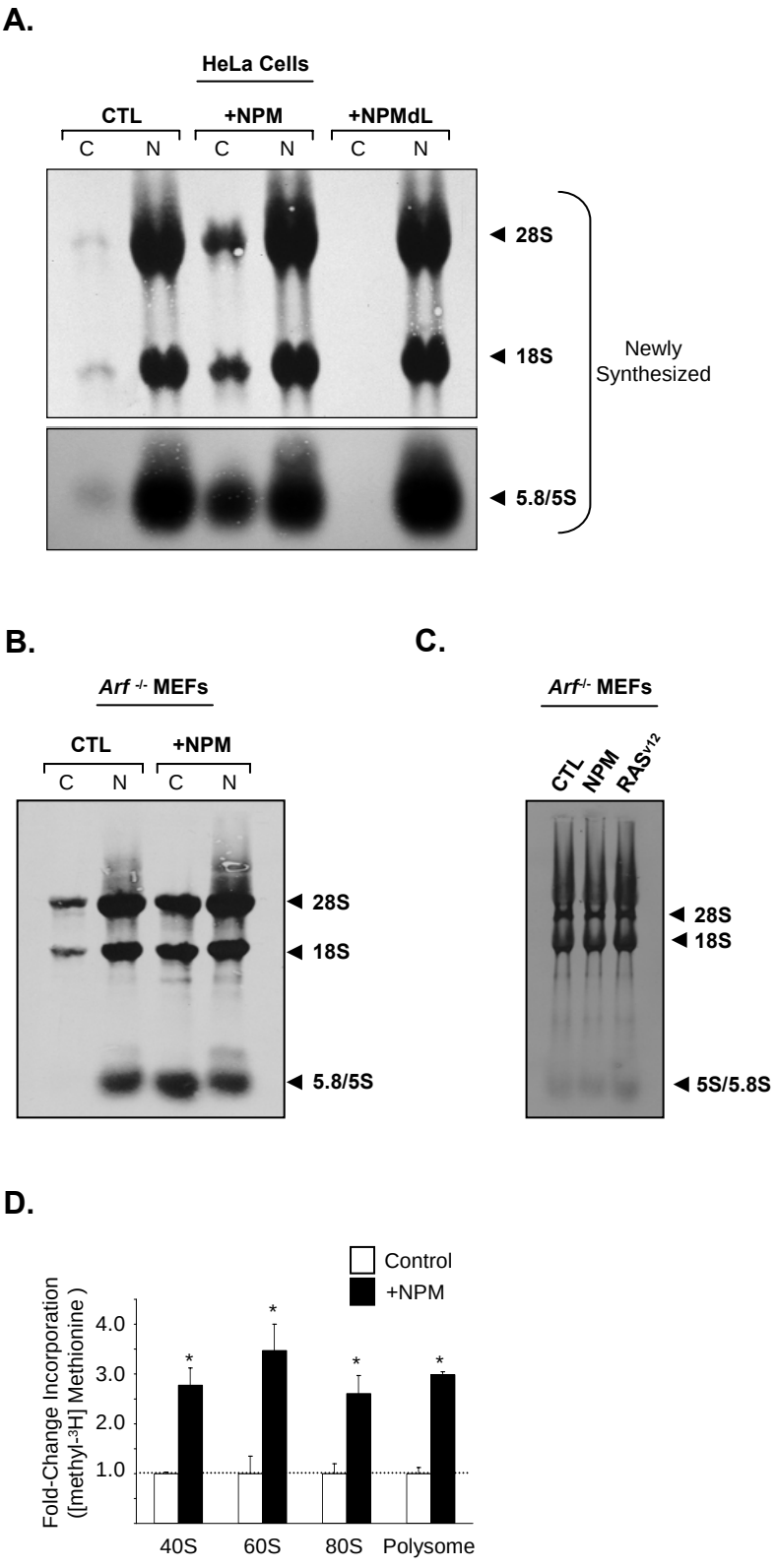

Figure 5- Maggi

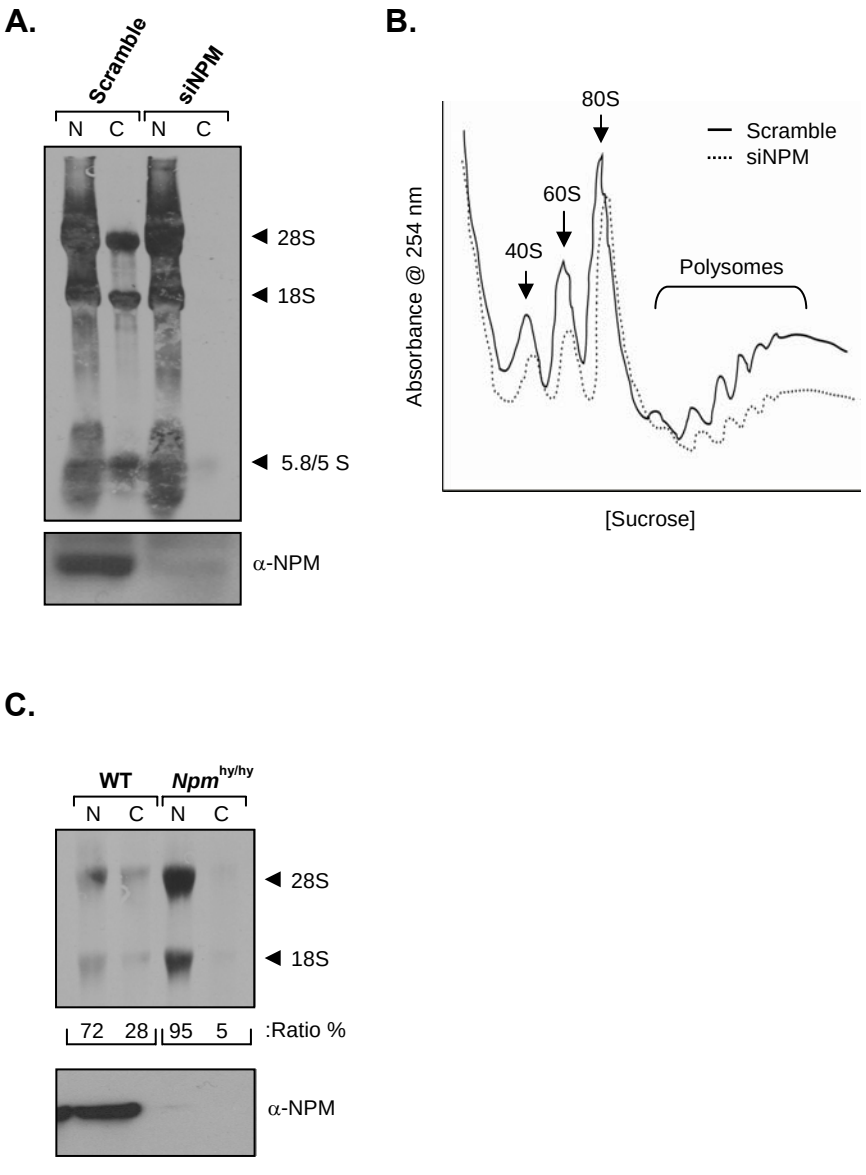

Figure 6- Maggi

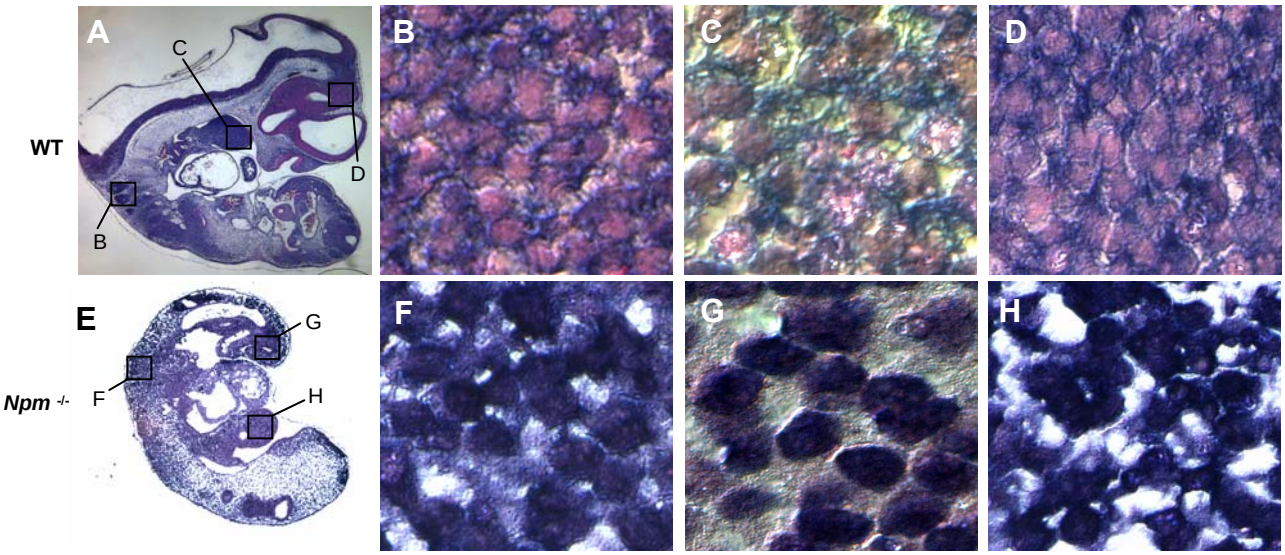

Curriculum Vitae

Leonard B Maggi, Jr.

Home Address and Phone:
14375 Jamestown Bay Dr.
Florissant, MO 63134
(314) 355-8677

Work Address, Phone, and Email:
Department of Internal Medicine
Division of Molecular Oncology
Washington University School of Medicine
660 South Euclid Ave., Box 8069
St. Louis, MO 63110
(314) 747-3898
lmaggi@im.wustl.edu

Birth Date: August 26, 1973
Birth Place: Peoria, IL

Citizenship: USA

Social Security Number: 322-58-3196

Present Position: Research Instructor Professor, Department of Internal Medicine, Division of Molecular Oncology, Washington University School of Medicine, St. Louis, MO

Education:

Undergraduate:

August 1991-May 1995	Cornell College Mount Vernon, IA	B.A., Biochemistry & Molecular Biology Philosophy Dr. Truman Jordan, Advisor

Graduate:

August 1997- November 2001	Saint Louis University Saint Louis, MO	Ph.D., Biochemistry & Molecular Biology Dr. John A. Corbett, Advisor

Postdoctoral:

October 2002-September 2006	Washington University Saint Louis, MO	Molecular Oncology Dr. Jason D. Weber, Advisor
December 2001- September 2002	Washington University Saint Louis, MO	Pathology & Immunology Dr. Barry Sleckman, Advisor

Work Experience:

October 1995-April 1996	**Protein Chemist** Today's Temporary Department of Molecular Immunology G.D. Searle Saint Louis, MO	Dr. Thomas J. Girard, Principal Investigator
April 1996-August 1997	**Sequencing Finisher** Genome Sequencing Center Washington University School of Medicine Saint Louis, MO	Dr. Robert Waterston, Group Leader and Head of the Genome Sequencing Center
October 2002-Present	**Research Instructor** Department of Internal Medicine Division of Molecular Oncology Washington University School of Medicine Saint Louis, MO	Dr. Jason D. Weber, Principle Investigator

Honors and Awards:

1st Place Student Presentation Biochemistry Departmental Retreat (1999)
Sigma Xi Outstanding Graduate Research Award (2000)
1st Place Student Oral Presentation Biochemistry Departmental Retreat (2000)
Alpha Sigma Nu Jesuit Honor Society (2000)

Teaching:

January 2000-April 2001	**Graduate Student Facilitator** 1st year Medical School Courses *Microbes and the Host Response* *Cell Biology and Pathology*	Velois Rauch, Director of Student Support Services Office of Multicultural Affairs Saint Louis University School of Medicine St. Louis, MO

Graduate Student Committees

1998-1999	Graduate Curriculum Committee
1999-2000	Departmental Library Committee
1999-2001	Wendell Griffith Lecture Committee (Student-invited lectureship series)
	Hosted Speakers: Dr. Natalie Ahn, University of Colorado at Boulder and HHMI (February 2000)
	Dr. James Darnell, The Rockefeller University (November 2000)

Funding

Completed:

NIH Institutional Training Grant T32-AI07163-24	December 1, 2001 – September 30, 2002
NIH Institutional Training Grant T32-HL707873	October 1, 2002 – September 30, 2004

Department of Defense Postdoctoral Traineeship Award October 1, 2004 – September 30, 2006
W81XWH-04-1-0909 "Role of the ARF Tumor Suppressor in Prostate Cancer"

Publications:

1. The *C. elegans* Sequencing Consortium. 1998. Genome Sequence of the Nematode *C. elegans*: A Platform for Investigating Biology. *Science*. 282:2012-2018.

2. **Maggi, LB, Jr.**, Sadeghi, H, Weigand, C, Scarim, AL, Heitmeier, MR, and Corbett, JA. 2000. Anti-inflammatory Actions of 15-d-$\Delta^{12,14}$-prostaglandin J_2 and Troglitazone: Evidence for Heat Shock-dependent and -independent Inhibition of Cytokine-induced iNOS Expression. *Diabetes*. 49:346-355.

3. **Maggi, LB, Jr.**, Heitmeier, MR, Scheuner, D, Kaufman RJ, Buller, RML, and Corbett, JA. 2000. Potential Role of PKR in dsRNA-induced Macrophage Activation. *EMBO J*. 19:3630-3638.

4. International Human Genome Sequencing Consortium. 2001. Initial Sequencing and Analysis of the Human Genome. *Nature*. 409:860-921.

5. Blair, LA, Heitmeier, MR, Scarim, AL, **Maggi, LB, Jr.**, and Corbett, JA**.** 2001. Double-stranded RNA-dependent Protein Kinase is Not Required for Double-stranded RNA-induced Nitric Oxide Synthase Expression or Nuclear Factor-κB Activation by Islets. *Diabetes*. 50:283-290.

6. Blair, LA, **Maggi, LB, Jr.**, Scarim, AL, and Corbett, JA. 2002. Role of Interferon Regulatory Factor-1 in iNOS expression by Mouse Islets. *J. Biol. Chem.* 277:359-365.

7. **Maggi, LB, Jr.**, Moran, JM, Scarim, AL, Ford, DA, Yoon, YW, McHowat J, Buller, RML and Corbett, JA. 2002. Novel Role for Calcium-independent Phospholipase A2 in the Macrophage Antiviral Response of Inducible Nitric-oxide Synthase Expression. *J. Biol. Chem.* 277:38449-38455

8. Steer, SA, Moran, JM, **Maggi, LB, Jr.,** Buller, RML, Perlman, H, Corbett, JA. 2003. Regulation of cyclooxygenase-2 expression by macrophages in response to double-stranded RNA and viral infection. *J. Immunol.* 170:1070-1076.

9. **Maggi, LB, Jr.,** Moran, JM, Buller, RML, and Corbett, JA. 2003. ERK Activation is Required for dsRNA- and Virus-induced IL-1 Expression by Macrophages. *J. Biol. Chem.* 278:16683-16689.

10. Brady, SN, Yu, Y, **Maggi, LB, Jr.**, Weber, JD. 2004. ARF Impedes NPM/B23 Shuttling in an Mdm2-Sensitive Tumor Suppressor Pathway. *Mol. Cell. Biol.* 24:9327-9338.

11. Kohr, B, Bredemeyer, AL, Huang, CY, Turnbull, I, Evans, R, **Maggi, LB, Jr.**, White, JM, Walker, LM, Carnes, K, Hess, R, and Sleckman, BP. 2005. Proteasome Activator PA200 Causes Defective Spermatogenesis. *Mol. Cell. Biol.* 26:2999-3007.

12. Yu, Y, **Maggi, LB, Jr.**, Brady, SN, Apicelli, AJ, Dai, MS, LU, H, and Weber, JD. 2006. Nucleophosmin is Essential for Ribosomal L5 Nuclear Export. *Mol. Cell. Biol.* 26:3798-3809.

13. Steer, SA, Moran, JM, Christmann, BS, **Maggi, LB, Jr.**, and Corbett, JA. 2006. Role of MAPK in the regulation of dsRNA and EMCV-induced COX-2 expression by macrophages. *J. Immunol.* 177:3413-3420.

14. Pelletier, CP, **Maggi, LB, Jr.**, Brady, SN, Scheidenhelm, DK, Gutmann, DH, and Weber, JD. 2006. mTOR/S6K1 Sets the Rate of Ribosome Export through Increased Nucleophosmin Translation and Stability. *In press Cancer Res.*

15. **Maggi, LB, Jr.**, Yu, Y, Grisendi, S, Pandolfi, PP, and Weber, JD. 2006. Regulation of Growth and Transformation by Nucleophosmin-mediated Ribosome Nuclear Export. *Under Review EMBO J.*

Invited Reviews:

1. **Maggi, LB, Jr.**, and Weber, JD. Nucleolar Adaptation in Human Cancer. 2005. *Cancer Invest.* 23:599-608.

Abstracts:

1. Maggi, LB, Jr., and Corbett, JA. 1999. Dominant Negative PKR Attenuates Double-stranded RNA-induced Nitric Oxide Production and Interleukin-1 Release by Murine Macrophages. *Diabetes* 48 Supplement 2:A434.

2. Maggi, LB, Jr., Weigand, C, Scarim, AL, Heitmeier, MR, and Corbett, JA. 2000. Anti-inflammatory Actions of 15-d-$\Delta^{12,14}$-prostaglandin J_2 and Troglitazone: Evidence for Heat Shock-dependent and -independent Inhibition of Cytokine-induced iNOS Expression. *Diabetes*. 49 Supplement 2:A260.

3. Blair, LA, Maggi, LB, Jr., and Corbett, JA. 2000. Potential Role of PKR in Double-stranded RNA-induced iNOS Expression by Mouse Islets. *Diabetes* 49 Supplement 2:A259.

4. Maggi, LB, Jr., and Corbett, JA. 2001. The Role of PKR and ERK in dsRNA-induced IL-1 Release from Macrophages. *Diabetes.* 50 Supplement 2:A404.

5. Moran, JM, Maggi, LB, Jr., Buller, RML, and Corbett, JA. 2002. Virus-Induced Macrophage Activation Is Mediated by a Novel iPLA$_2$ Signaling Pathway. *Diabetes*. 51 Supplement 2:A370.

6. Maggi, LB, Jr., Yu, Y, Grisendi, S, Zhang, W, Towsend, R, McLeod, HL, Pandolfi, PP, and Weber, JD. 2006. Nucleophosmin Directs Ribosome Nuclear Export and Cell Growth. Cold Spring Harbor Laboratory Meeting: *Mechanisms and Models of Cancer* pg. 170.

7. Pelletier, CP, Maggi, LB, Jr., and Weber, JD. 2006. mTOR/S6K sets the rate of ribosome export through increased nucleophosmin translation. Cold Spring Harbor Laboratory Meeting: *Mechanisms and Models of Cancer* pg. 209.

Invited Lectureships:

Regulation of Growth and Transformation by Nucleophosmin-mediated Ribosome Export	2006	2nd Annual Postdoc Symposium Washington University School of Medicine Saint Louis, MO

References:

Jason D. Weber
Assistant Professor
Department of Internal Medicine
Division of Molecular Oncology
Washington University School of Medicine
660 S Euclid, Campus Box 8069
Saint Louis, MO 63110
Phone: (314) 747-3898
Fax (314) 747-2797
Email: jweber@im.wustl.edu

Sheila Stewart
Assistant Professor
Department of Cell Biology and Physiology
Washington University School of Medicine
660 S. Euclid, Campus Box 8228
St. Louis, MO 63110
Phone (314) 362-7437
Fax (314) 362-7463
Email: sheila.stewart@cellbiology.wustl.edu

John A. Corbett
Associate Professor
Department of Biochemistry and Molecular Biology
Saint Louis University School of Medicine
1402 S. Grand Blvd.
St. Louis, MO 63104
Phone (314) 977-9247
Fax (314) 977-9205
Email: corbettj@slu.edu

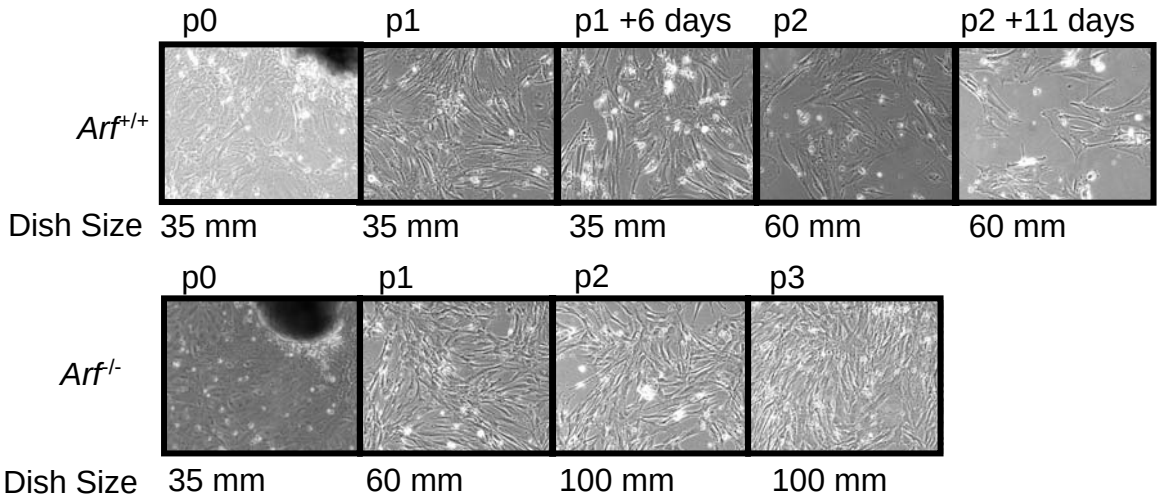

Figure 1. *Arf*$^{-/-}$ Prostate Cell Cultures. Prostates isolated from *Arf*$^{+/+}$ and *Arf*$^{-/-}$ mice were chopped in to ~1mm^3 pieces and grown in 35mm wells of a 6 well plate. When confluent the cells were passaged to larger plates as indicated. These data are representative of 2 independent isolations.

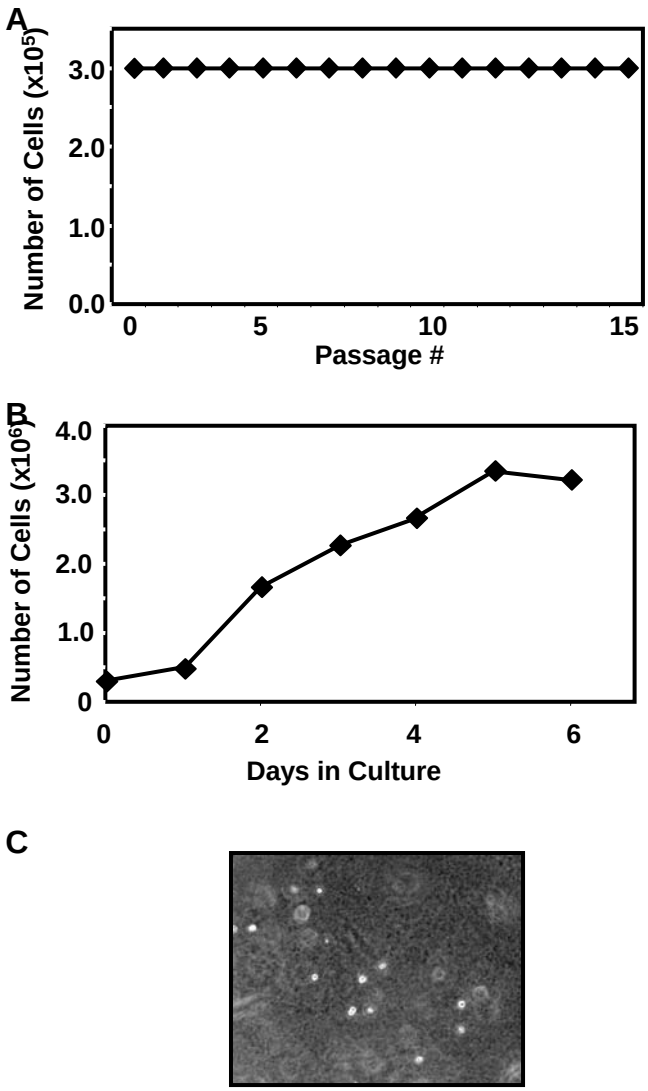

Figure 2. *Arf*$^{-/-}$ Prostate Cells are Immortal not Transformed. **A** *Arf*$^{-/-}$ prostate ($3x10^5$ cells) were seeded on 35 mm dishes and $3x10^5$ cells were passaged every 3 days. **B** *Arf*$^{-/-}$ prostate cells ($3x10^5$ cells) were seeded on 100 mm dishes and cell number was determined every 24 h. **C** *Arf*$^{-/-}$ prostate cells (1000 cells) were seeded in media containing soft agar and colony formation was assessed fourteen days later. 3T3 protocol (**A**) and growth curve (**B**) are representative of 2 independent experiments performed in triplicate. Colony formation in soft agar (**C**) is representative of 3 independent experiments performed in quadruplicate.

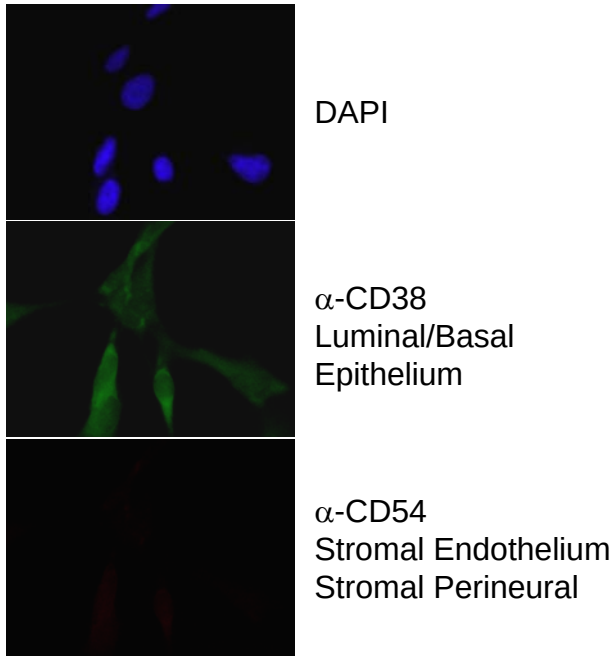

Figure 3. *Arf*$^{-/-}$ Prostate Cells are Epithelial Cells. *Arf*$^{-/-}$ prostate cells were stained with antibodies against CD38 (Epithelial Prostate marker) or CD54 (Stromal Prostate marker). Nuclei are demarcated with DAPI. These data are representative of two independent isolations.

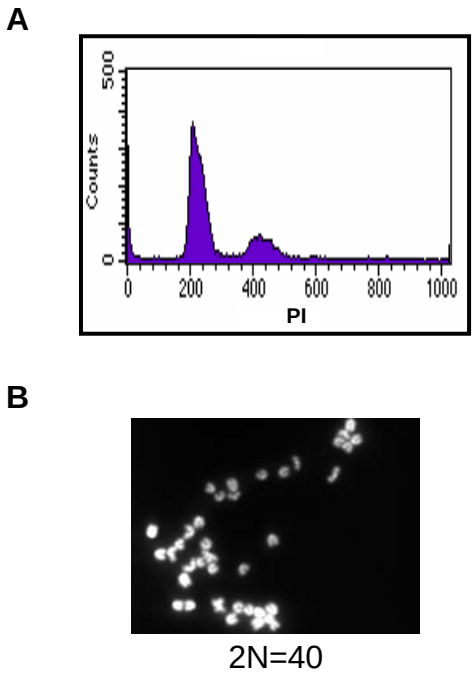

Figure 4. *Arf*$^{-/-}$ PEpC are Diploid. **A** *Arf*$^{-/-}$ PEpC were fixed and stained with PI prior to DNA content analysis by flow cytometry. **B** *Arf*$^{-/-}$ PEpC were treated with colcemid and fixed. Chromosomes were prepared and visualized with DAPI. Results from flow cytometry (**A**) are representative of 3 independent experiments. Results from Chromosome analysis (**B**) are representative of 5 metaphase spreads.

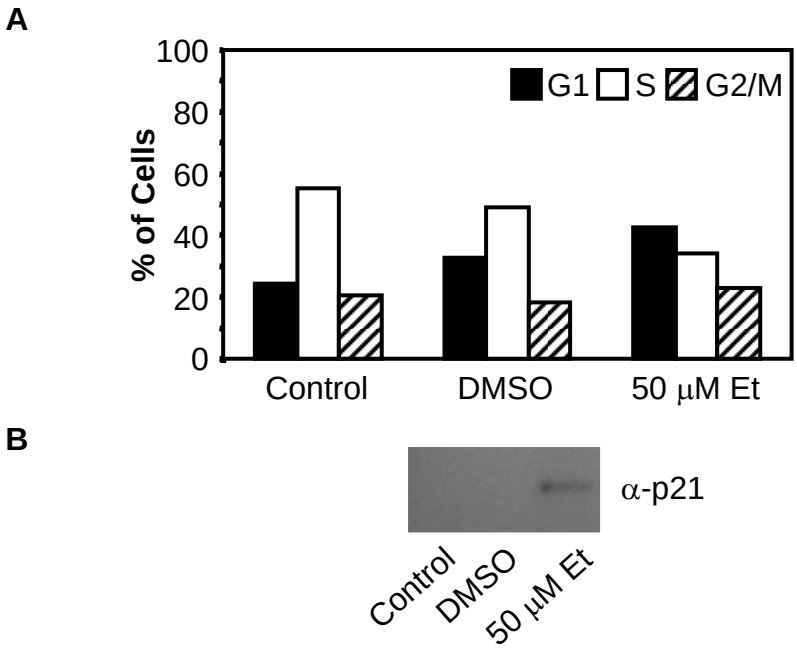

Figure 5. *Arf*$^{-/-}$ PEpC Have an Intact p53 Response. **A** *Arf*$^{-/-}$ PEpC ($1x10^6$) were treated for 18 h with DMSO or 50 μM Etoposide prior to being fixed and stained with PI. DNA content was analyzed by flow cytometry. **B** A portion of the cells from **A** were used in western blot analysis to assess p21 levels. These data are representative of 3 independent experiments.

Figure 6. p19ARF Overexpression Inhibits *Arf*$^{-/-}$ PEpC Cell Cycle Progression

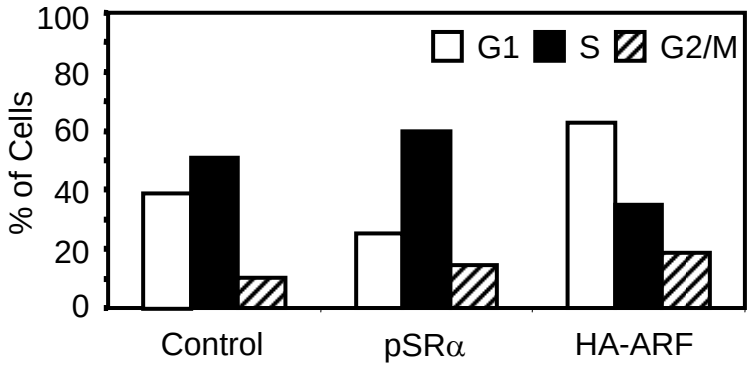

Figure 6. p19ARF Overexpression Inhibits *Arf*$^{-/-}$ PEpC Cell Cycle Progression. *Arf*$^{-/-}$ PEpC were infected with HA-p19ARF expressing retroviruses. DNA content was analyzed 48 h later by flow cytometry. This data is representative of 2 independent experiments.

Figure 7. Effects of Androgen Receptor Inhibition on *Arf*$^{-/-}$ PEpC Cell Growth

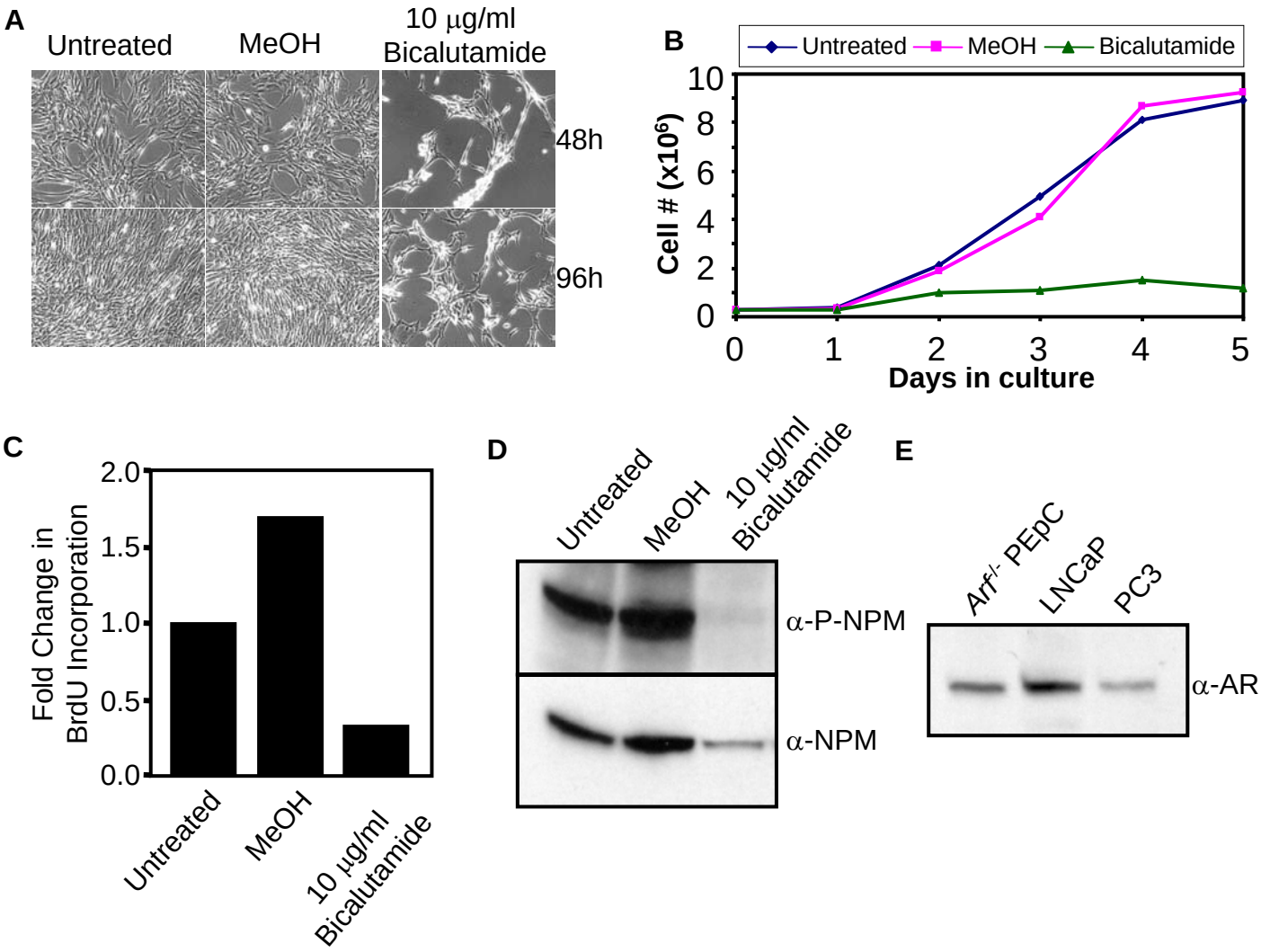

Figure 7. Androgen Receptor Signaling is Required for *Arf*$^{-/-}$ PEpC Growth. **A** *Arf*$^{-/-}$ PEpC ($1x10^6$) were treated with MeOH or 10 μg/ml bicalutamide as indicated and cell denisty assesses at the indicated times. **B** *Arf*$^{-/-}$ PEpC ($3x10^5$) were seeded onto 100 mm dishes in the presence or absence of MeOH or 10 μg/ml bicalutamide as indicated and cell number determined every 24 h. **C** *Arf*$^{-/-}$ PEpC ($7.5x10^4$) were seeded onto glass cover slips in the presence or absence of MeOH or 10 μg/ml bicalutamide for 48 h. Cells were labeled with 10 μM BrdU for 18 h prior to fixation and staining with antibodies recognizing BrdU incorporated into replicating DNA. DAPI was used to demarcate cell nuclei. **D** *Arf*$^{-/-}$ PEpC treated with MeOH or 10 μg/ml bicalutamide for 96 h were analyzed by western blot with antibodies against phosphorylated Thr198 NPM or NPM as indicated. **E** Cell lysates (10 μg) from *Arf*$^{-/-}$ PEpC, LNCaP, and PC3 cells were analyzed for androgen receptor expression by western blot. These data are representative of three independent experiments.

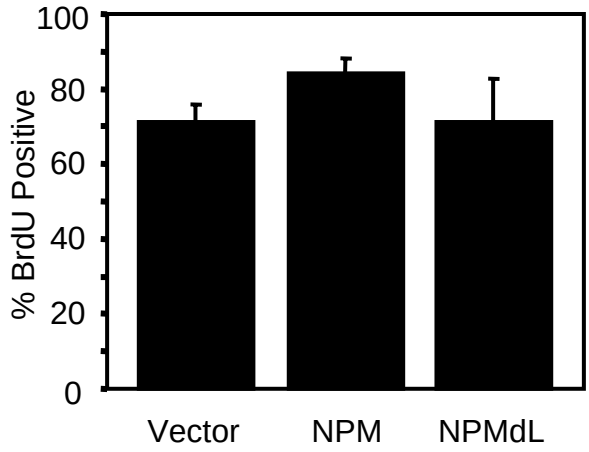

Figure 8. PC3 Cell S Phase Progression Is Not Affected By NPM Shuttling. PC3 cells nucleofected with empty vector or GFP-tagged NPM or NPMdL were labeled with BrdU for 18 h prior to fixation and staining with antibodies against BrdU incorporated in to replicating DNA. DAPI was used to demarcate nuclei. These data are representative three independent experiments performed in triplicate ± SEM.

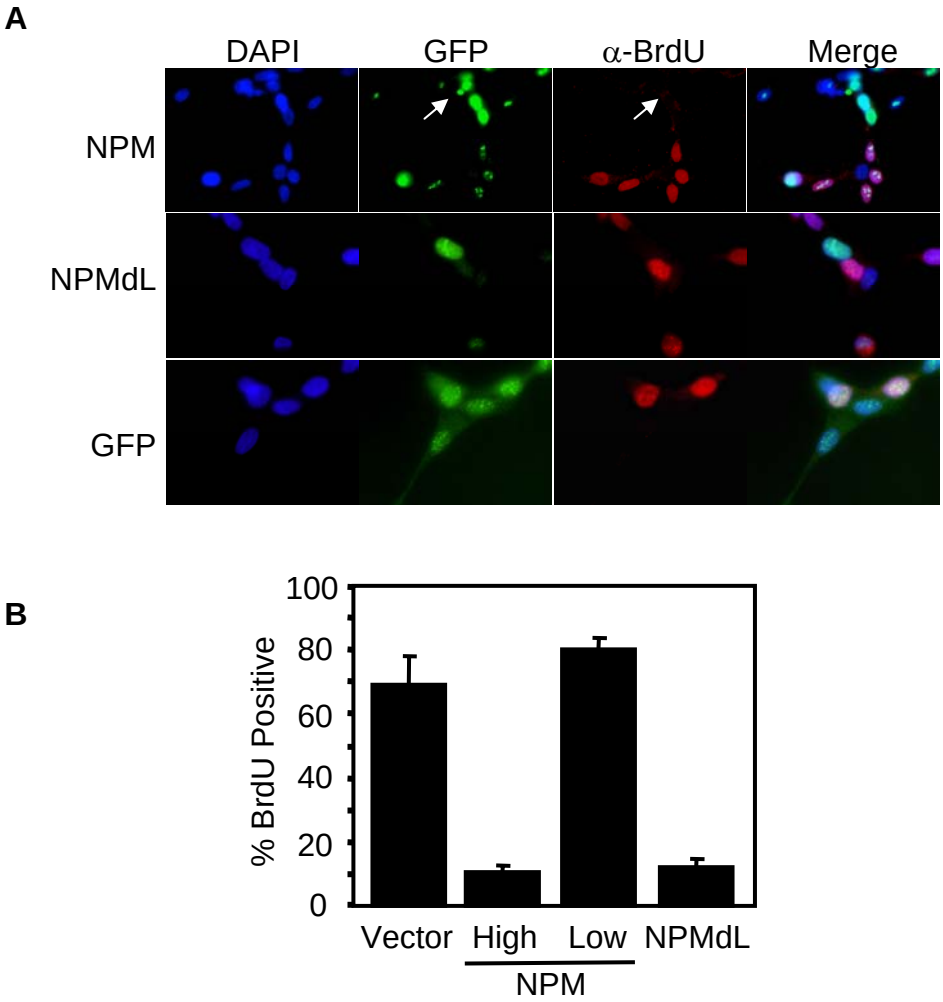

Figure 9. LNCaP Cell S Phase Progression Is Affected By Inhibition of NPM Shuttling or High Expression of NPM. A LNCaP cells nucleofected with empty vector or GFP-tagged NPM or NPMdL were labeled with BrdU for 18 h prior to fixation and staining with antibodies against BrdU incorporated in to replicating DNA. DAPI was used to demarcate nuclei. **B** Quantification of BrdU postive cells shown in A. These data are representative two independent experiments performed in triplicate ± SD.

Figure 11. *Arf* Loss Increases Protein Synthesis Rates of PEpC

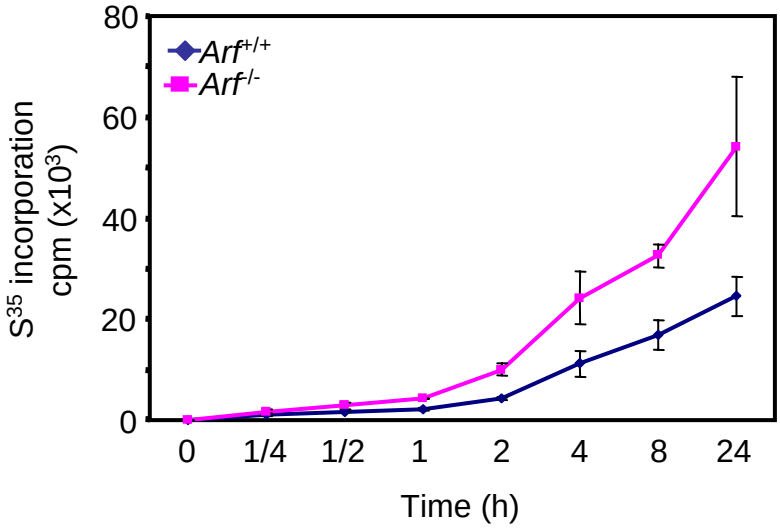

Figure 10. *Arf* loss Increases Protein Synthesis Rates of PEpC. $Arf^{+/+}$ or $Arf^{-/-}$ PEpC were labeled with 35S-methionine in methionine-free media for the indicated times. Equal numbers of cells ($2.5x10^4$) were lysed and TCA-precipitable counts were measured. This data is representative of two experiments performed in triplicate ± SD.

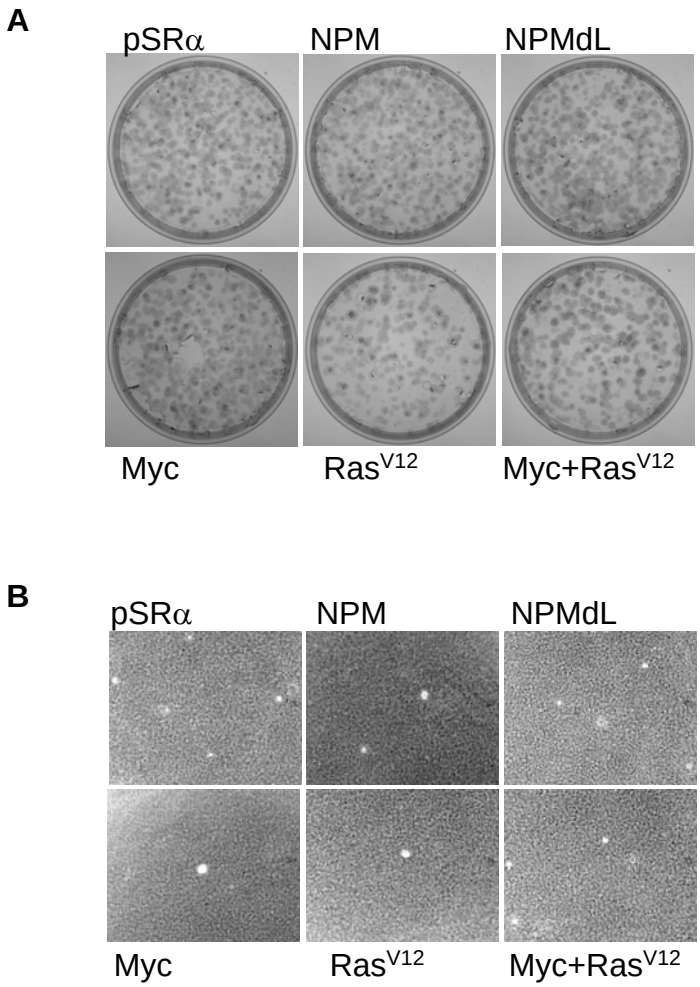

Figure 11. *Arf*$^{-/-}$ PEpC Cannot Be Transformed. *Arf*$^{-/-}$ PEpC were infected with the indicated retroviruses. **A** Forty-eight hours post infection $3x10^5$ cells were seeded in media containing 800 μg/ml G418 and foci formation was assessed fourteen days later. **B** Forty-eight hours post infection $1x10^4$ cells were seeded in media containing soft agar and 800 μg/ml G418. Colony formation was assessed fourteen days later. These data are representative of two independent experiments.

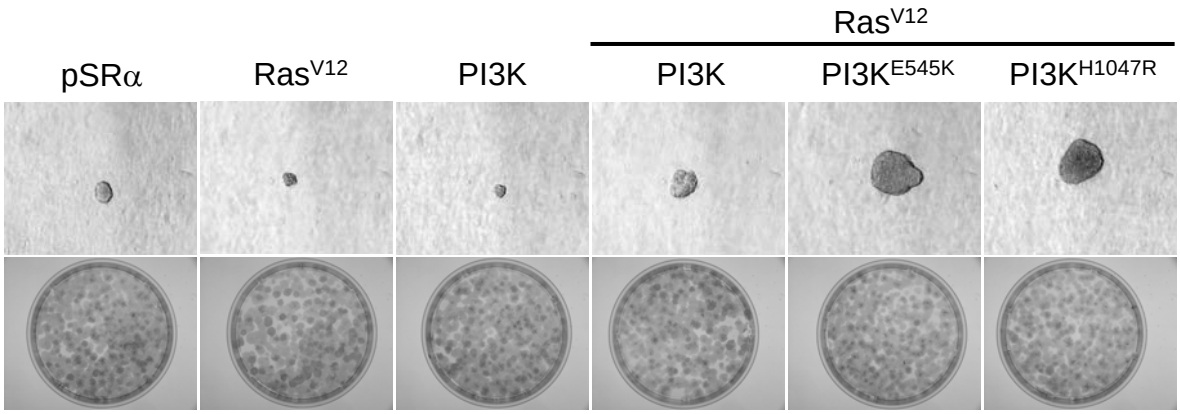

Figure 12. *Arf*$^{-/-}$ PEpC Can Be Trasnformed by Ras and PI3K mutants. *Arf*$^{-/-}$ PEpC were infected with the indicated retroviruses. Forty-eight hours post infection $1x10^4$ cells were seeded in media containing soft agar and 800 μg/ml G418 (pSRα and PI3K constructs) and/or 1 μg/ml puromycin (RasV12). Colony formation was assessed fourteen days later (Top Panels). Forty-eight hours post infection $3x10^5$ cells were seeded in media containing 800 μg/ml G418 (pSRα and PI3K constructs) and/or 1 μg/ml puromycin (Ras^{V12}) and foci formation was assessed fourteen days later (Bottom Panels). These data are representative of two independent experiments.

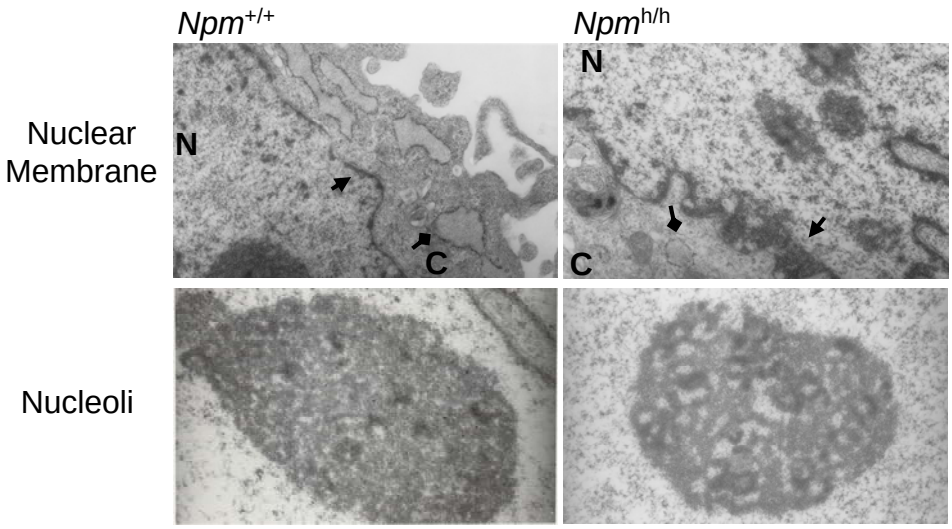

Figure 13. Loss of *Npm* Inhibits Ribosome Nuclear Export and Alters Nucleolar Morphology. *Npm*$^{+/+}$ or *Npm*$^{h/h}$ Mouse Embryo Fibroblasts were fixed and subjected to electron microscopic analysis. **Top panels** Arrows ⟶ point to nuclear membrane with increased ribosomes in the *Npm*$^{h/h}$ cells. Diamond headed arrows ⟶◆ point to cytoplasmic rough ER which is dramatically decreased in *Npm*$^{h/h}$ cells. **Bottom panels** Increased magnification focused on nucleoli of *Npm*$^{+/+}$ or *Npm*$^{h/h}$ cells.

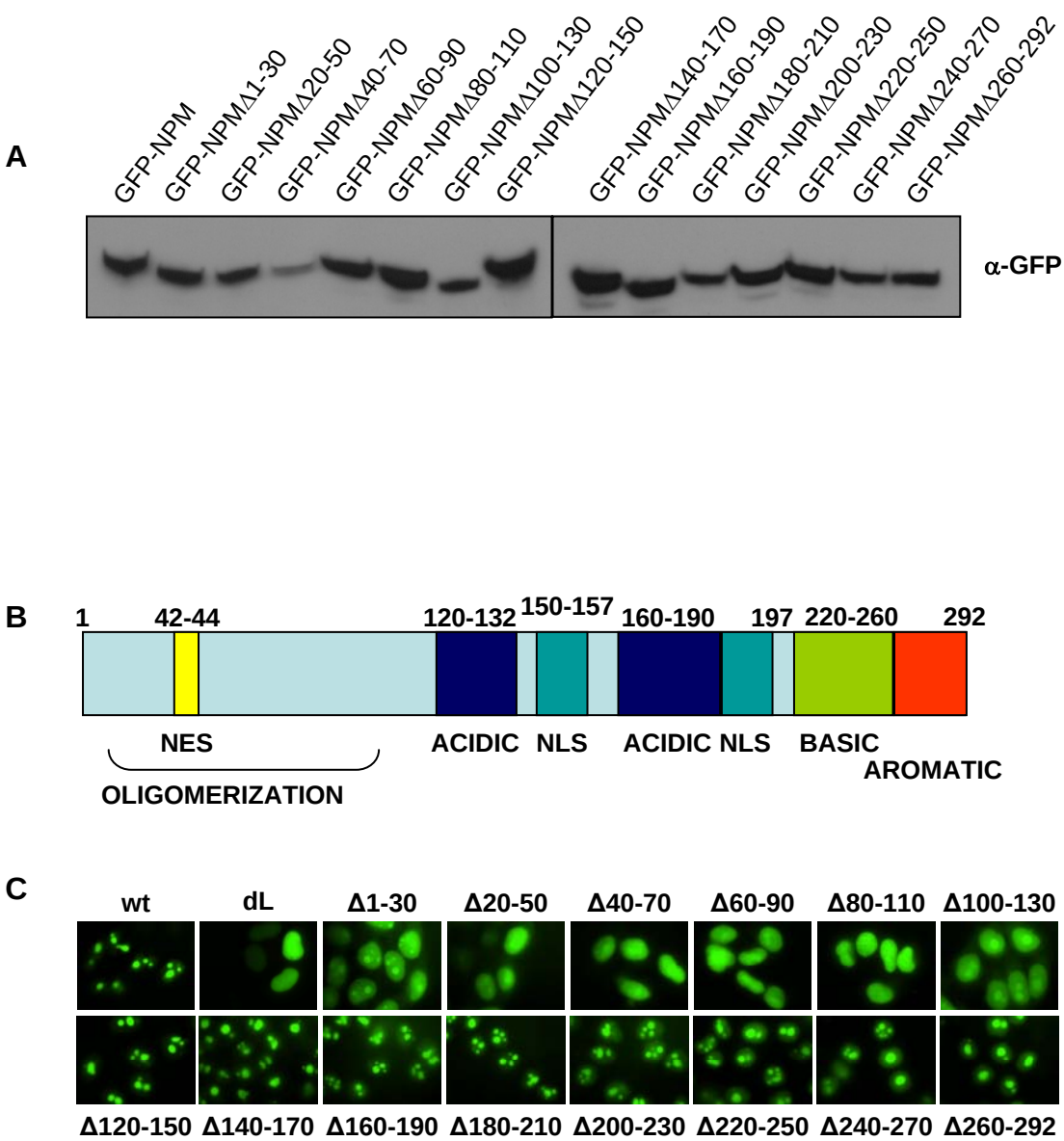

Figure 14. Expression and Localization of NPM Deletion Mutants. **A.** HeLa cells ($2x10^6$) were nucleofected with 2 μg of the indicated GFP-NPM constructs and 24 h later analyzed for GFP expression by western blot. **B** Domain structure of NPM. **C** HeLa cells nucleofected with the indicated GFP-NPM constructs were plated on cover slips. Cells were fixed and visualized for GFP localization by flourescence microscopy. Pictures are at 100X magnification. These data are representative of two independent experiments.

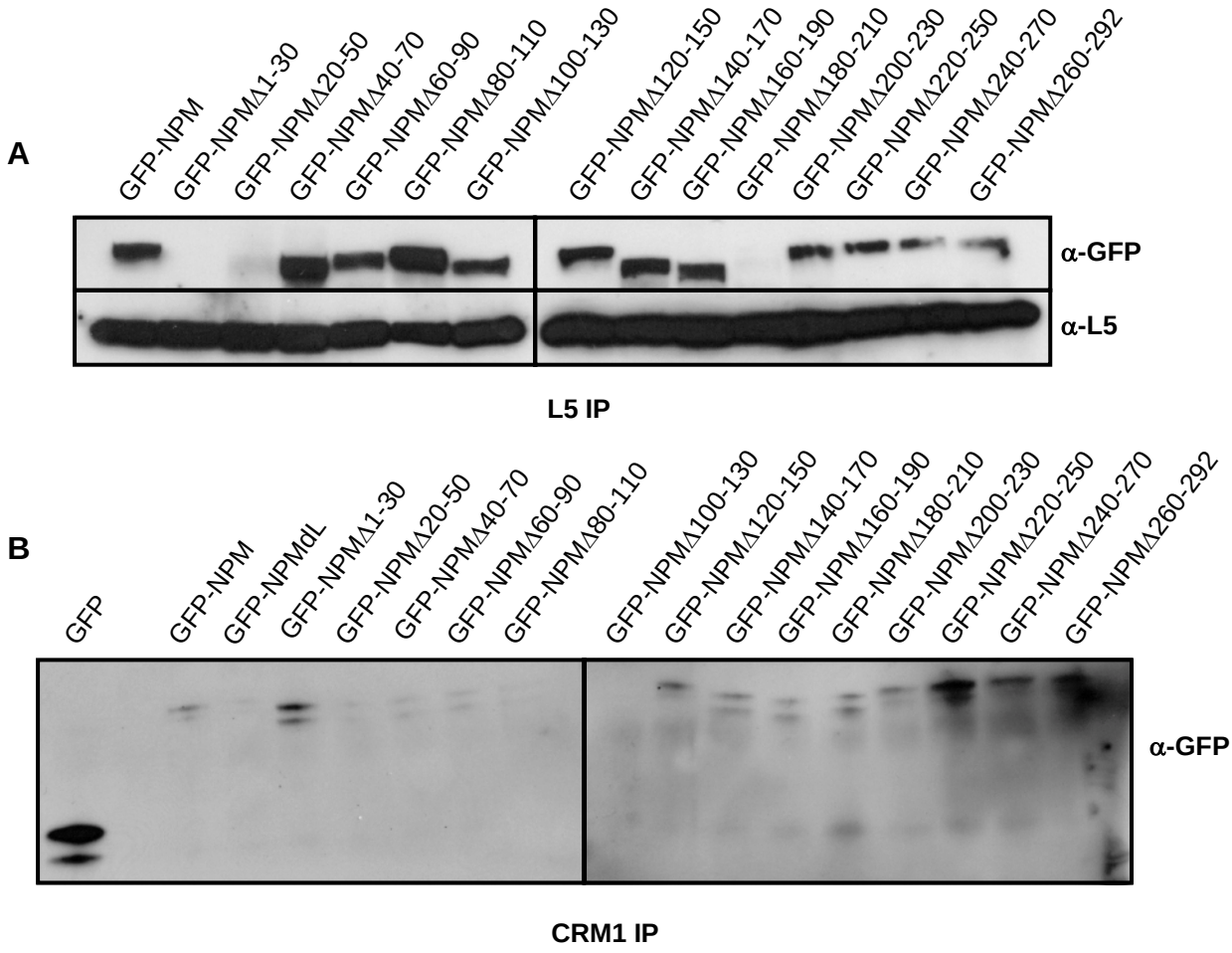

Figure 15. Regions of NPM required for L5 and CRM-1 interaction. HeLa cells ($2x10^6$) were nucleofected with the indicated GFP-NPM constructs and 24 h later, lysed and subjected to IP with an L5 (**A**) or Crm1 (**B**) anitibody. Immunoprecipitated proteins were analyzed by western blot for GFP (**A** and **B**) and L5 (**A**). These results are representative of two independent experiments.

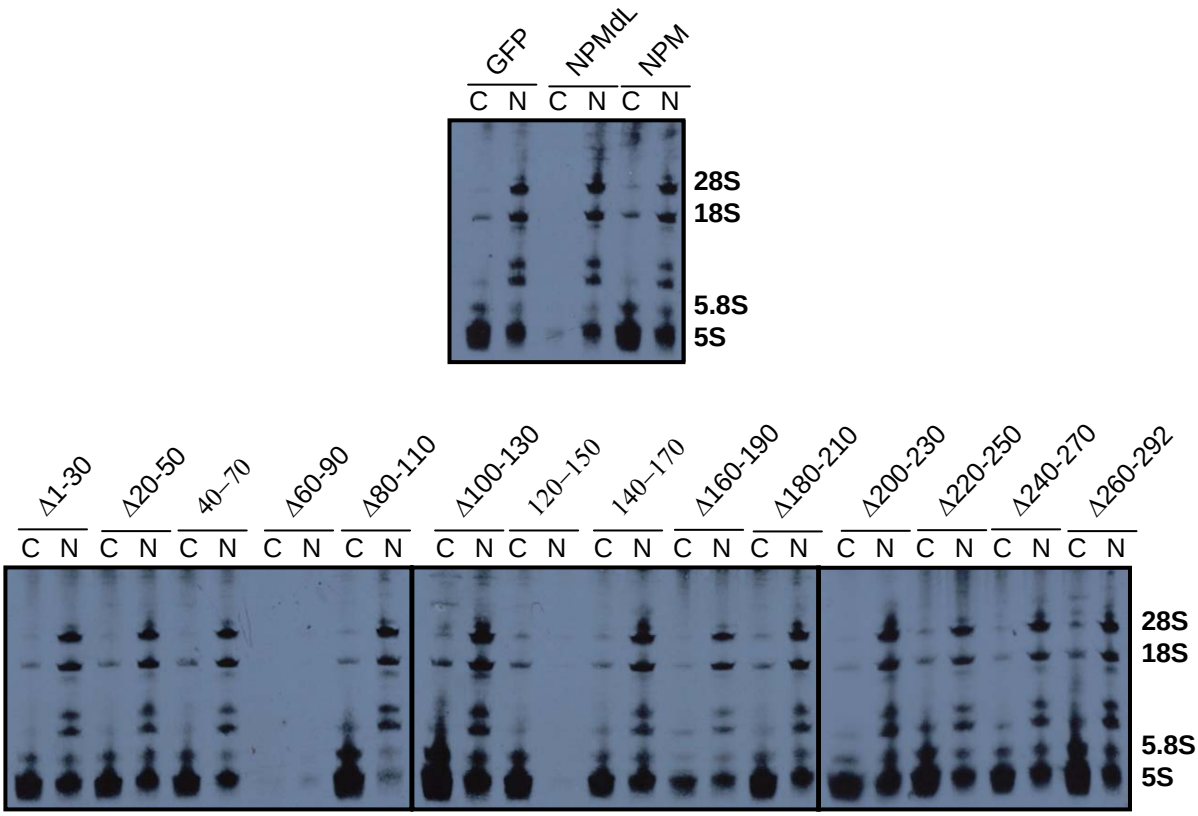

Figure 16. Regions of NPM required for rRNA Export. HeLa cells were nucleofected with the indicated GFP-NPM constructs. Twenty-four hours later cells were labeled with [methyl-^{3}H] methionine to label newly synthesized rRNAs. Equal numbers of cells were fractionated into cytosolic and nuclear fractions, total RNA isolated, separated on 10% TBE-Urea Gels, transferred to nylon membrane and visualized by autoradiography.